Electronic Supplementary Information

To Accompany

Bulk Gold Catalyzes Hydride Transfer in the Cannizzaro and Related Reactions

Kristopher M. Fecteau,[a,1] Ian R. Gould,[a] Lynda B. Williams,[b] Hilairy E. Hartnett,[a,b] Garrett D. Shaver,[a] Kristin N. Johnson,[a,2] and Everett L. Shock[a,b]

[a]School of Molecular Sciences, Arizona State University, Tempe, AZ 85287 USA
[b]School of Earth and Space Exploration, Arizona State University, Tempe, AZ 85287 USA

[1] Corresponding author. Present address: School of Earth and Space Exploration, Arizona State University, Tempe, AZ 85287. email: kfecteau@asu.edu
[2] Present address: Tokyo Institute of Technology, Earth-Life Science Institute, 2-12-1-IE-1 Ookayama, Meguro-ku, Tokyo, 152-8550, Japan

Materials

All reagents employed in this study were obtained commercially. Benzene (99.9%), toluene (99.9%), benzaldehyde (redistilled, 99.5%), decane (99%), benzyl alcohol (99.8%), benzoic acid (99.5%), diphenylmethane (99%), bibenzyl (99%), and benzyl ether (99%) were all obtained from Sigma-Aldrich (St. Louis, MO, USA) and used as received. 4-Methyldiphenylmethane (Matrix Scientific, Columbia, SC, USA) and 2-methyldiphenylmethane (Synquest Laboratories, Alachua, FL, USA) were both obtained at 98% purity while 3-methyldiphenylmethane (97%) was obtained from AK Scientific (Union City, CA, USA); all were used as received. Dichloromethane (99.9%) was obtained from Fisher Scientific (Pittsburg, PA, USA) and used as received. Deionized water was obtained from a Barnstead Diamond water purification system fed with locally produced reverse osmosis water to yield a final resistivity of 18.2 MΩ•cm.

Bulk gold powder was obtained at 99.995% purity from Salt Lake Metals (Salt Lake City, UT, USA). Before use, the powder was rinsed repeatedly with deionized water in a fine fritted filter, allowed to air dry, then rinsed with multiple aliquots of dichloromethane and allowed to air dry. The powder was then heated at 110 °C overnight before use. For reuse, the used gold was collected on the fritted filter under reduced pressure and the same cleaning procedure was then employed. Gold powders with 0.5-0.8 and 5.5-9.0 micron particle sizes were obtained from Alfa Aesar (Ward Hill, MA, USA) at 99.96% purity. Upon receipt, these powders were transferred to a 4 mL silanized vial with a Teflon-lined cap, suspended in deionized water, and allowed to settle. The water was decanted and the procedure was repeated twice. Subsequently, 3 aliquots of methanol (spectroscopy grade) followed by dichloromethane were similarly used and the residual dichloromethane was evaporated under a gentle stream of nitrogen. The surface areas of these

powders were determined via Brunauer-Emmett-Teller adsorption of N_2 in a vacuum background at -196 °C using a Micromeritics (Norcross, GA, USA) Tristar 3020 surface area and porosity system with ~2 g of the 0.5-0.8 micron powder and ~5 g of the 5.5-9.0 micron powder. Prior to measurement, the powders were dried overnight at 100 °C under a stream of nitrogen. Free space was reduced by use of a glass filler rod and the cold and ambient free space volumes were determined using helium. Measurement of the surface area of the large bulk powder obtained from Salt Lake Metals was also attempted but the surface area was too low to obtain serviceable results.

Methods

All experiments were conducted in clear fused silica tubes (8 mm inner diameter, 12 mm outer diameter) produced from tubing obtained commercially (GM Associates, Oakland, CA, USA). The tubing was cut into ~25 cm lengths, flame sealed on one end using a glass blowing lathe, and annealed. Each tube was weighed empty using a foam holder and then weighed again after addition of an aliquot of gold powder. Benzaldehyde (41.0 µL) or benzyl alcohol (41.5 µL) was added dropwise via a 50 µL syringe followed by the addition of water (4.00 mL) via syringe after the water had been purged with argon for at least one hour, resulting in final organic concentrations of ~100 millimolal. For ~200 millimolal experiments, the volume of organic loaded was doubled. Solutions in these experiments are characterized in terms of molality, rather than molarity, because the solutions are prepared at room temperature, but the experiments are conducted at a higher temperature (200 °C) where the density (and hence, solution volume) is different, thereby avoiding the potential confusion in regard to what temperature the concentrations reference, as molality is independent of temperature. The tube was degassed on a vacuum line via two freeze-pump-thaw cycles using liquid nitrogen and then frozen and flame sealed under vacuum with a hydrogen-oxygen flame, resulting in a final experimental tube length of ~14 cm. The tubes

were thawed, thoroughly mixed via vortexing, and placed horizontally in the middle of a muffle furnace (Fisher Isotemp) preheated with a galvanized steel pipe as secondary containment, as previously described.[1] All experiments were conducted at 200 °C and the temperature was monitored using a thermocouple probe; the variability in temperature over the course of the experiment was estimated to be ± 2 °C. To end the experiment, the tubes were quenched under tap water, requiring ~2 minutes to reach ambient temperature. The tubes were then frozen at -20 °C until analysis.

Dichloromethane-soluble organics were quantified by liquid-liquid extraction and gas chromatography-flame ionization detection (GC-FID) analysis. Experiment tubes were thawed, scored above the liquid level with a tubing cutter, and broken open, whereupon the contents were poured into a 20 mL amber vial containing ~1.4 g of sodium chloride. Sodium chloride was added to increase the ionic strength of the aqueous layer and improve partitioning of polar organics into the organic layer. Dichloromethane (8.00 mL) containing 9.23 mM n-decane (internal standard) was then added to the vial, with a portion of this solution first being added to the open tube to extract organics adhered to the inside of the tube, then being combined with the other fluids in the vial. Once combined, the vial was sealed with a Teflon-lined septum and vigorously shaken for 45 seconds then allowed to stand for several minutes until phase separation had occurred. The shaking and standing procedure was repeated twice. A portion of the bottom dichloromethane layer was then transferred to 2 mL amber autosampler vials via a Pasteur pipet and sealed with a Teflon-lined septum. Samples were then analyzed by GC-FID on either a Varian CP-3800 or Bruker Scion 456 gas chromatograph, both of which were equipped with a Varian CP-8400 autosampler. Injection volumes were 1 μL and all data are based on the means of at least 3 injections. The injector (CP-1177) was isothermal at 275 °C and operated at a split ratio of 15. The carrier gas was

helium held constant at 1.5 mL/minute through a capillary column (Supelco 5% phenyl, 95% polydimethylsiloxane, 30 m x 0.25 mm, 0.25 μm film thickness). The column oven temperature was initially 40 °C but upon injection was increased to 140 °C over 10 minutes then raised to 300 °C over 32 minutes, after which it was held at 300 °C for 8 minutes. The flame ionization detector temperature was held isothermally at 300 °C.

Integrated peak area ratios of each analyte relative to that of the decane internal standard were expressed in millimolarity units (as dichloromethane solutions) using response factors obtained from calibration curves, which were constructed with at least 4 solutions of known quantities of each analyte and 9.23 mM decane. The response factor of 4-methyldiphenylmethane, determined as described above, was used for all 3 isomers of methyldiphenylmethane. The concentrations of each analyte were then converted to yields of each compound in each experiment. Mass balance was determined via comparison of the equivalents of aromatic rings added to each experiment to the number of equivalents quantified upon analysis, thereby assuming aromatic rings are inert under the experimental conditions. Hydrogen balance was calculated as the ratio of the total number of moles of hydrogen present in the quantified organic products to the number of moles of hydrogen present in a number of moles of the starting reactant (benzaldehyde or benzyl alcohol) equal to the total number of moles of aromatic rings quantified upon analysis, expressed as a percentage. In other words, hydrogen balance is reported as the ratio of moles of hydrogen in the products to moles of hydrogen in the reactant normalized to 100% mass balance (based on aromatic rings).

Gold powders were analyzed using a FEI XL30 Environmental SEM-FEG for surface morphology and particle size analysis. The powders were mounted on 12.7 mm round aluminum pin stubs (Ted Pella, Redding, CA, USA) and adhered to the surface of the mounts by carbon tape.

Images were taken in secondary electron (SE) mode at 15.00 to 20.00 kV, spot size 3.0 to 4.0. Gold samples remained uncoated during SEM analysis.

Uncatalyzed Benzaldehyde Reactions and Correction of Benzoic Acid Yield

The reaction product yields of experiments starting with benzaldehyde were corrected for the small amounts of products formed in competing aqueous, uncatalyzed reactions. In the absence of gold, benzaldehyde conversion was low and small quantities of both benzyl alcohol and benzoic acid were formed (Figure S1, data reported in Table S1). When the initial concentration of benzaldehyde was doubled, the yield of benzyl alcohol increased roughly by a factor of four, suggesting it was produced via an aqueous phase second-order reaction, consistent with the Cannizzaro disproportionation. However, the yield of benzoic acid greatly exceeded that of the alcohol and more closely doubled when the starting benzaldehyde concentration was doubled. These observations suggest most of the benzoic acid produced in the absence of gold arises by a first-order oxidative reaction of benzaldehyde. The oxidant could be traces of residual oxygen that remain after the sample degassing procedure (**Scheme S1**, Reaction **a**). Minor amounts of benzoic acid in these experiments arise via disproportionation, equivalent to the corresponding yield of benzyl alcohol. Thus, the yield of benzoic acid in each experiment (both with and without gold) was corrected by subtracting this minor amount of benzoic acid derived independently of disproportionation, i.e., by subtracting the yield of benzoic acid in experiments without gold minus the yield of benzyl alcohol in those same experiments. This correction was minor with respect to the yield of benzoic acid obtained in the presence of gold.

Minor Reactions of Benzyl Alcohol and Analysis of Disproportionation Yields

Minor products in addition to the major products benzaldehyde and toluene were also observed with benzyl alcohol as the starting material, including benzene, benzoic acid, benzyl

ether, diphenylmethane, methyldiphenylmethanes (*i.e.*, benzyltoluenes), and bibenzyl (Figure S2, data reported in Table S2). The sum of these minor products amounted to no more than 6% of the total product yield. Benzene and benzoic acid are readily explained as arising from the gold-catalyzed reactions of benzaldehyde, since their yields increased with increasing quantities of added gold. In contrast, the other products were likely derived from the alcohol and their production *decreased* with increasing amounts of gold, with the exception of bibenzyl. This decrease, along with their very low yields, suggests that these products arise from reactions in the aqueous phase that are not gold-catalyzed, since higher gold loadings increase the amount of alcohol that reacts via a surface-catalyzed mechanism and decrease the rate of uncatalyzed pathways. Benzyl alcohol can be protonated and lose water to form a benzyl cation, which can then perform electrophilic aromatic substitution (EAS) with benzene or toluene to yield diphenylmethane or methyldiphenylmethanes, respectively (**Scheme S1**, Reactions **c** and **d**). Alcohols are known to be readily protonated and dehydrate under hydrothermal conditions,[2–6] owing to the greater autoionization of water (pK_w = 5.64 at 200 °C),[7,8] and EAS has previously been observed with benzyl alcohol.[9–11] The relative yields of the three methyldiphenylmethane isomers (Figure S3) are consistent with the *ortho*- and *para*-directing effect of the methyl substituent, with the yield of the *ortho*-isomer being slightly less than that of the *para*-isomer, presumably due to a steric effect.[12] Benzyl ether arises from condensation of two equivalents of benzyl alcohol (**Scheme S1**, Reaction **e**).

In order to discern whether the yields of benzaldehyde and toluene reflect the disproportionation of benzyl alcohol, the benzaldehyde and toluene yields were adjusted to reflect the secondary reactions discussed above. The benzaldehyde yield was first corrected by subtracting the small amount of benzaldehyde observed in the absence of gold that seems to be produced by

oxidation of benzyl alcohol (**Scheme S1**, Reaction **b**) rather than by disproportionation, since toluene was not observed in experiments without gold. The presumed oxidant is residual air-derived oxygen that was not completely removed during the degassing procedure conducted during experiment preparation. Assuming cross-disproportionation is the major pathway for the production of benzoic acid in experiments starting with benzyl alcohol, the total benzaldehyde yield in each experiment was: corrected benzaldehyde + benzoic acid + benzene + diphenylmethane. Since the benzoic acid yield is stoichiometrically equal to the amount of toluene produced via cross-disproportionation, the corresponding toluene yield due to benzyl alcohol disproportionation was: toluene + methyldiphenylmethanes – benzoic acid. These yields were then compared with each other as evidence for benzyl alcohol disproportionation as the primary reaction in experiments starting with benzyl alcohol.

References

1 Z. Yang, H. E. Hartnett, E. L. Shock and I. R. Gould, Organic oxidations using geomimicry, *J. Org. Chem.*, 2015, **80**, 12159–12165.

2 X. Xu, M. J. Antal Jr. and D. G. M. Anderson, Mechanism and temperature-dependent kinetics of the dehydration of tert-butyl alcohol in hot compressed liquid water, *Ind. Eng. Chem. Res.*, 1997, **36**, 23–41.

3 M. J. Antal Jr., M. Carlsson, X. Xu and D. G. M. Anderson, Mechanism and kinetics of the acid-catalyzed dehydration of 1- and 2-propanol in hot compressed liquid water, *Ind. Eng. Chem. Res.*, 1998, **37**, 3820–3829.

4 N. Akiya and P. E. Savage, Kinetics and mechanism of cyclohexanol dehydration in high-temperature water, *Ind. Eng. Chem. Res.*, 2001, **40**, 1822–1831.

5 Z.-B. Xu and J. Qu, Hot water-promoted SN1 solvolysis reactions of allylic and benzylic alcohols, *Chem. - A Eur. J.*, 2013, **19**, 314–323.

6 C. Bockisch, E. D. Lorance, H. E. Hartnett, E. L. Shock and I. R. Gould, Kinetics and mechanisms of dehydration of secondary alcohols under hydrothermal conditions, *ACS Earth Sp. Chem.*, 2018, **2**, 821–832.

7 W. L. Marshall and E. U. Franck, Ion product of water substance, 0-1000 °C, 1-10,000 bars, new international formulation and its background, *J. Phys. Chem. Ref. Data*, 1981, **10**, 295–304.

8 A. V. Bandura and S. N. Lvov, The ionization constant of water over wide ranges of temperature and density, *J. Phys. Chem. Ref. Data*, 2006, **35**, 15–30.

9 A. R. Katritzky, M. Balasubramanian and M. Siskin, Aqueous high-temperature chemistry of carbo- and heterocycles. 2. Monosubstituted benzenes: benzyl alcohol, benzaldehyde and benzoic acid, *Energy & Fuels*, 1990, **4**, 499–505.

10 K. J. Robinson, I. R. Gould, K. M. Fecteau, H. E. Hartnett, L. B. Williams and E. L. Shock, Deamination reaction mechanisms of protonated amines under hydrothermal conditions, *Geochim. Cosmochim. Acta*, 2019, **244**, 113–128.

11 K. M. Fecteau, I. R. Gould, C. R. Glein, L. B. Williams, H. E. Hartnett and E. L. Shock, Production of carboxylic acids from aldehydes under hydrothermal conditions: A kinetics study of benzaldehyde, *ACS Earth Sp. Chem.*, 2019, **3**, 170–191.

12 G. A. Olah, Aromatic substitution. XXVIII. Mechanism of electrophilic aromatic substitutions, *Acc. Chem. Res.*, 1971, **4**, 240–248.

Table S1. Experimental details and product yields of experiments starting with benzaldehyde using small and large gold powders.

powder grams	conversion %	mass balance %	H balance %	benzaldehyde µmol	benzyl alcohol µmol	benzoic acid µmol	benzene µmol	toluene µmol
no powder, 100 millimolal								
0	0.92	108.44	100.02	432.33	0.25	3.72	0.04	<0.01[a]
0	1.16	110.77	100.02	440.57	0.26	4.86	0.04	<0.01
large bulk powder, 100 millimolal								
0.0618[b]	7.37	103.97	100.98	387.51	12.32	18.02	0.50	<0.01
0.1547	17.70	102.36	102.75	338.98	33.82	38.11	0.82	0.15
0.1547	14.34	101.82	102.12	350.94	26.03	31.40	1.24	0.09
0.3004	36.62	101.84	105.73	259.74	68.95	75.99	3.64	1.48
0.4851	55.93	93.73	107.67	166.22	59.85	116.02	8.15	26.93
0.7505	49.45	91.42	105.95	185.95	30.94	107.13	9.14	34.68
1.0075	48.47	97.98	104.98	203.17	16.43	122.57	9.59	42.50
1.0076	37.60	91.44	104.27	229.58	15.35	85.32	5.90	31.79
small 0.5-0.8 micron powder, 100 millimolal								
0.0153	2.73	96.81	100.28	378.92	3.06	6.62	0.78	0.18
0.0197	2.60	91.48	100.18	358.54	1.91	6.80	0.78	0.10
0.0811	8.04	96.96	101.10	358.78	11.71	14.68	3.78	1.20
0.0829	7.31	94.94	100.98	354.10	10.14	13.10	3.54	1.14
0.2008	11.36	97.10	101.61	346.32	17.04	19.08	6.44	1.83
0.2008	12.87	96.44	101.83	338.11	19.16	20.55	8.10	2.15
0.2022	12.89	94.40	102.23	330.89	23.02	15.76	7.76	2.42
small 0.5-0.8 micron powder, 200 millimolal								
0.2009	8.75	97.60	101.26	716.76	27.34	26.04	12.89	2.43
0.2022	8.59	98.45	101.29	724.28	28.17	24.91	12.46	2.51
no powder, 200 millimolal								
0	1.36	99.54	100.04	790.18	0.86	10.04	0.05	<0.01
0	1.33	97.06	100.04	770.70	0.88	9.50	0.06	<0.01
small 0.5-0.8 micron powder, 100 millimolal, half time[c]								
0.0810	6.53	97.46	100.92	366.59	9.91	11.76	2.97	0.95
0.2032	11.96	96.62	101.73	342.30	18.10	20.17	6.10	2.14
0.2032	27.04	93.78	104.35	275.32	45.39	47.07	5.72	3.87

[a]below detection limits. [b]masses in italics refer to gold that had been previously used once. [c]1451 minutes; all other experiments were 2902 minutes.

Table S2. Experimental details and product yields of experiments starting with benzyl alcohol (using small 0.5-0.8 micron gold powder).

powder	conv.	mass balance	H balance	benzald-ehyde	benzyl alcohol	benzoic acid	benzene	toluene	benzyl ether	DPM[b]	4-BT[c]	3-BT	2-BT	bibenzyl
grams	%	%	%	µmol	µmol	µmol	µmol	µmol	µmol	µmol	µmol	µmol	µmol	µmol
0	0.20	103.00	100.12	0.22	411.81	<0.01[a]	<0.01	<0.01	0.31	<0.01	<0.01	<0.01	<0.01	<0.01
0	0.16	103.55	100.08	0.21	414.21	<0.01	<0.01	<0.01	0.23	<0.01	<0.01	<0.01	<0.01	<0.01
0.0505	34.25	100.07	95.78	68.17	263.61	2.21	0.61	63.18	0.64	0.029	0.38	0.11	0.34	0.08
0.2030	52.22	94.63	93.87	85.39	181.16	5.94	2.63	101.49	0.31	0.028	0.34	0.11	0.31	0.17
0.2031	50.86	95.99	94.00	85.08	188.97	6.03	2.45	99.47	0.34	0.028	0.35	0.11	0.32	0.16
0.3391	53.46	93.43	93.64	84.72	174.20	8.40	2.83	101.88	0.26	0.025	0.29	0.09	0.26	0.22

[a]below detection limits. [b]diphenylmethane. [c]benzyltoluene (*i.e.*, methyldiphenylmethane)

Table S3. Experimental details and product yields of experiments starting with benzaldehyde using medium 5.5-9.0 micron gold powder.

powder grams	time minutes	conversion %	mass balance %	H balance %	benzaldehyde µmol	benzyl alcohol µmol	benzoic acid µmol	benzene µmol	toluene µmol
0.5007	720	5.14	95.63	101.61	365.00	2.14	12.85	1.26	3.54
0.5004	1451	6.58	95.28	102.06	358.17	2.67	15.76	1.58	5.22
0.4999	2160	4.36	96.62	101.37	371.85	1.50	11.04	0.95	3.47
0.5003	2925	2.83	96.85	100.90	378.69	1.11	7.23	0.46	2.24
0.5002	2925	7.52	96.19	102.36	357.94	2.98	18.56	1.68	5.89

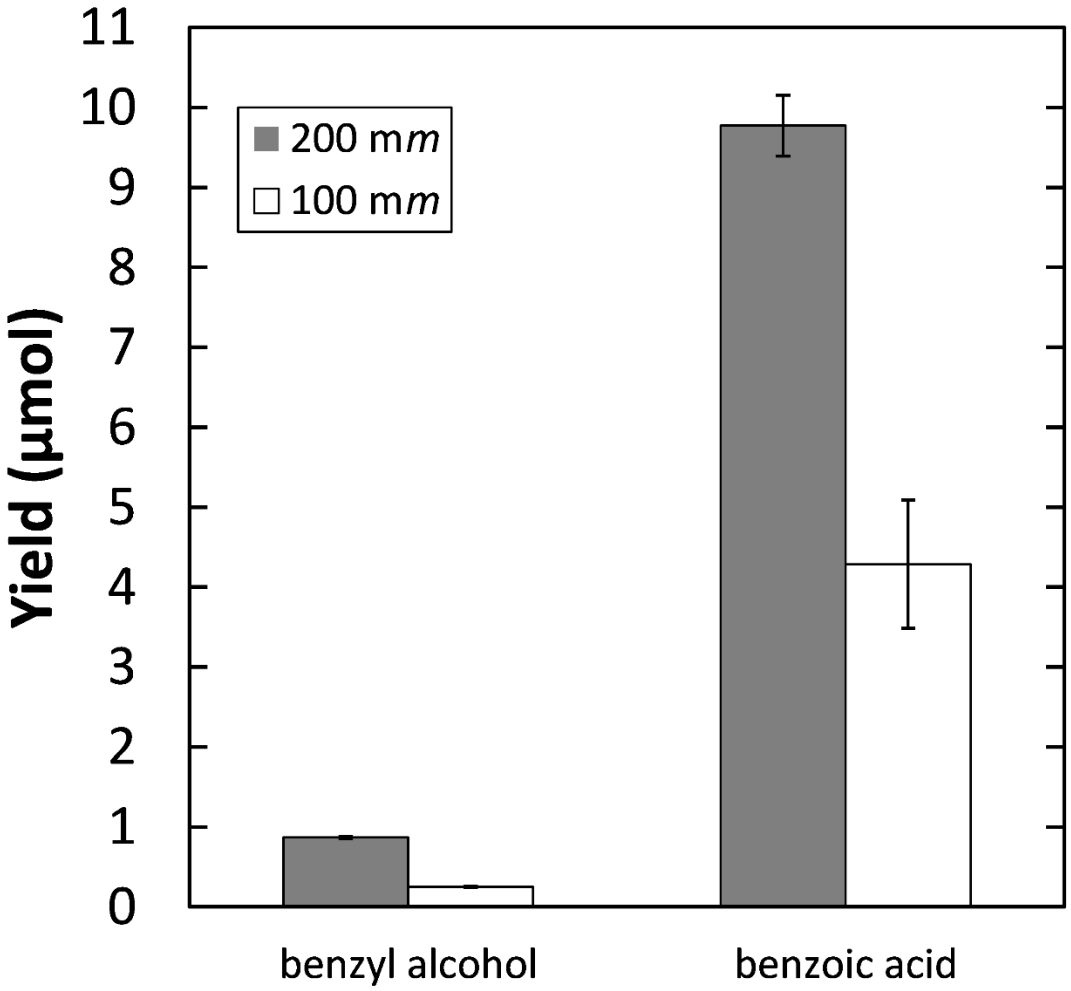

Figure S1. Yields of benzyl alcohol and benzoic acid in experiments without gold at 200 °C and 1.5 MPa for 2902 minutes with 100 and 200 millimolal initial benzaldehyde concentrations. Error bars represent the standard deviation of duplicate experiments.

Scheme S1. Aqueous Phase (Uncatalyzed) Reactions of Benzaldehyde and Benzyl Alcohol Solutions (200 °C, 1.5 MPa)

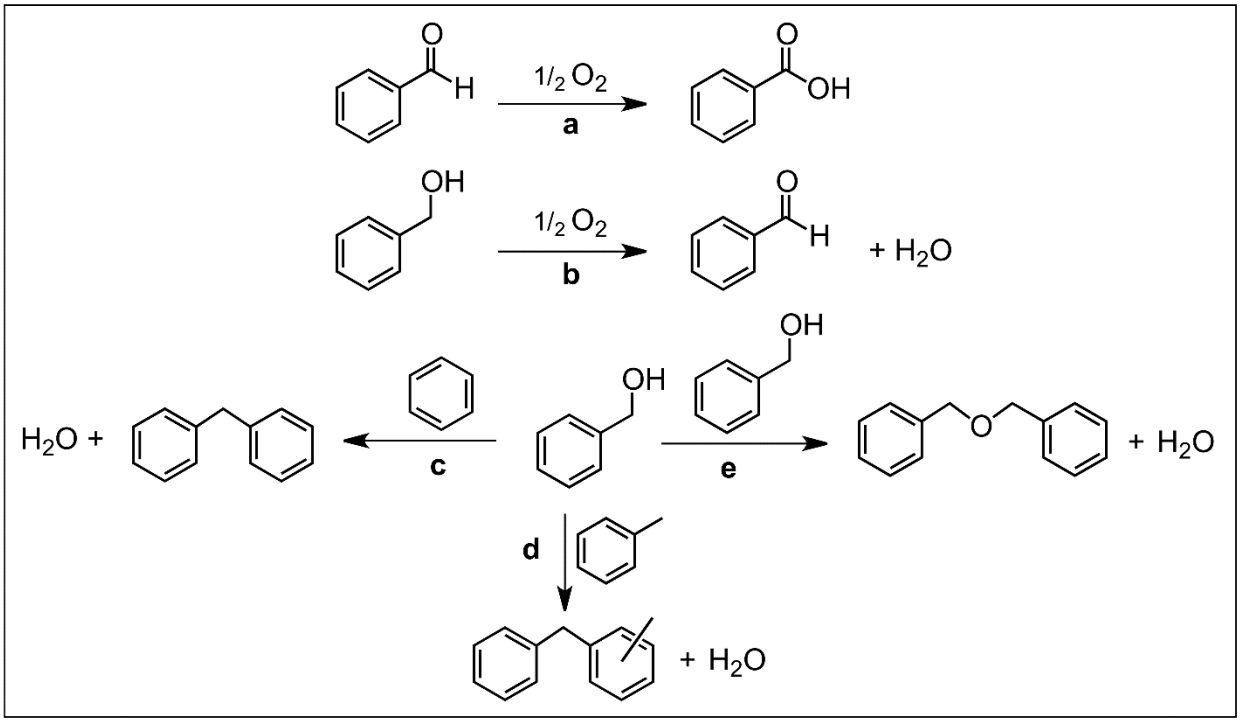

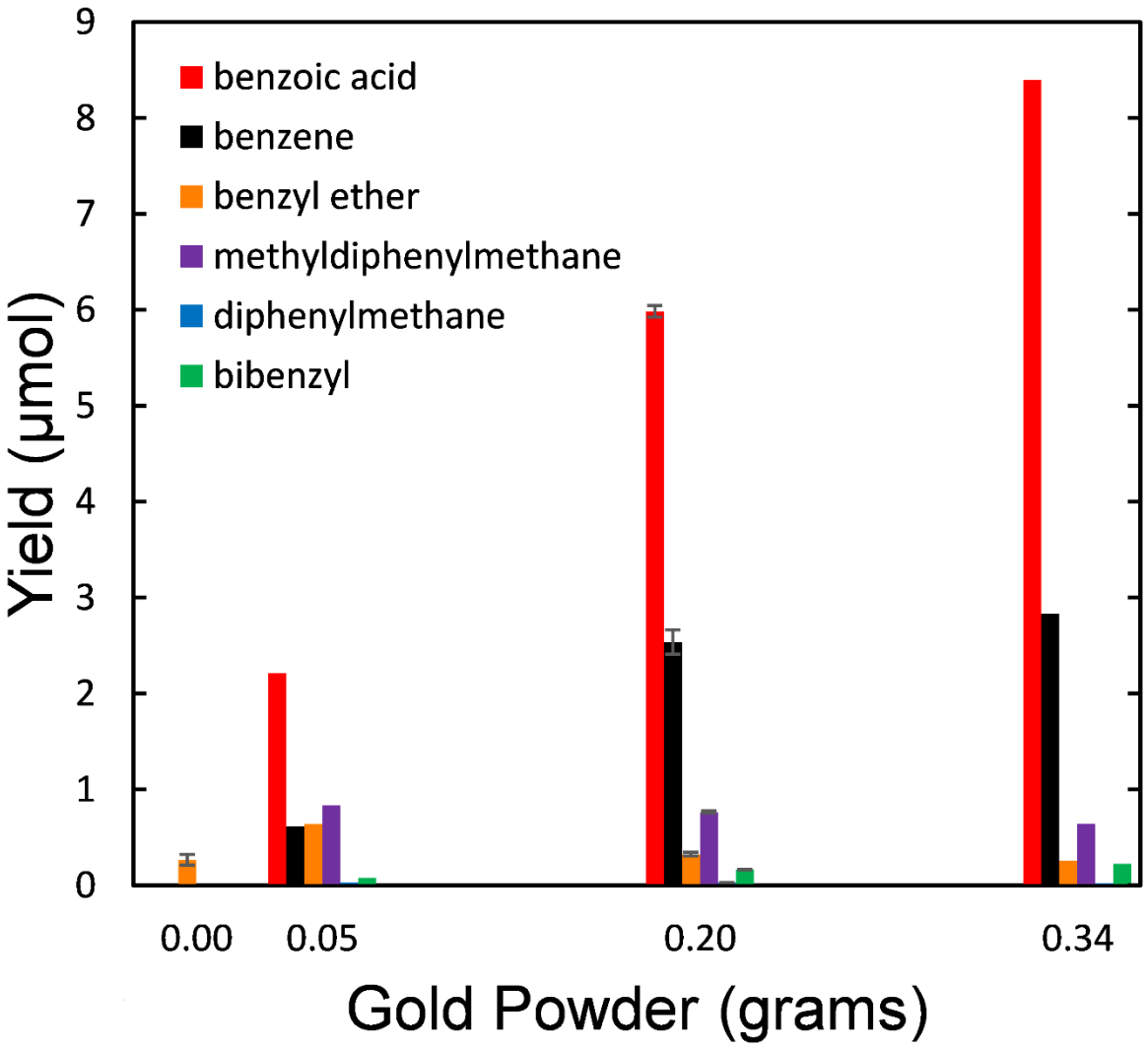

Figure S2. Yields of minor products (collectively representing no than 6% of the total yield of products in a given experiment) in experiments starting with benzyl alcohol and the small particle size 0.5-0.8 micron gold powder. Uncertainties are the standard deviation of duplicate experiments, which were completed only with no gold and 0.2 grams of gold.

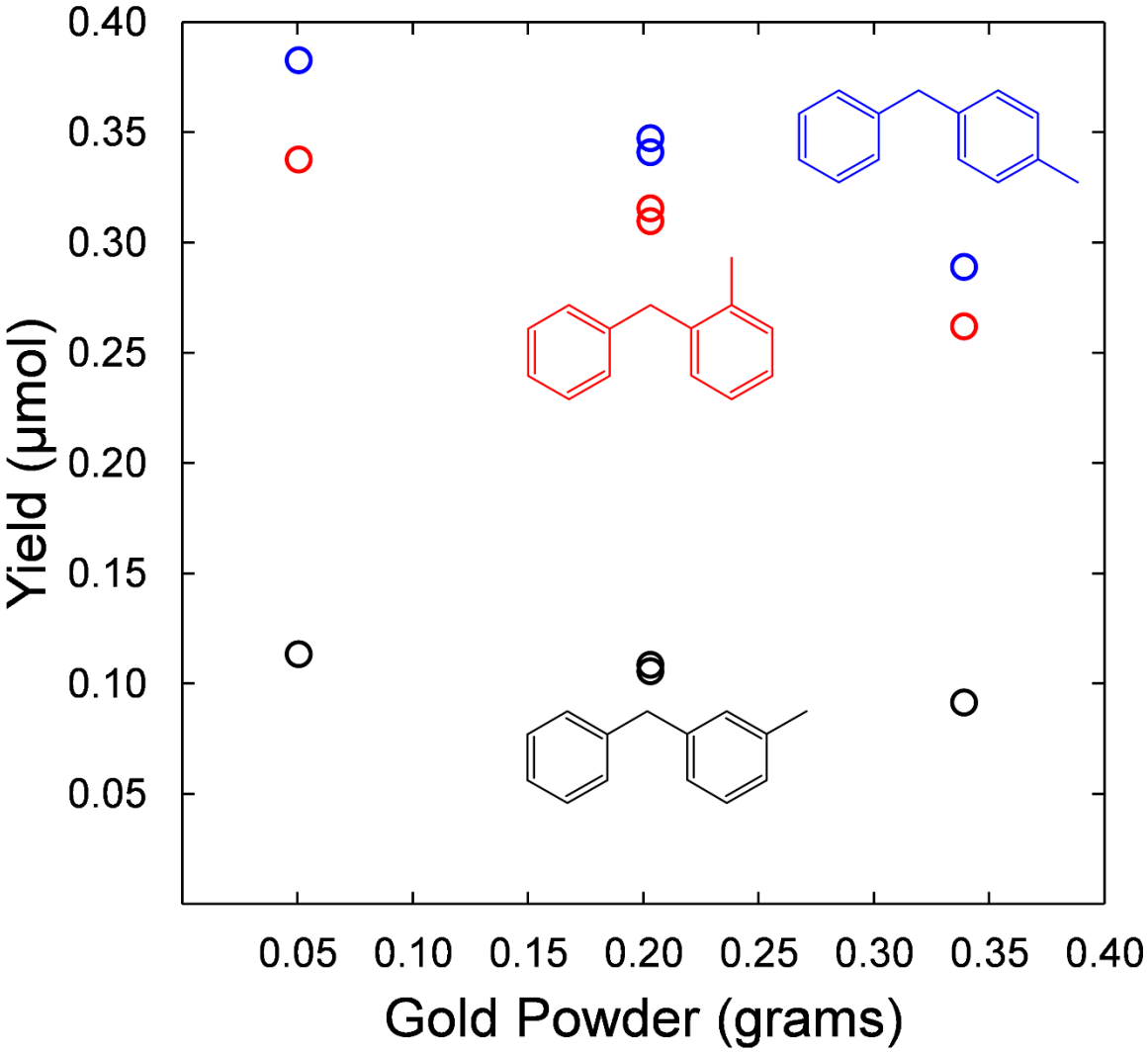

Figure S3. Yields of each isomer of methyldiphenylmethane (*i.e.*, benzyltoluene) with respect to the amount of smaller 0.5-0.8 micron gold powder present for experiments starting with 100 millimolal benzyl alcohol (200 °C, 1.5 MPa, 2902 minutes).

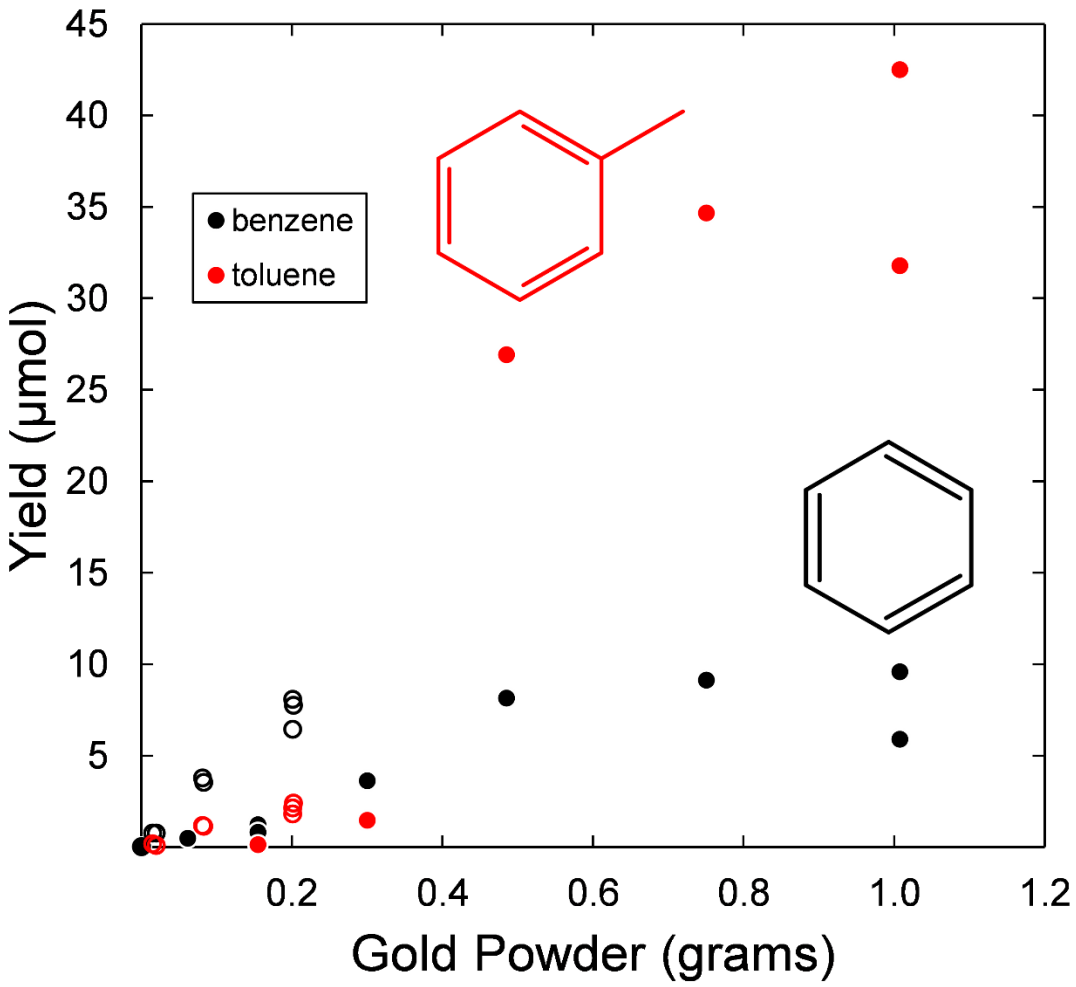

Figure S4. Yields of benzene (black circles) and toluene (red circles) in experiments with 0.1 molal benzaldehyde at 200 °C and 1.5 MPa for a constant duration of 2902 minutes in the presence of larger bulk (filled circles) or smaller 0.5-0.8 micron (open circles) gold powder.

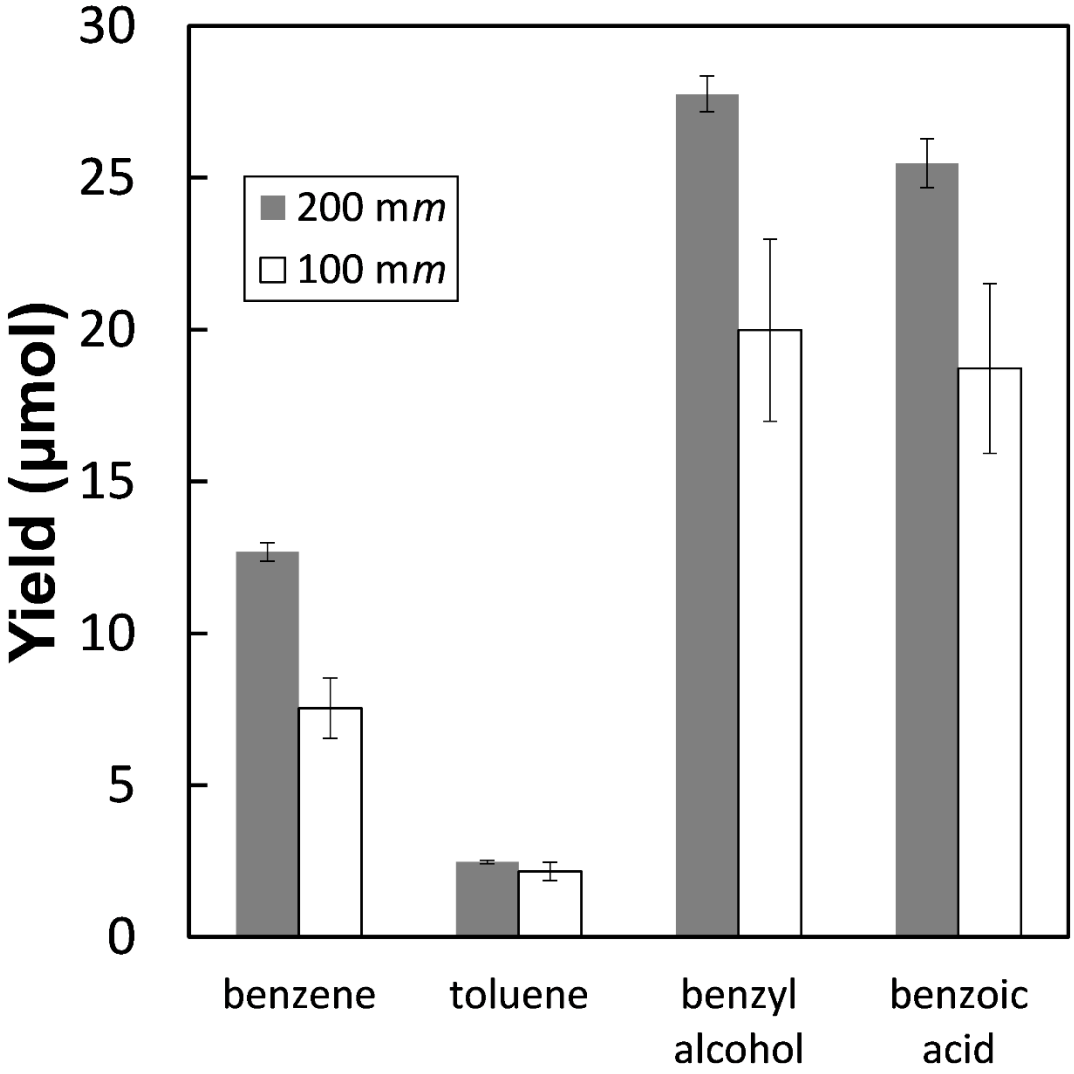

Figure S5. Yields of major products in experiments (200 °C, 1.5 MPa, 2902 minutes) with approximately 200 mg of smaller 0.5-0.8 micron gold for 100 and 200 millimolal starting benzaldehyde concentrations. Results are the mean and standard deviation of replicate experiments.

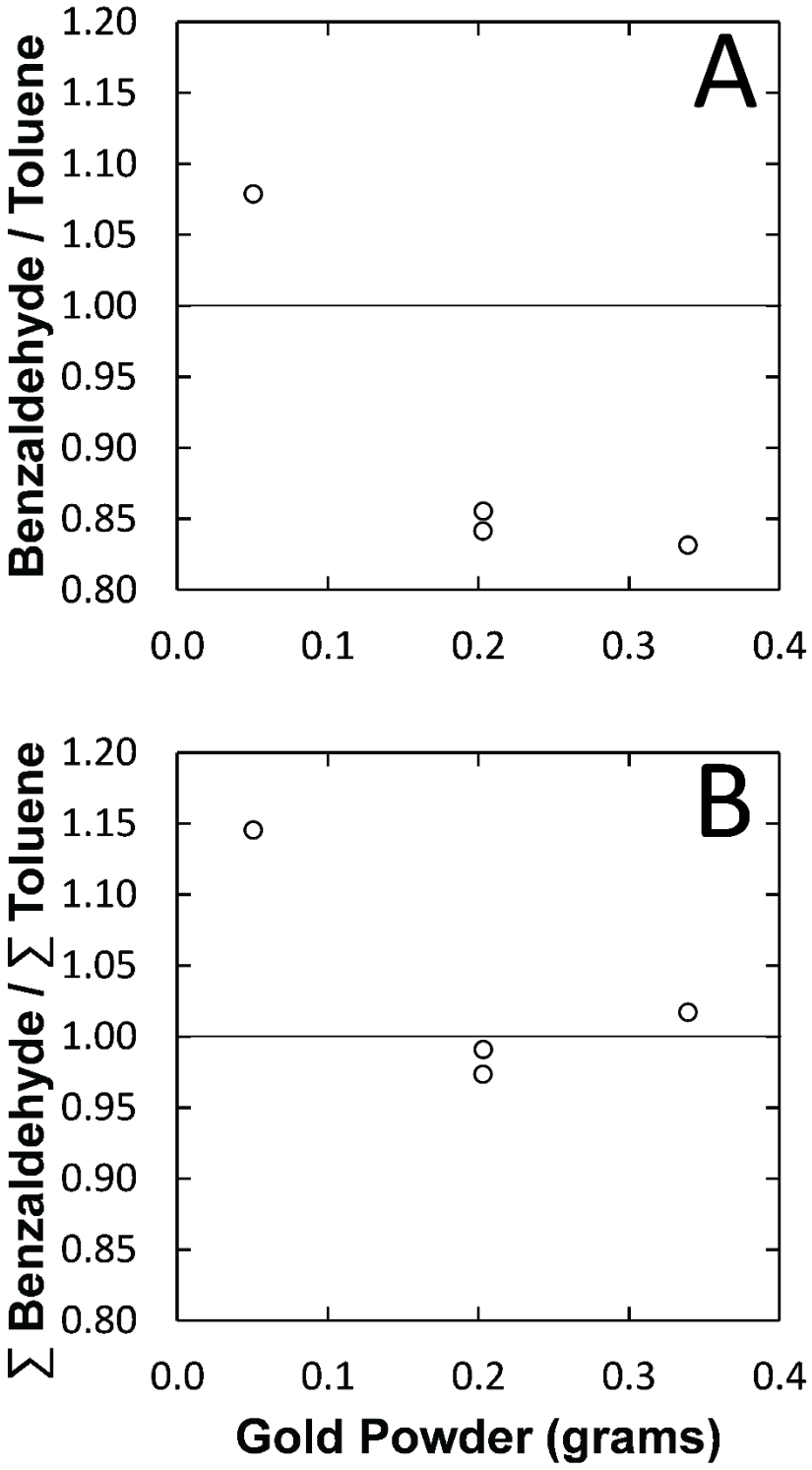

Figure S6. A) Ratios of benzaldehyde to toluene in experiments starting with benzyl alcohol relative to the amount of smaller 0.5-0.8 micron gold powder present. B) The same ratios corrected for consumption of benzaldehyde and toluene by secondary reactions and by subtracting the small amount of benzaldehyde derived in the absence of gold.

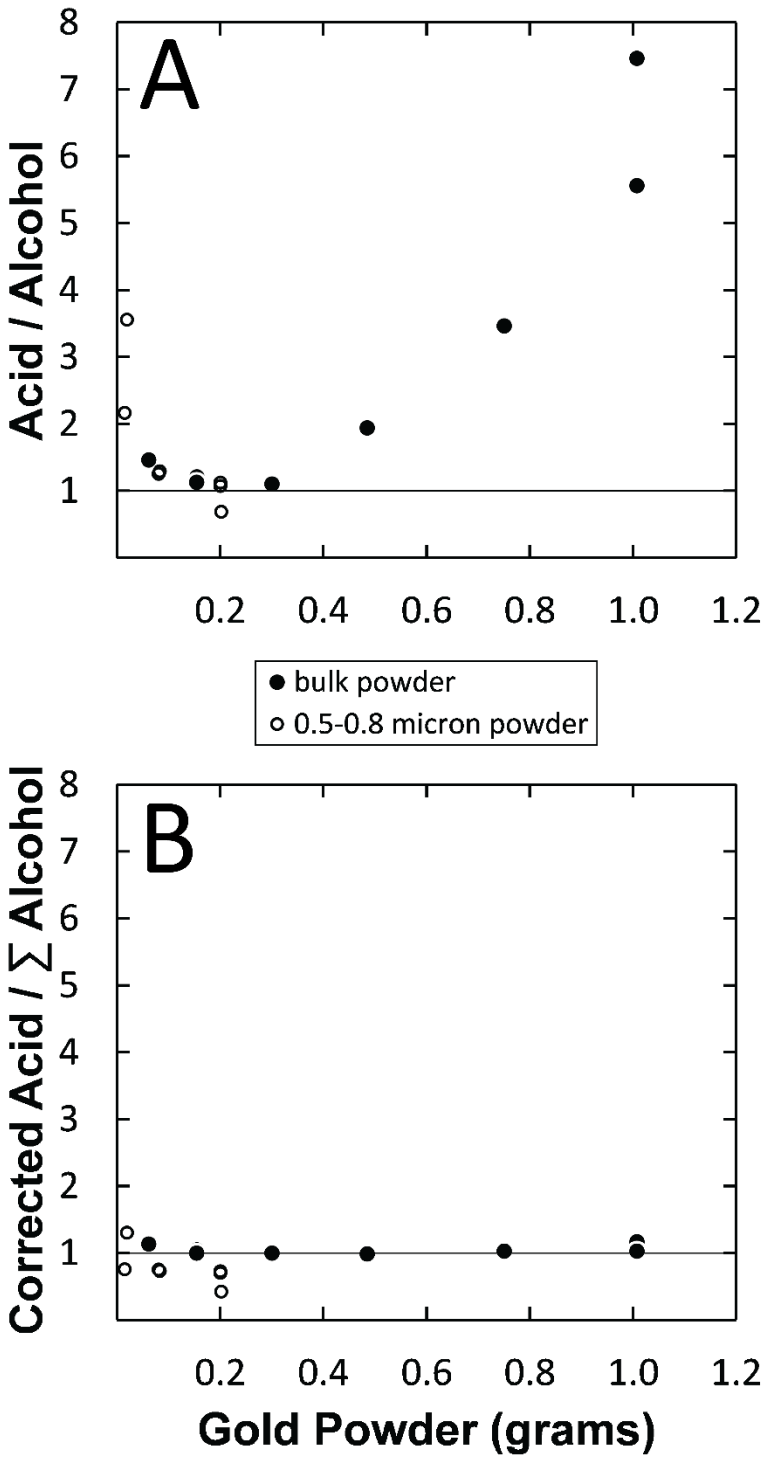

Figure S7. A) Ratio of benzoic acid to benzyl alcohol observed in experiments starting with benzaldehyde relative to the amount of larger bulk (filled circles) or smaller 0.5-0.8 micron (open circles) gold powder present. B) The same ratios corrected by assuming benzyl alcohol disproportionation is the source of toluene (*i.e.*, total alcohol = benzyl alcohol + 2 * toluene) and also corrected for the small amount of benzoic acid putatively obtained via oxidation.

SEM of new small 0.5-0.8 micron gold powder

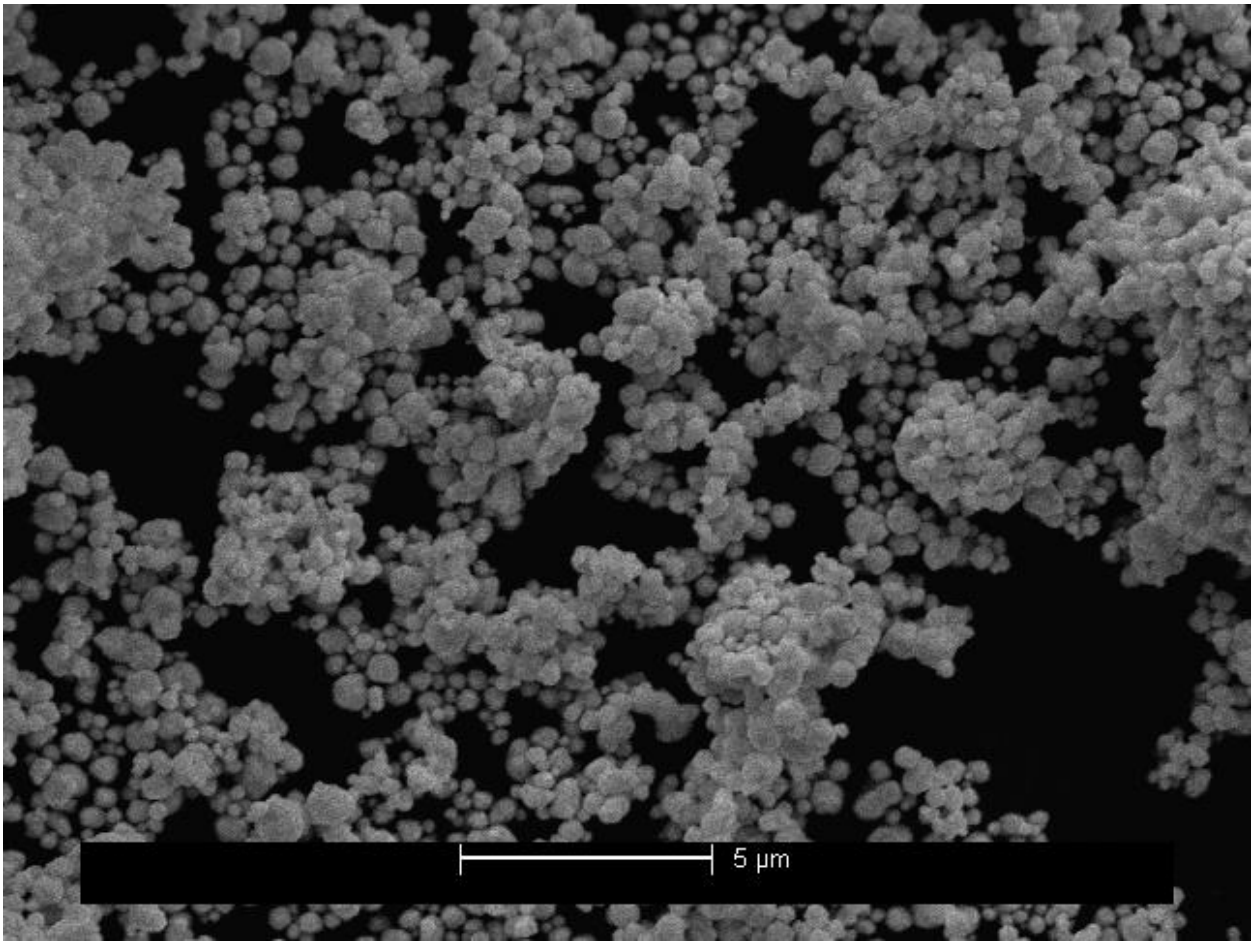

Figure S8. New small 0.5-0.8 micron gold powder.

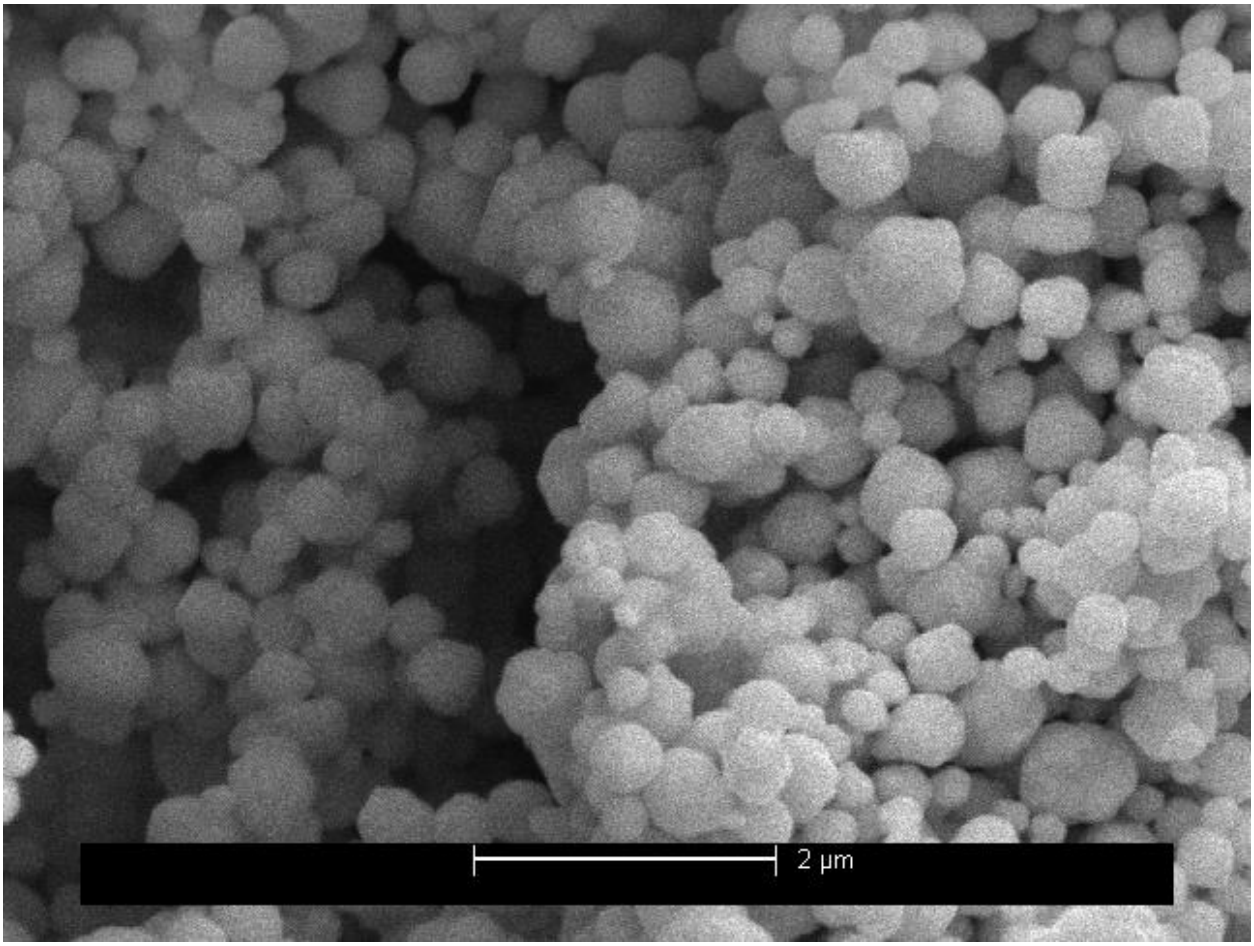

Figure S9. New small 0.5-0.8 micron gold powder.

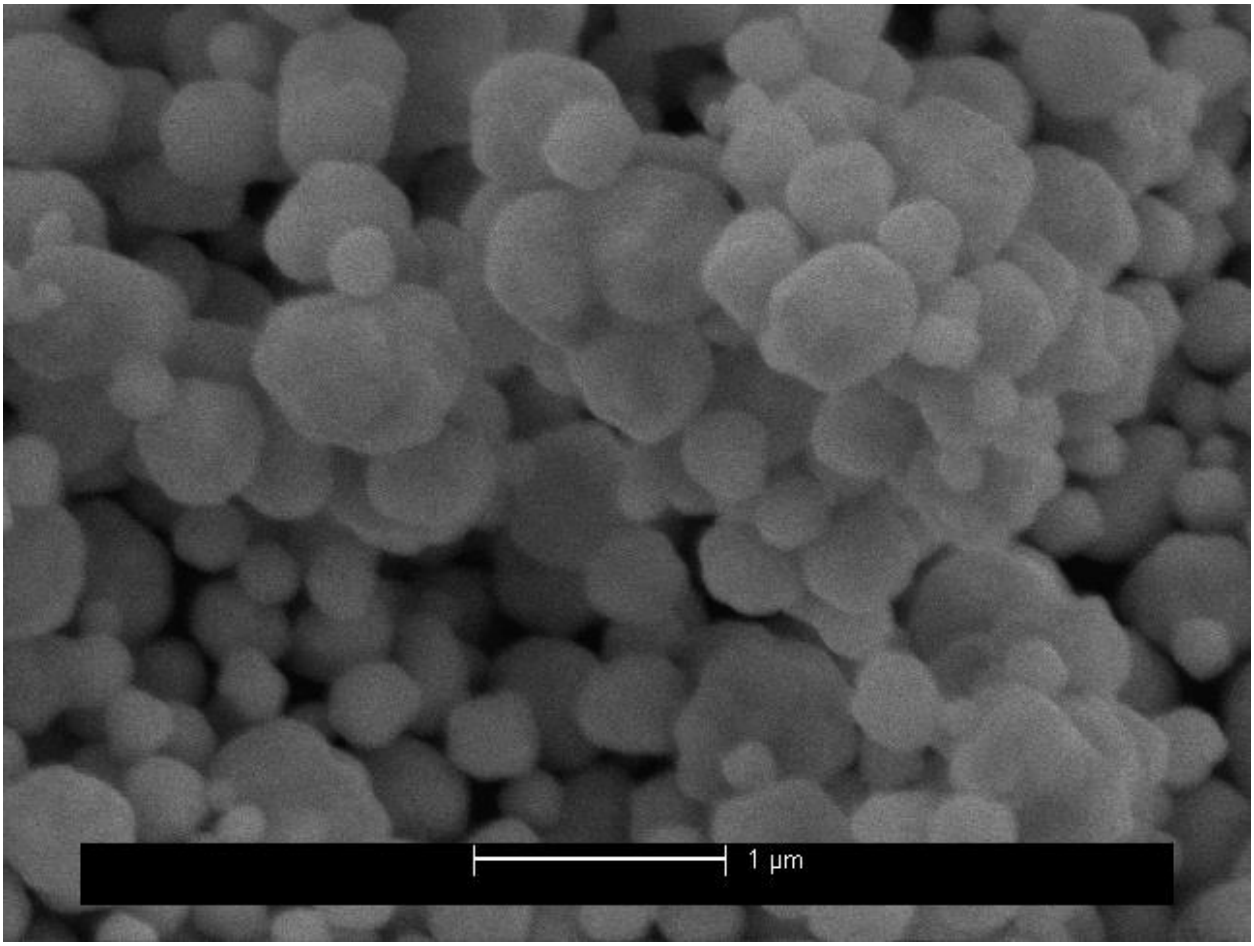

Figure S10. New small 0.5-0.8 micron gold powder.

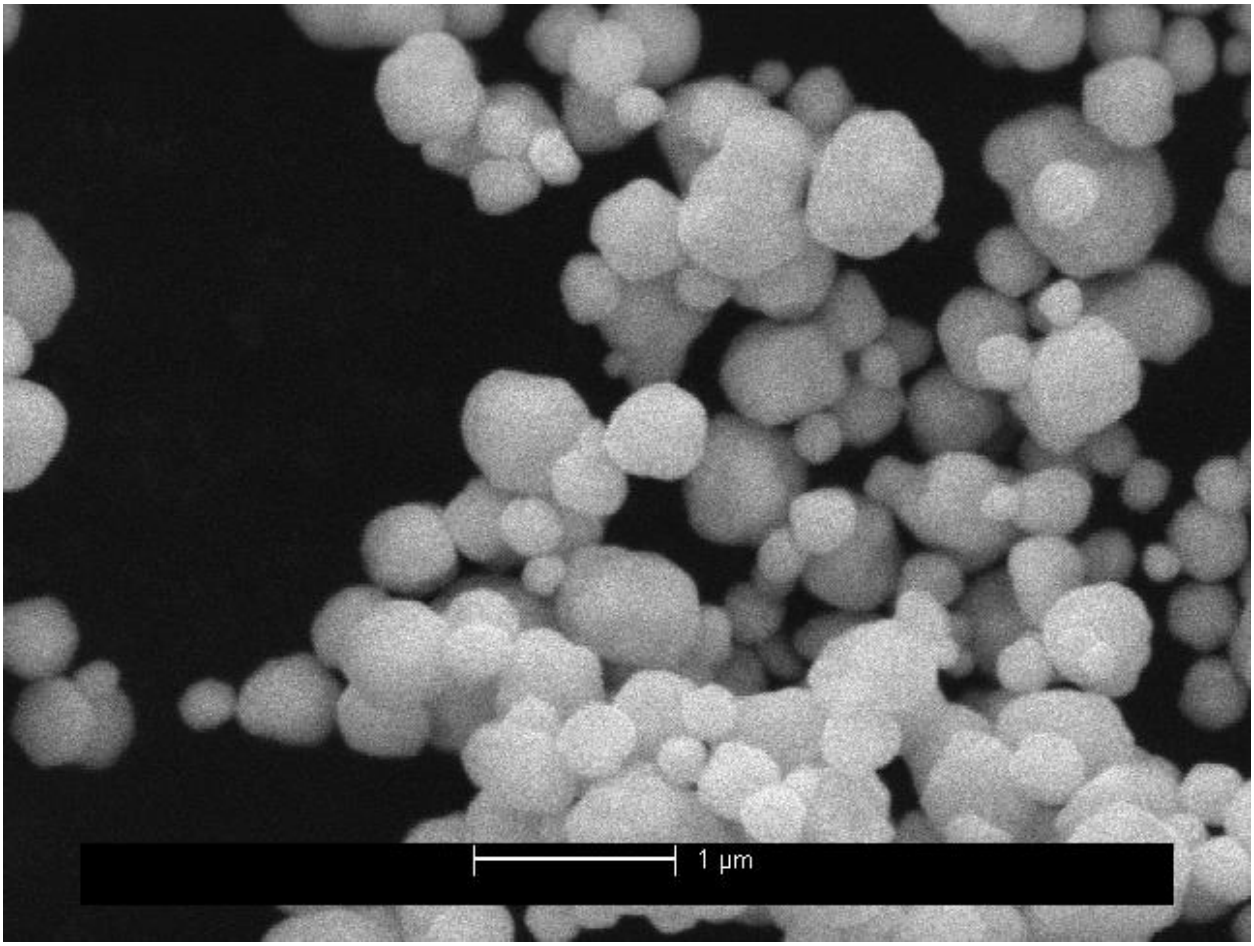

Figure S11. New small 0.5-0.8 micron gold powder.

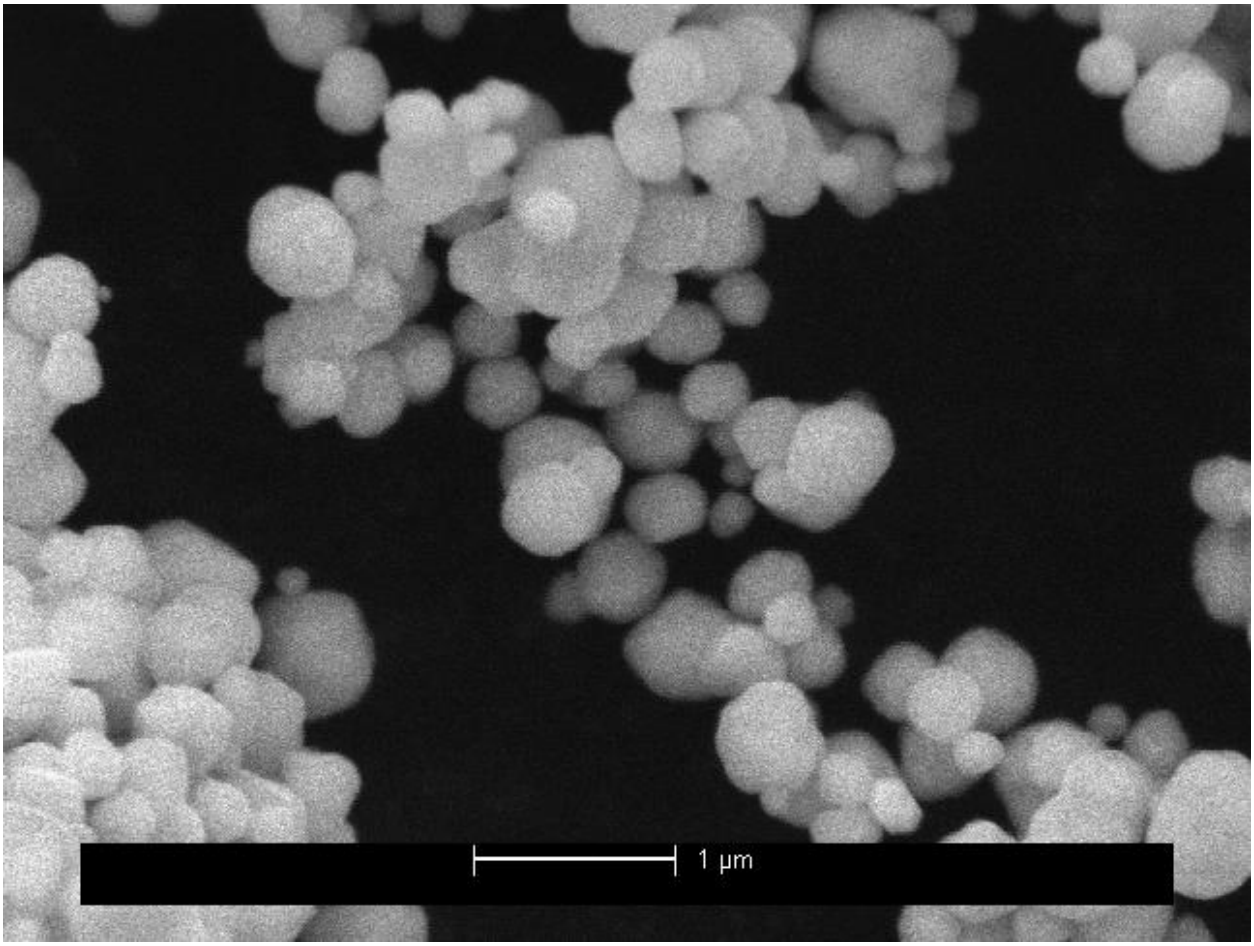

Figure S12. New small 0.5-0.8 micron gold powder.

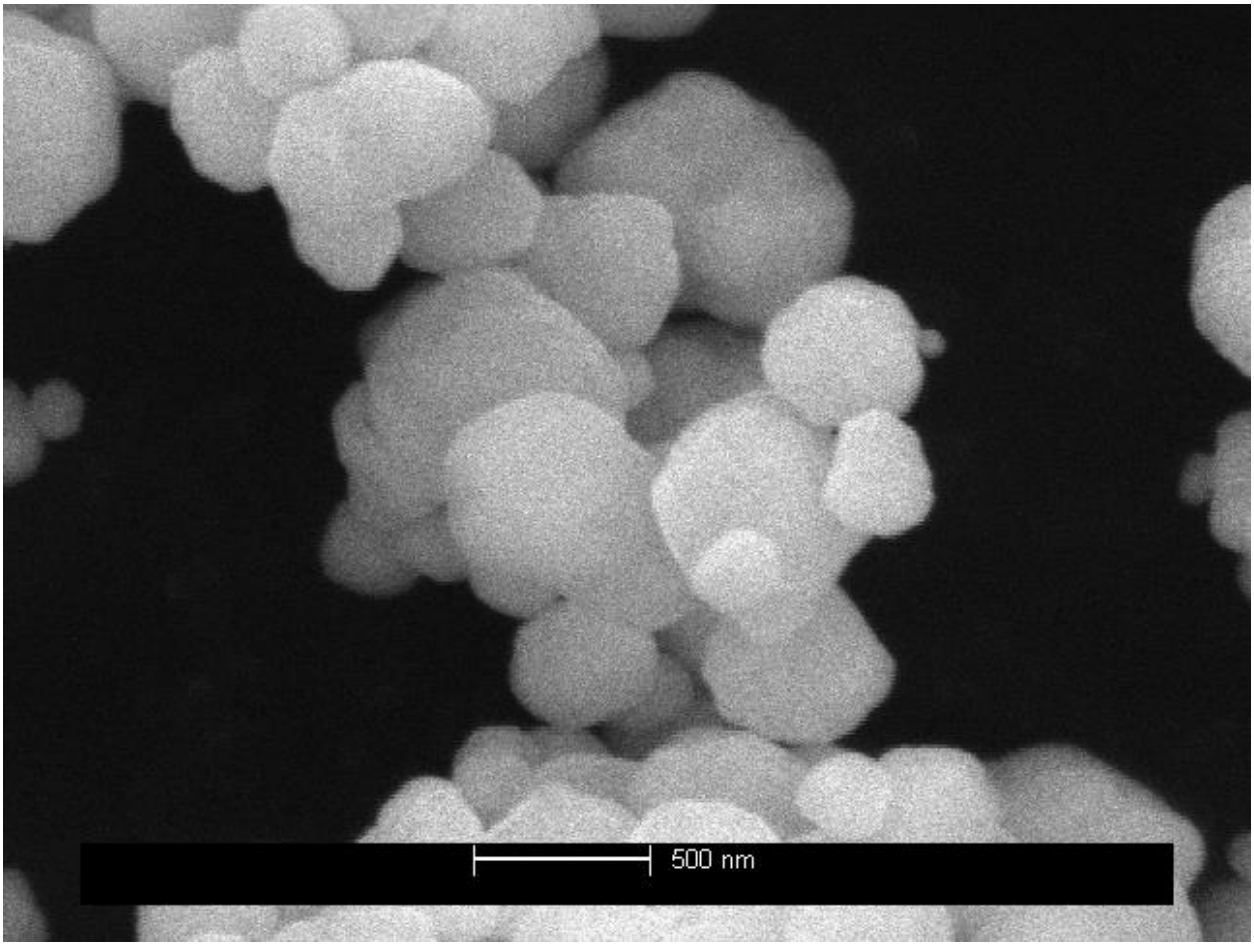

Figure S13. New small 0.5-0.8 micron gold powder.

SEM of used small 0.5-0.8 micron gold powder

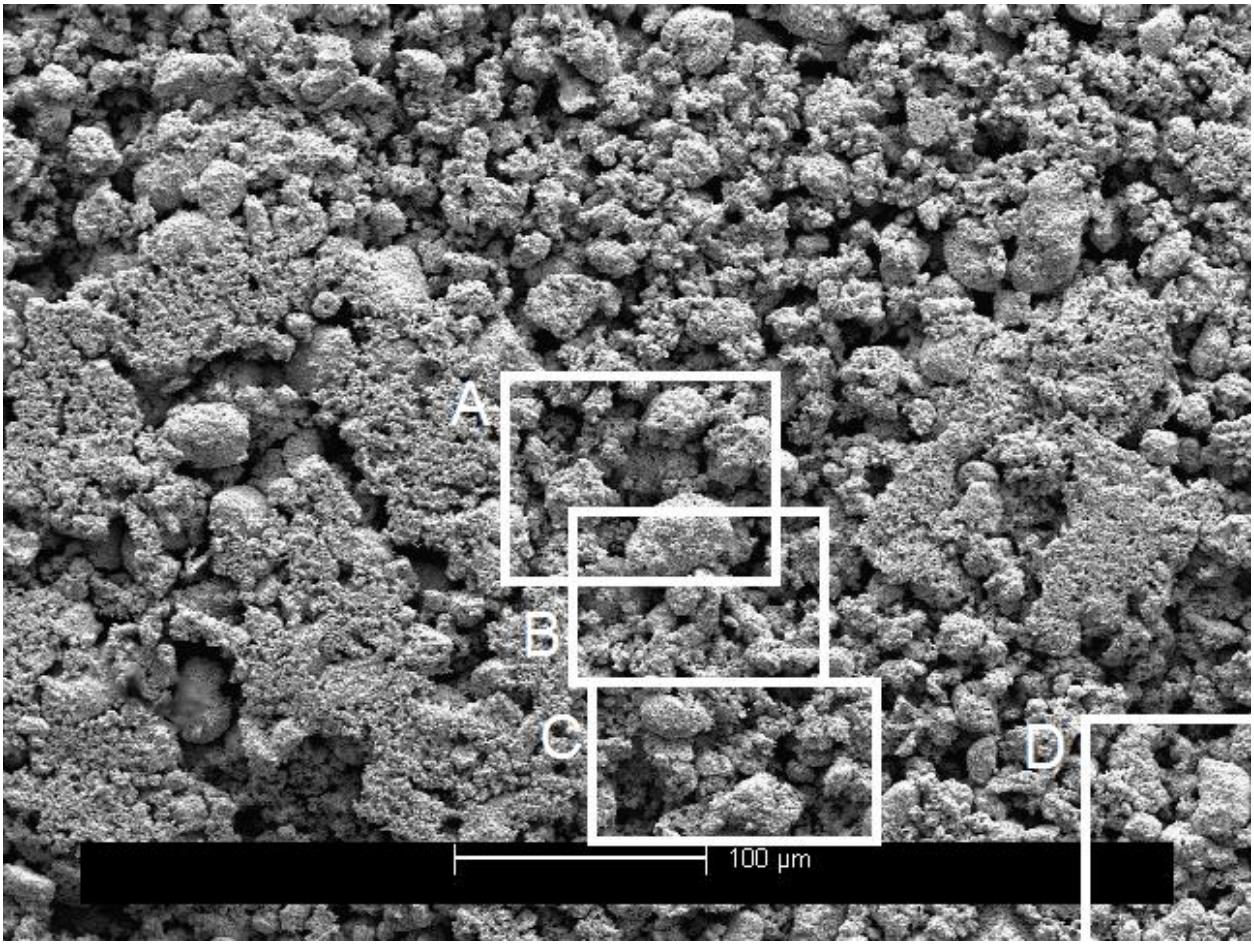

Figure S14. Used small 0.5-0.8 micron gold powder (broad view with regions indicated).

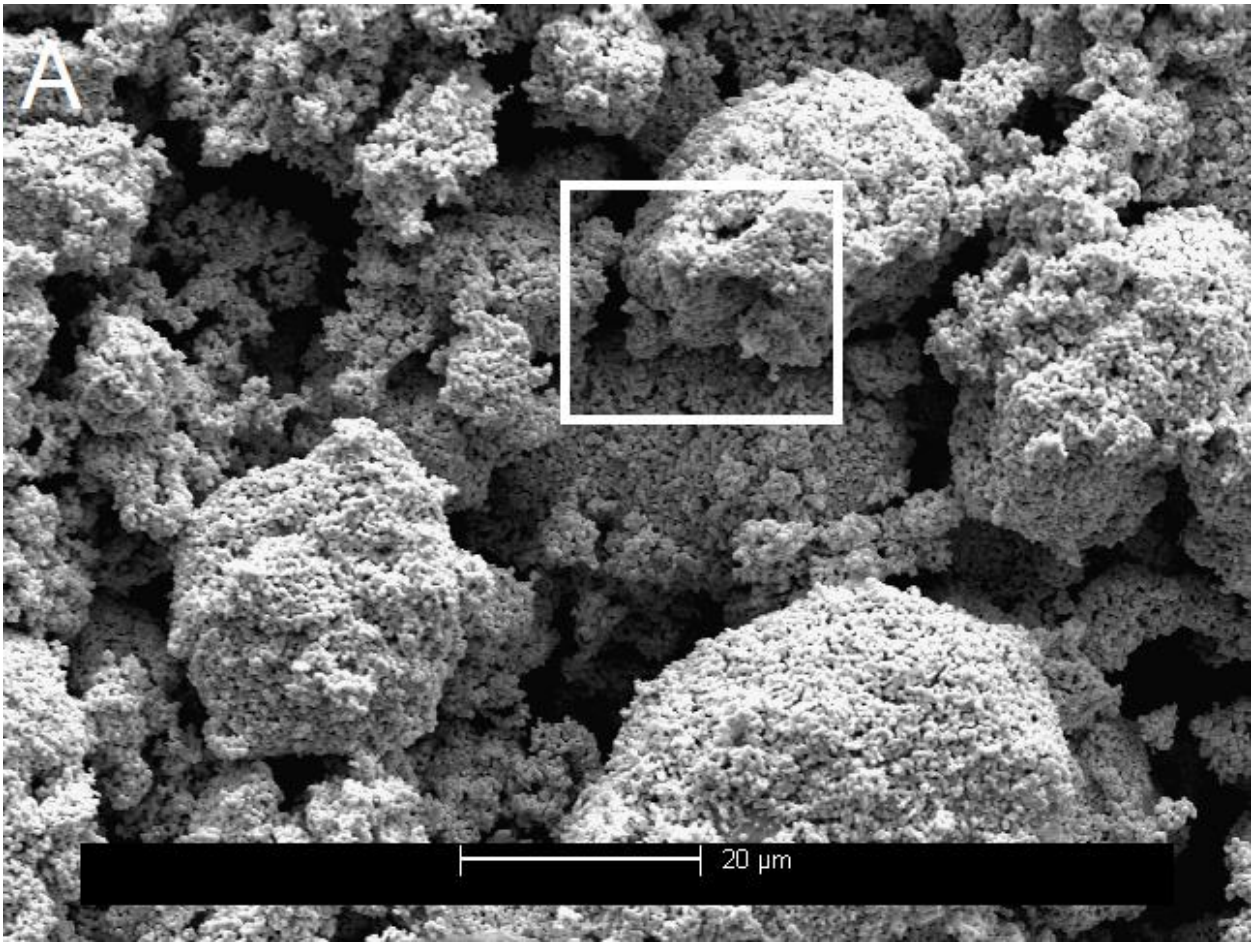

Figure S15. Used small 0.5-0.8 micron gold powder (region A in Figure S14).

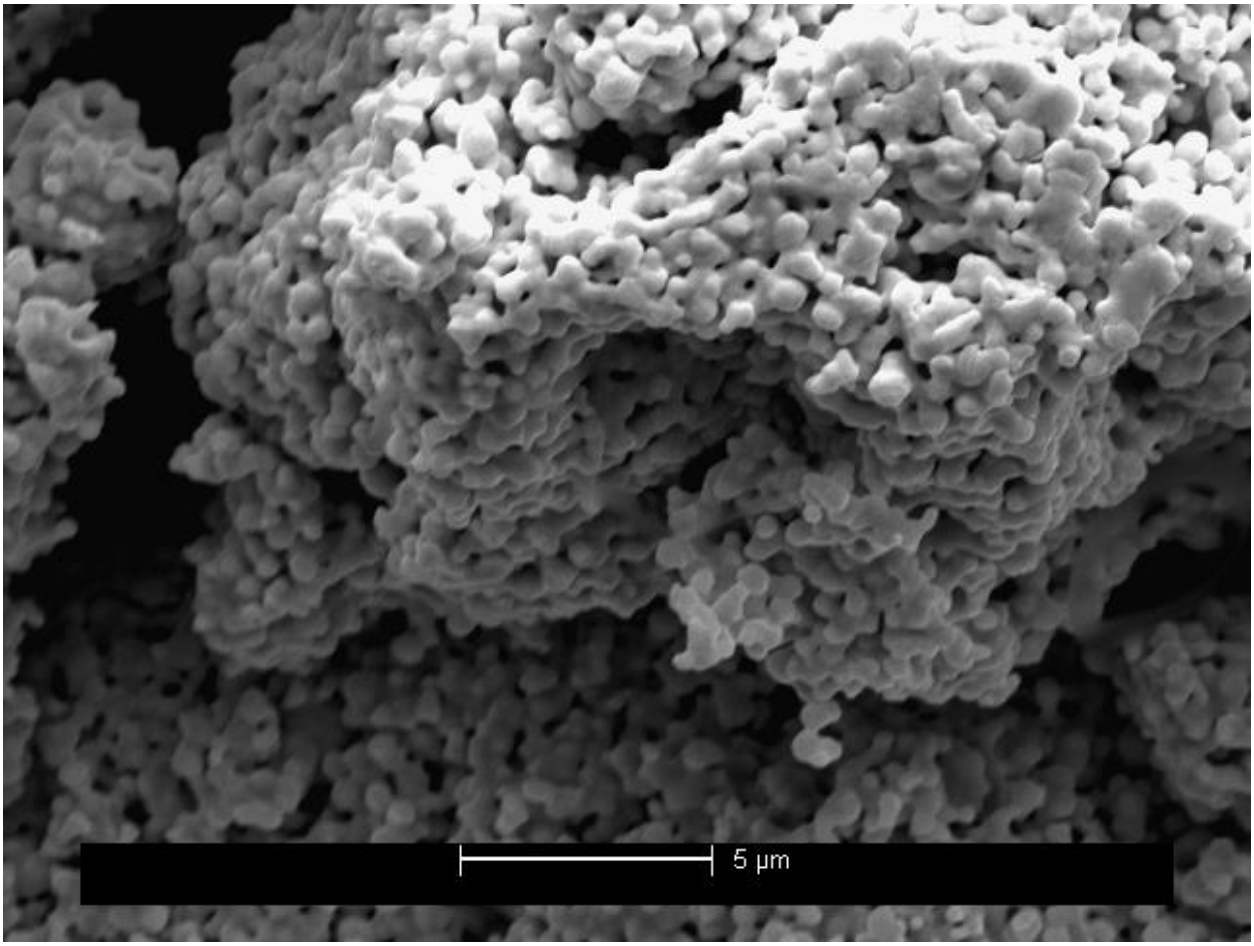

Figure S16. Used small 0.5-0.8 micron gold powder (boxed area in Figure S15).

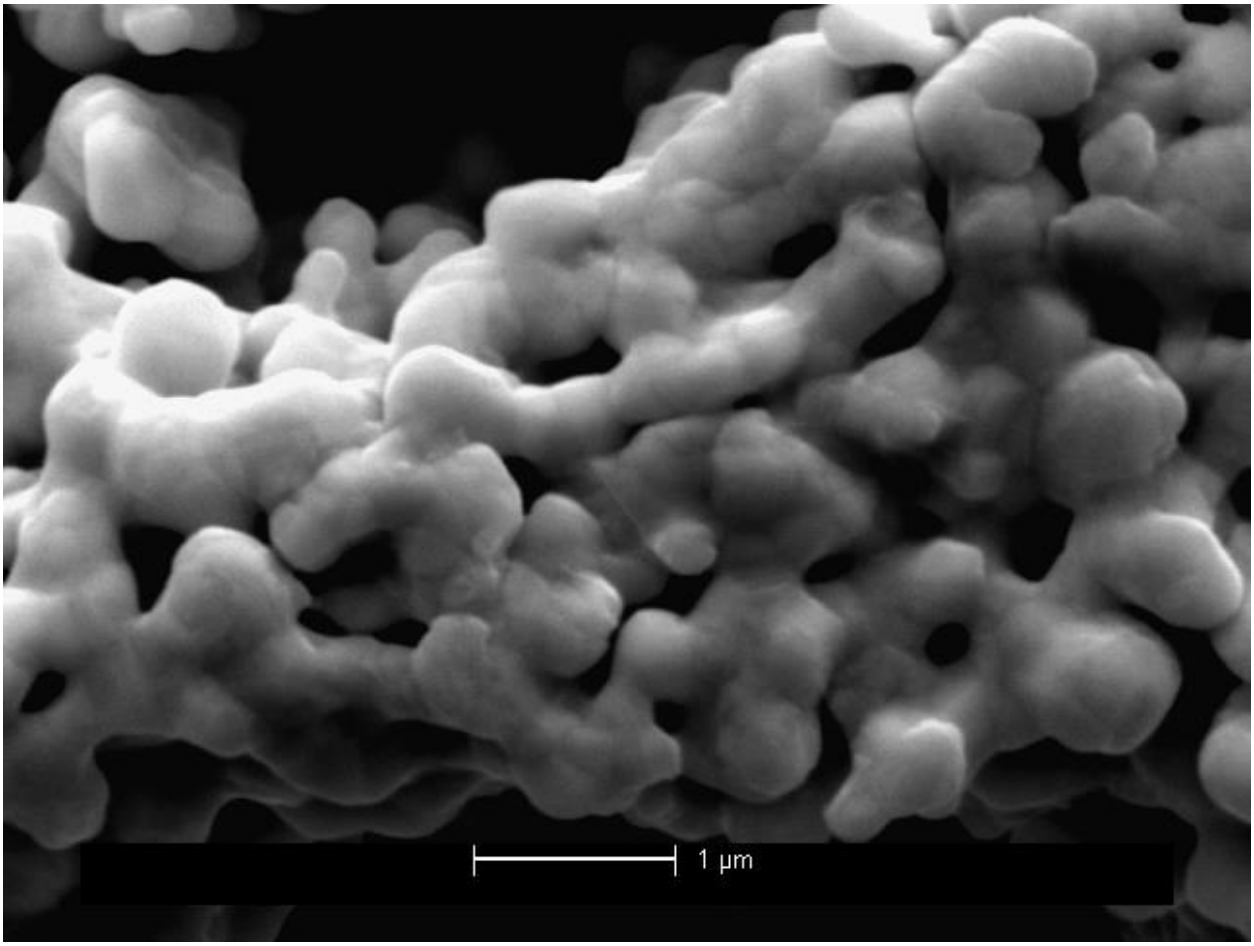

Figure S17. Used small 0.5-0.8 micron gold powder (region A in Figure S14, zoomed in).

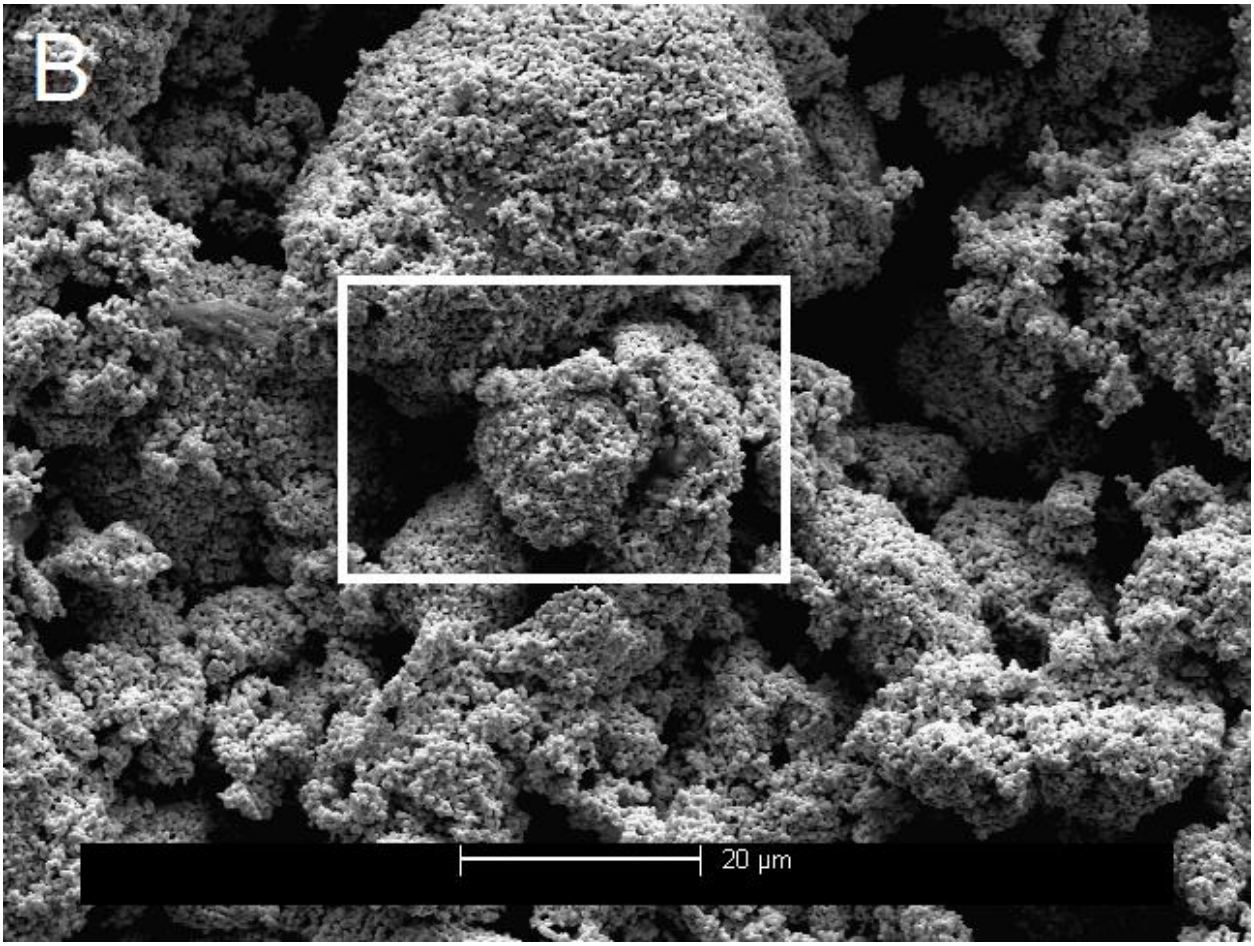

Figure S18. Used small 0.5-0.8 micron gold powder (region B in Figure S14).

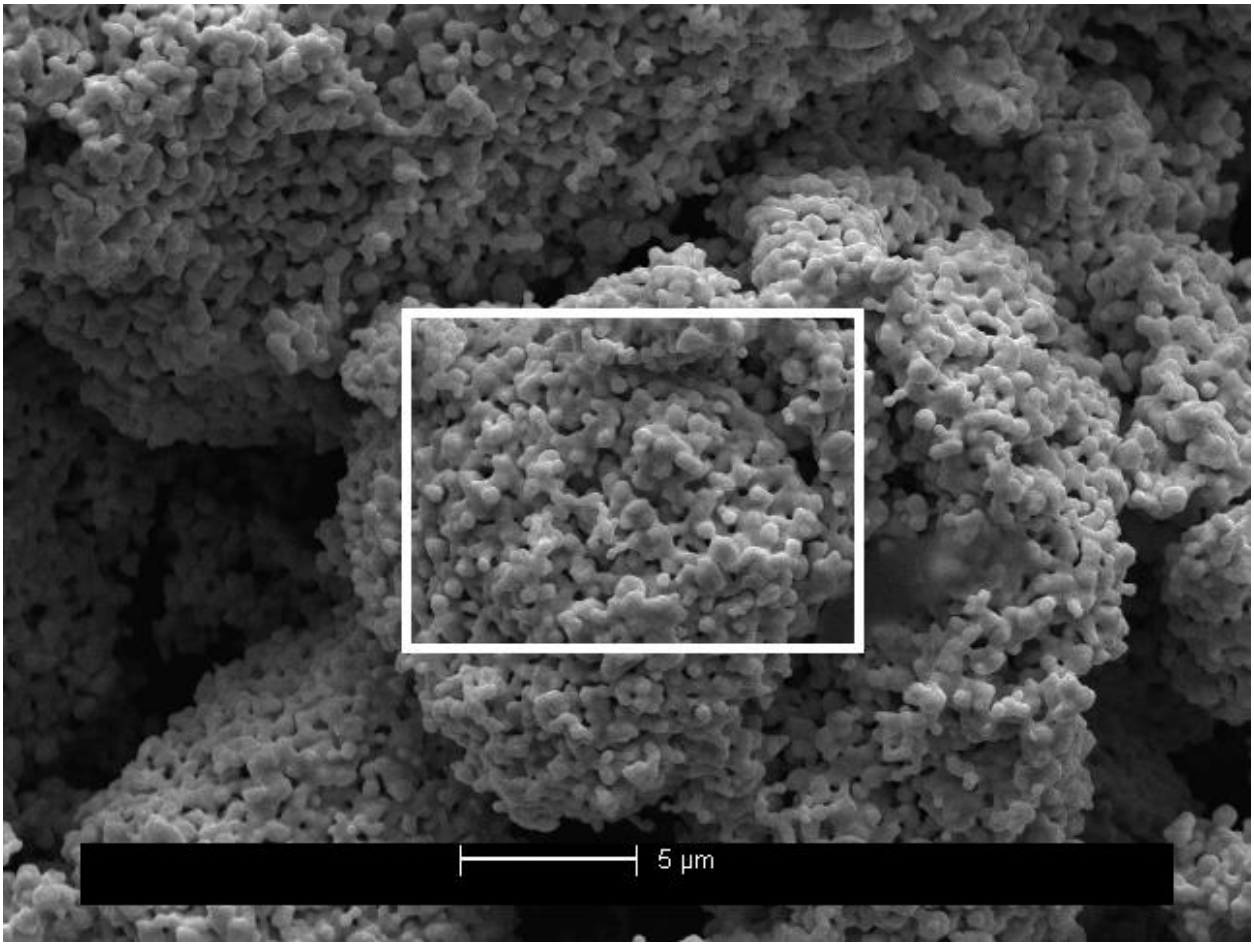

Figure S19. Used small 0.5-0.8 micron gold powder (boxed area in Figure S18).

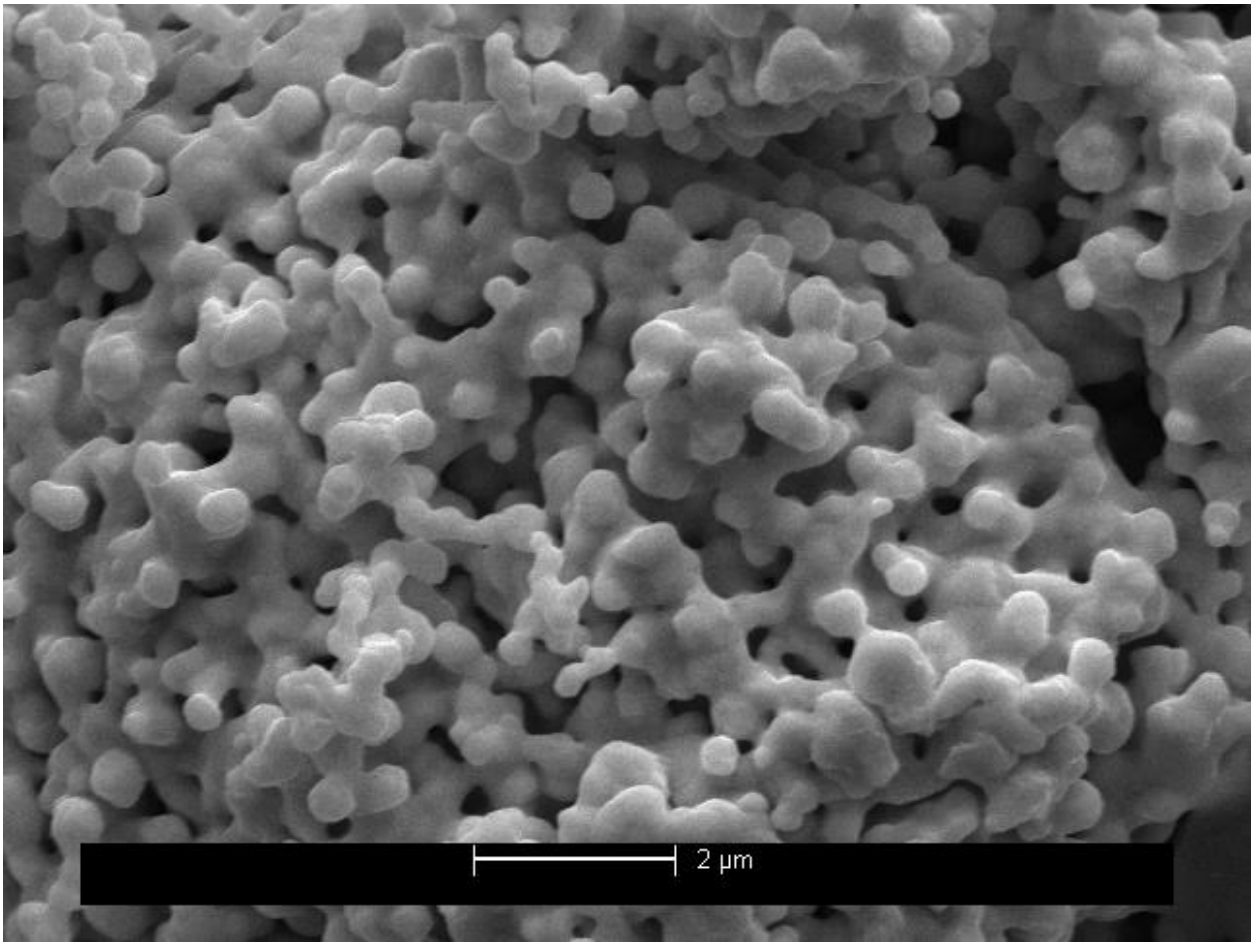

Figure S20. Used small 0.5-0.8 micron gold powder (boxed area in Figure S19).

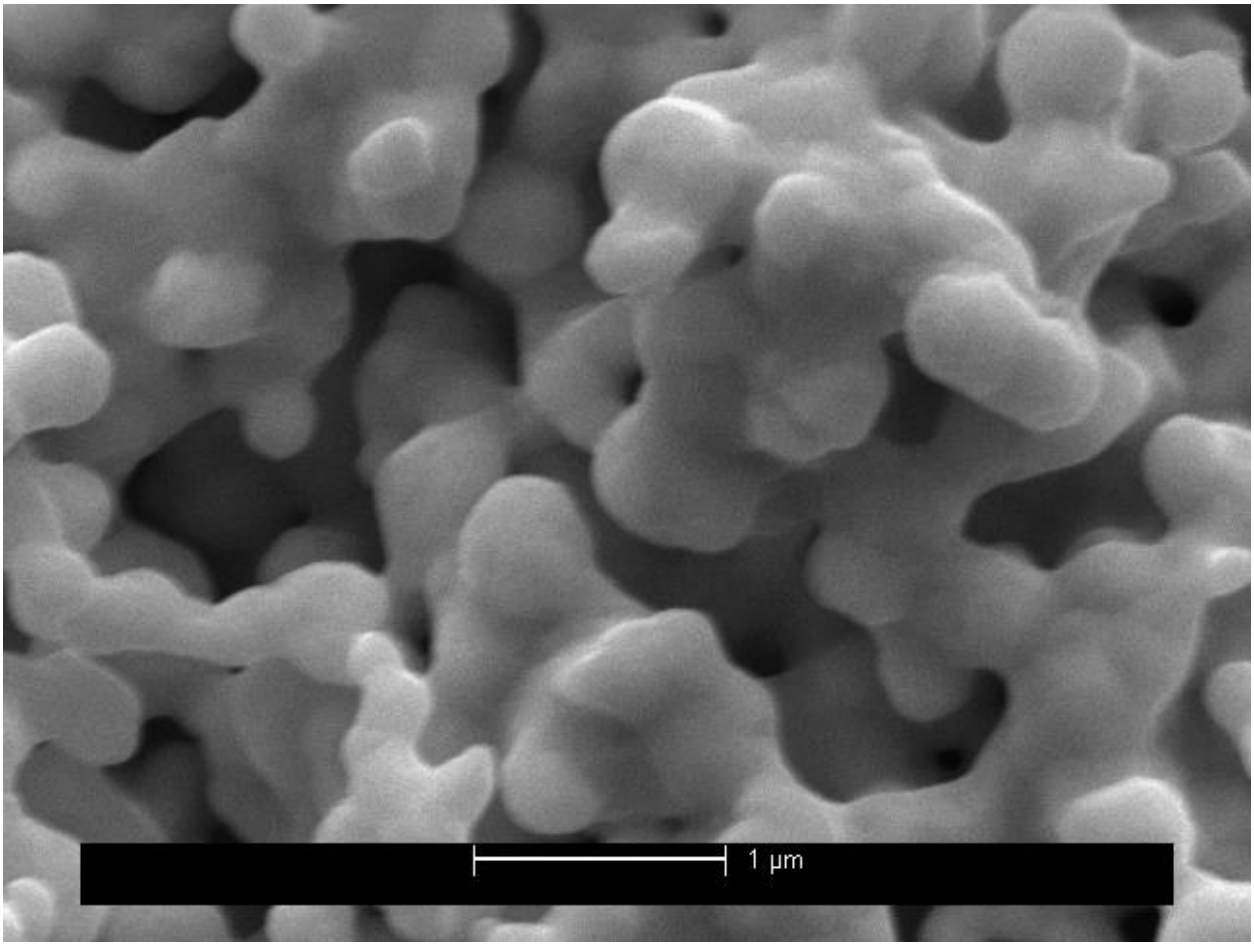

Figure S21. Used small 0.5-0.8 micron gold powder (region B in Figure S14, zoomed in).

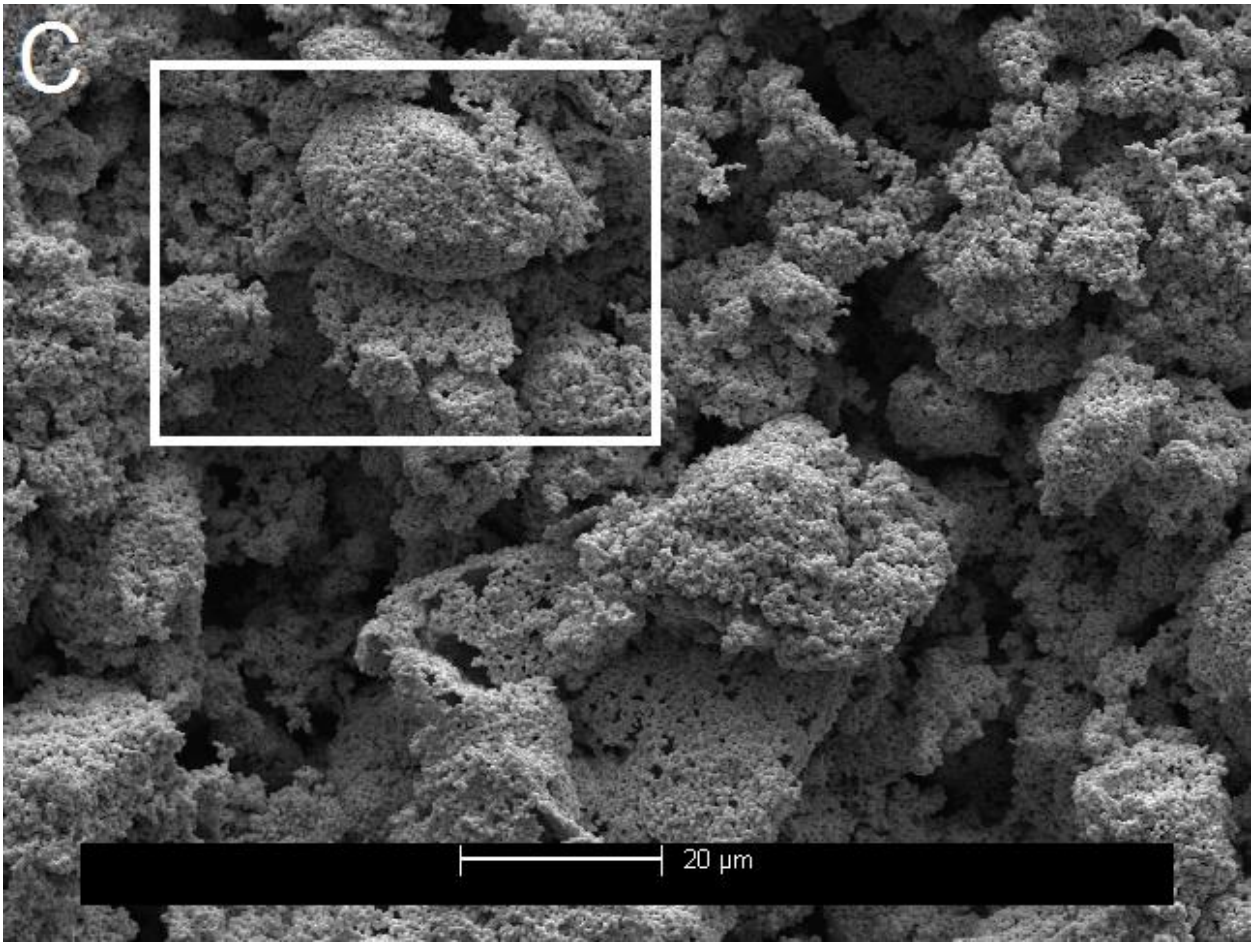

Figure S22. Used small 0.5-0.8 micron gold powder (region C in Figure S14).

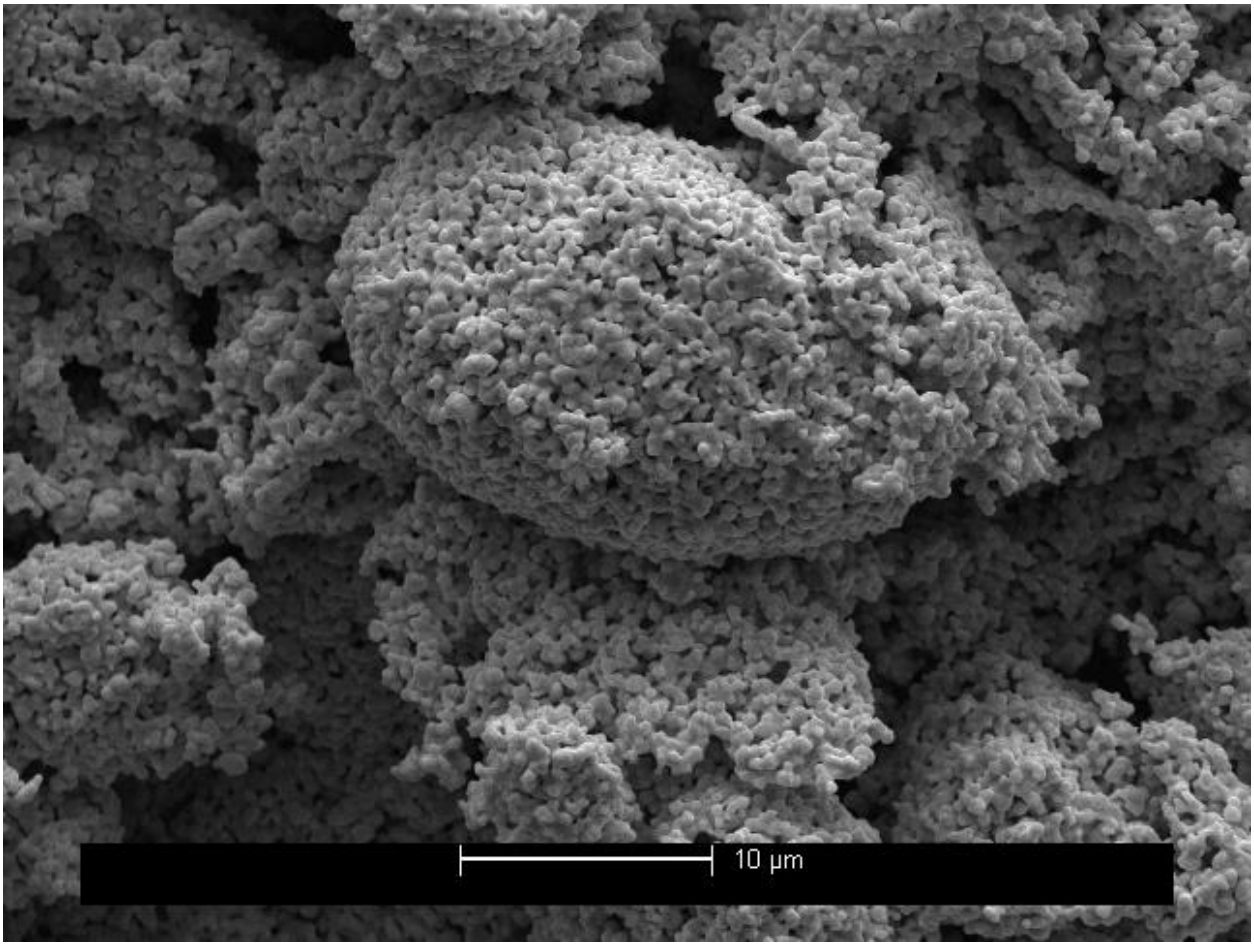

Figure S23. Used small 0.5-0.8 micron gold powder (boxed area in Figure S22).

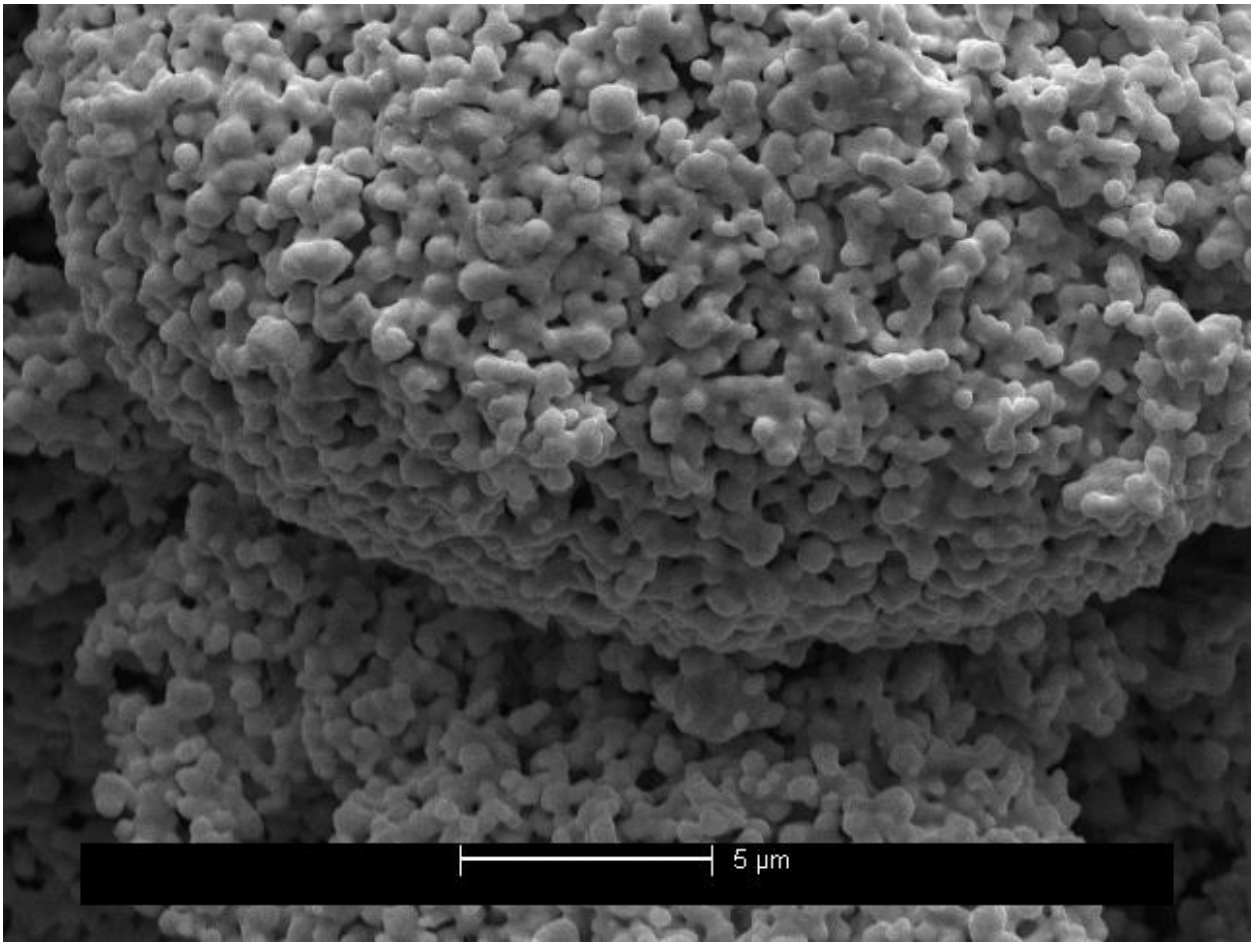

Figure S24. Used small 0.5-0.8 micron gold powder (region C in Figure S14, zoomed in).

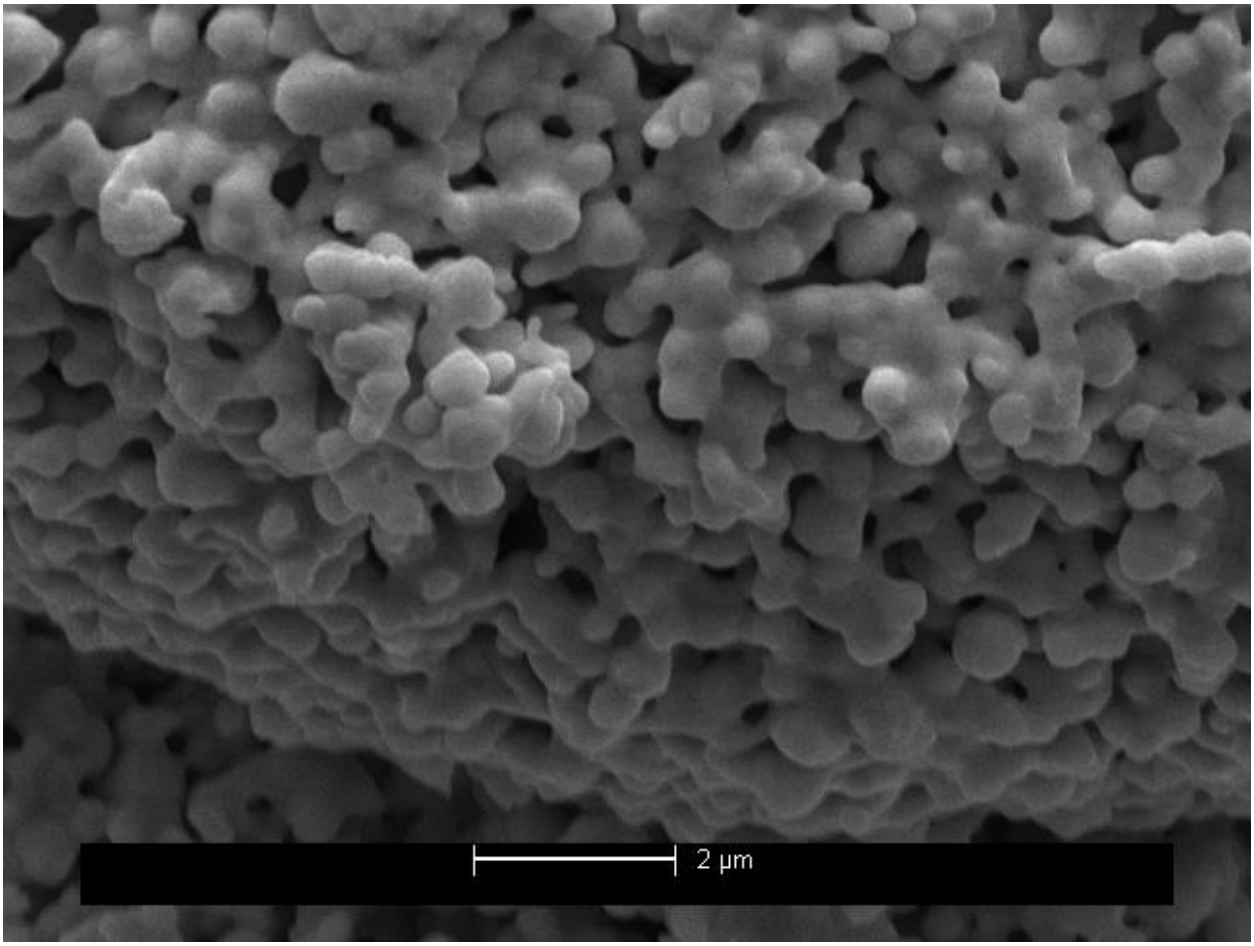

Figure S25. Used small 0.5-0.8 micron gold powder (region C in Figure S14, zoomed in).

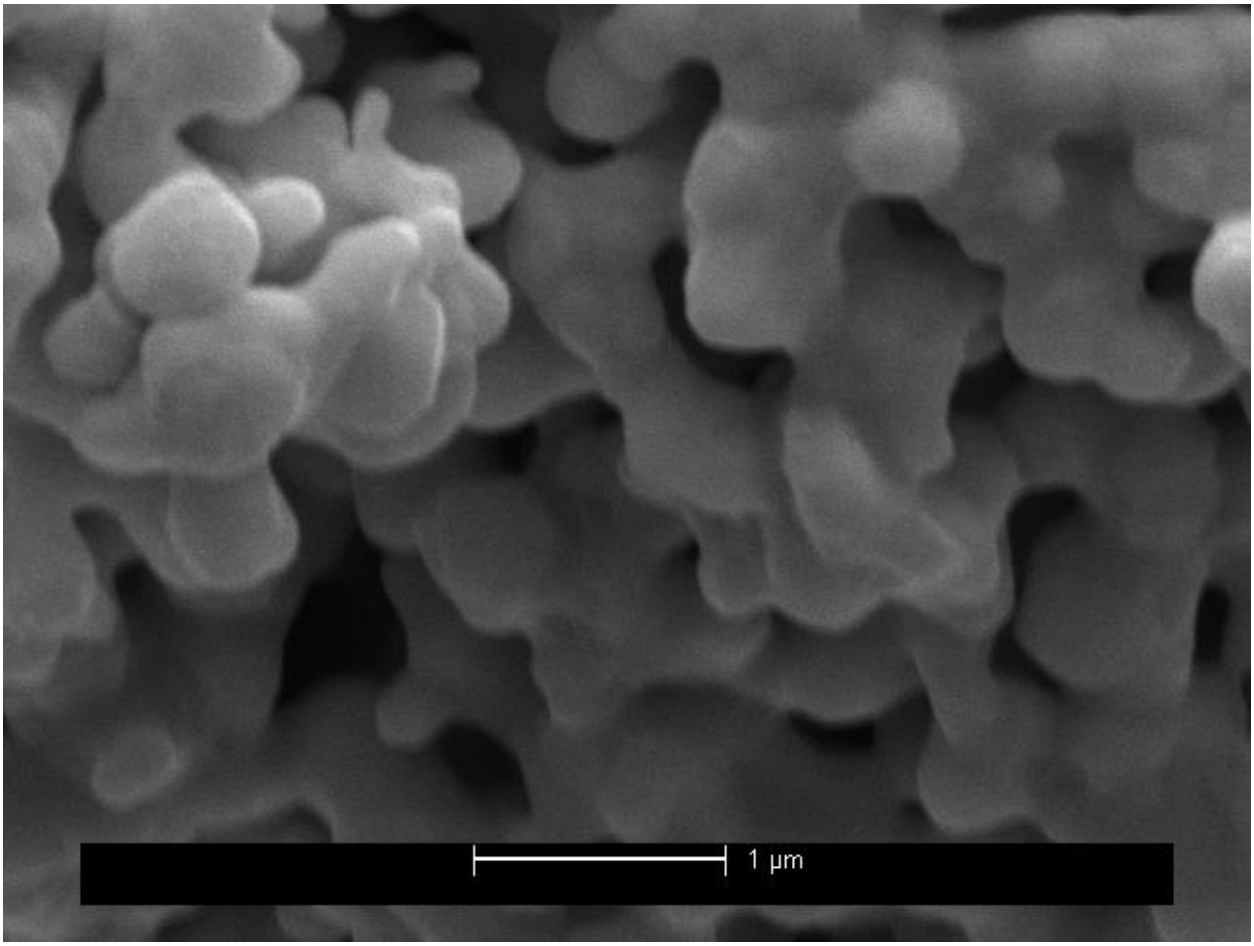

Figure S26. Used small 0.5-0.8 micron gold powder (region C in Figure S14, zoomed in).

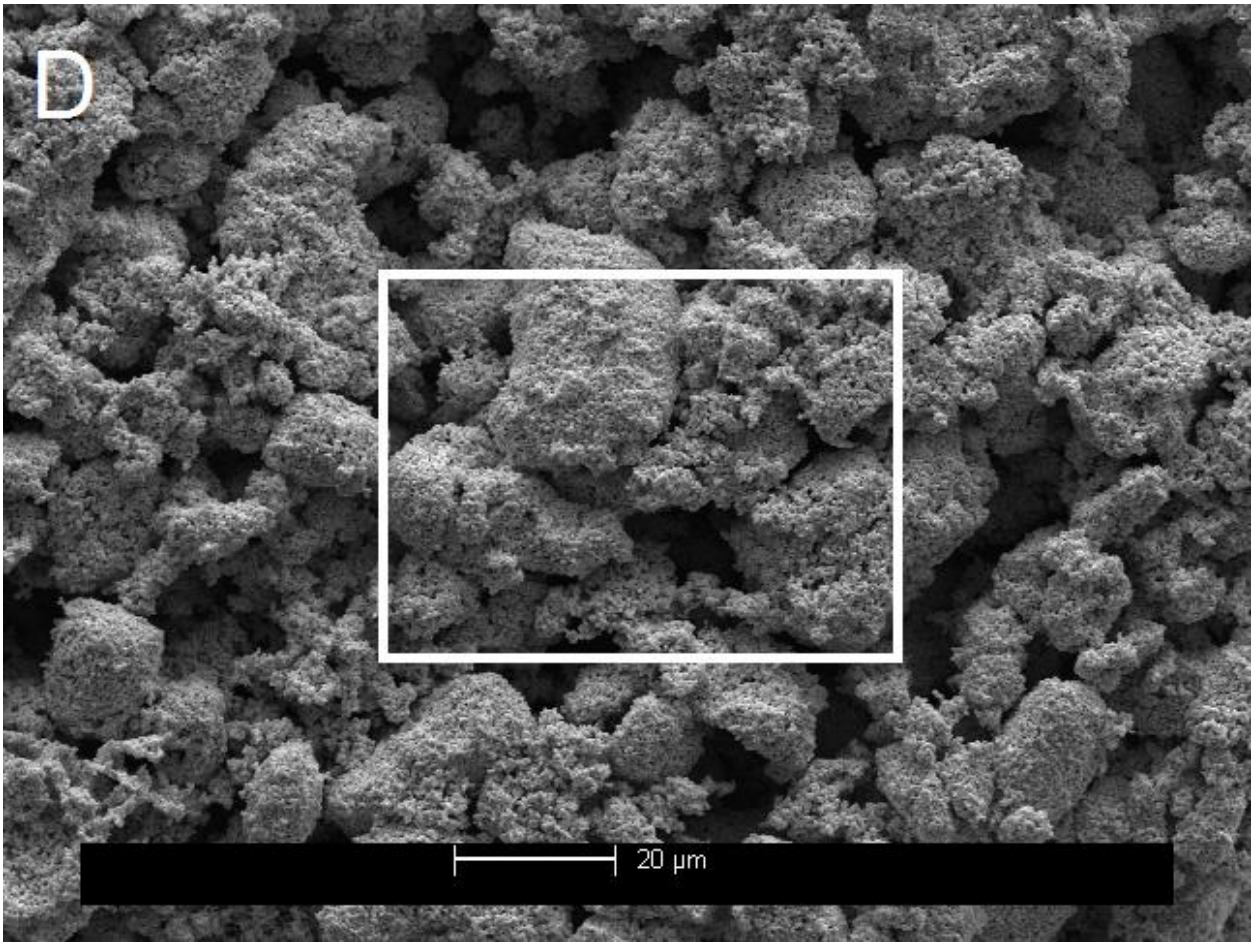

Figure S27. Used small 0.5-0.8 micron gold powder (region D, not shown in Figure S14).

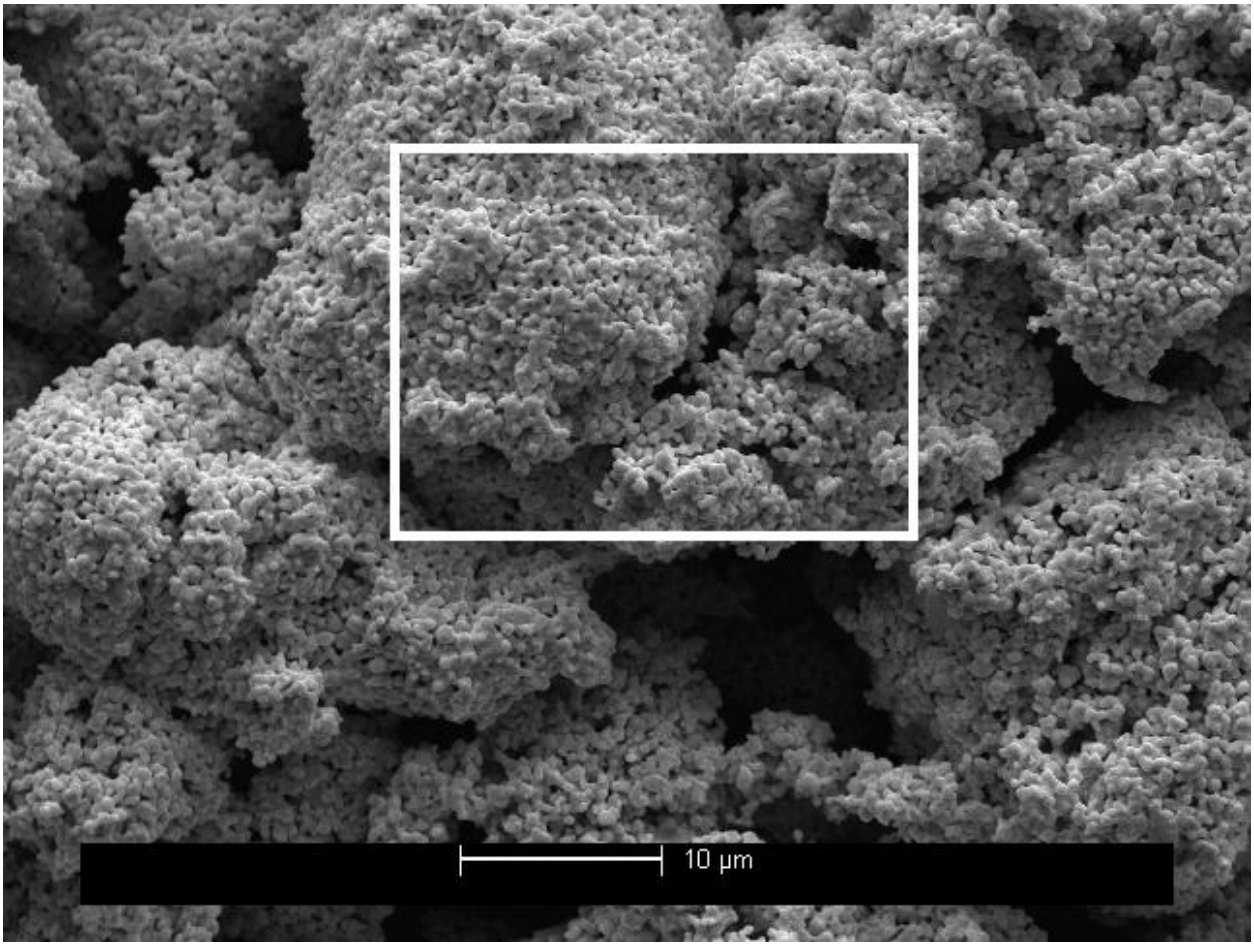

Figure S28. Used small 0.5-0.8 micron gold powder (boxed area in Figure S27).

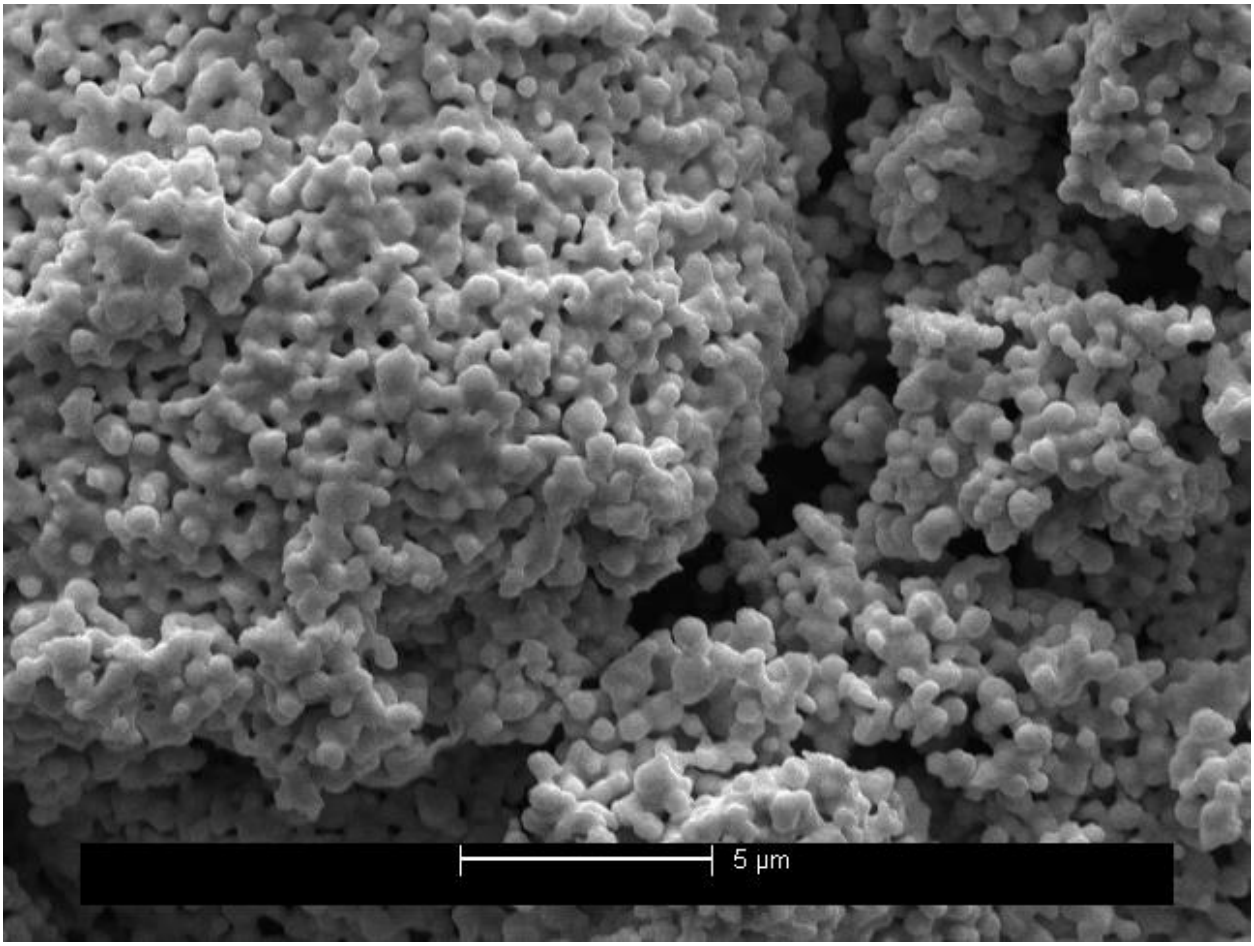

Figure S29. Used small 0.5-0.8 micron gold powder (boxed area in Figure S27).

SEM of new medium 5.5-9.0 micron gold powder

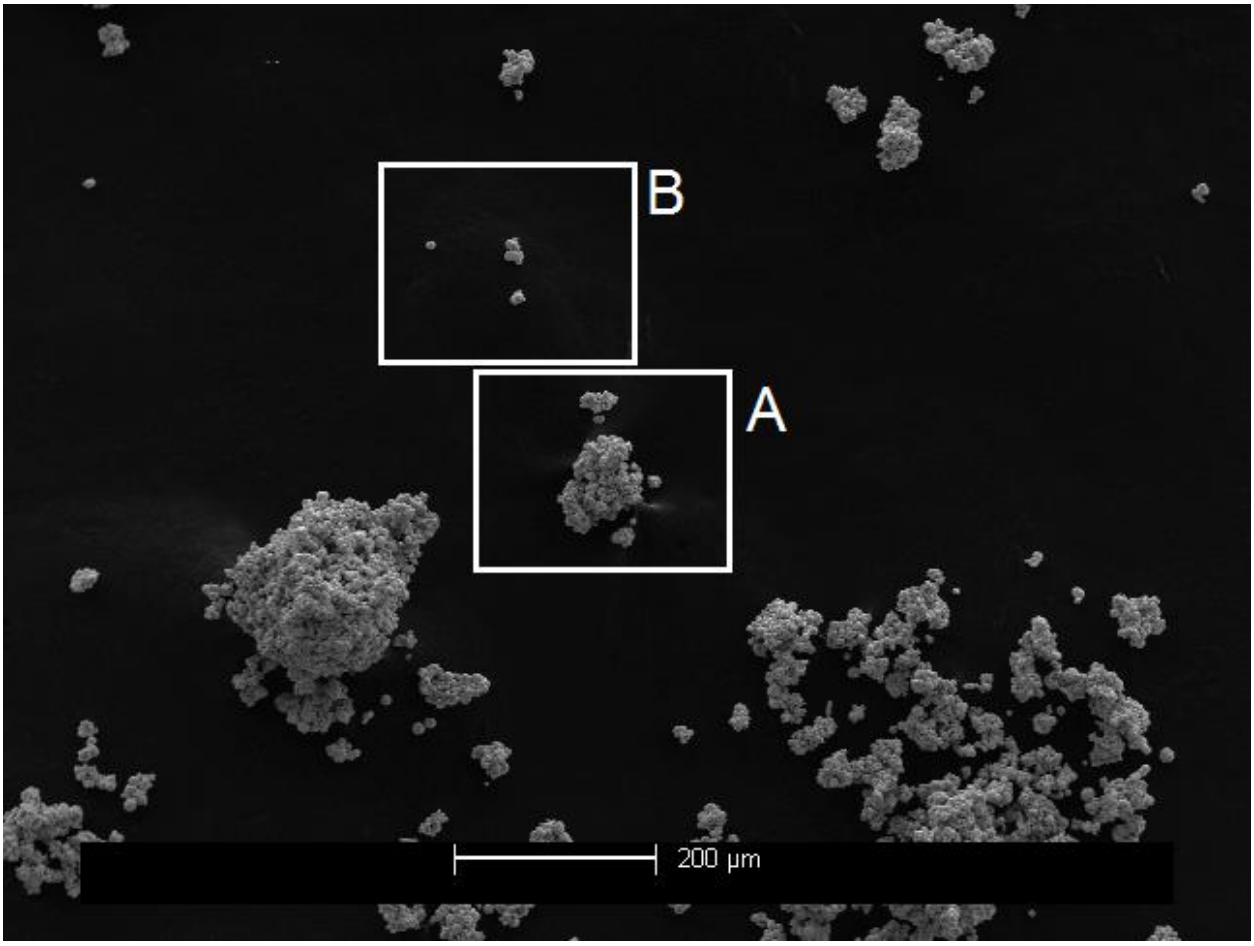

Figure S30. New medium 5.5-9.0 micron gold powder (broad view with regions indicated).

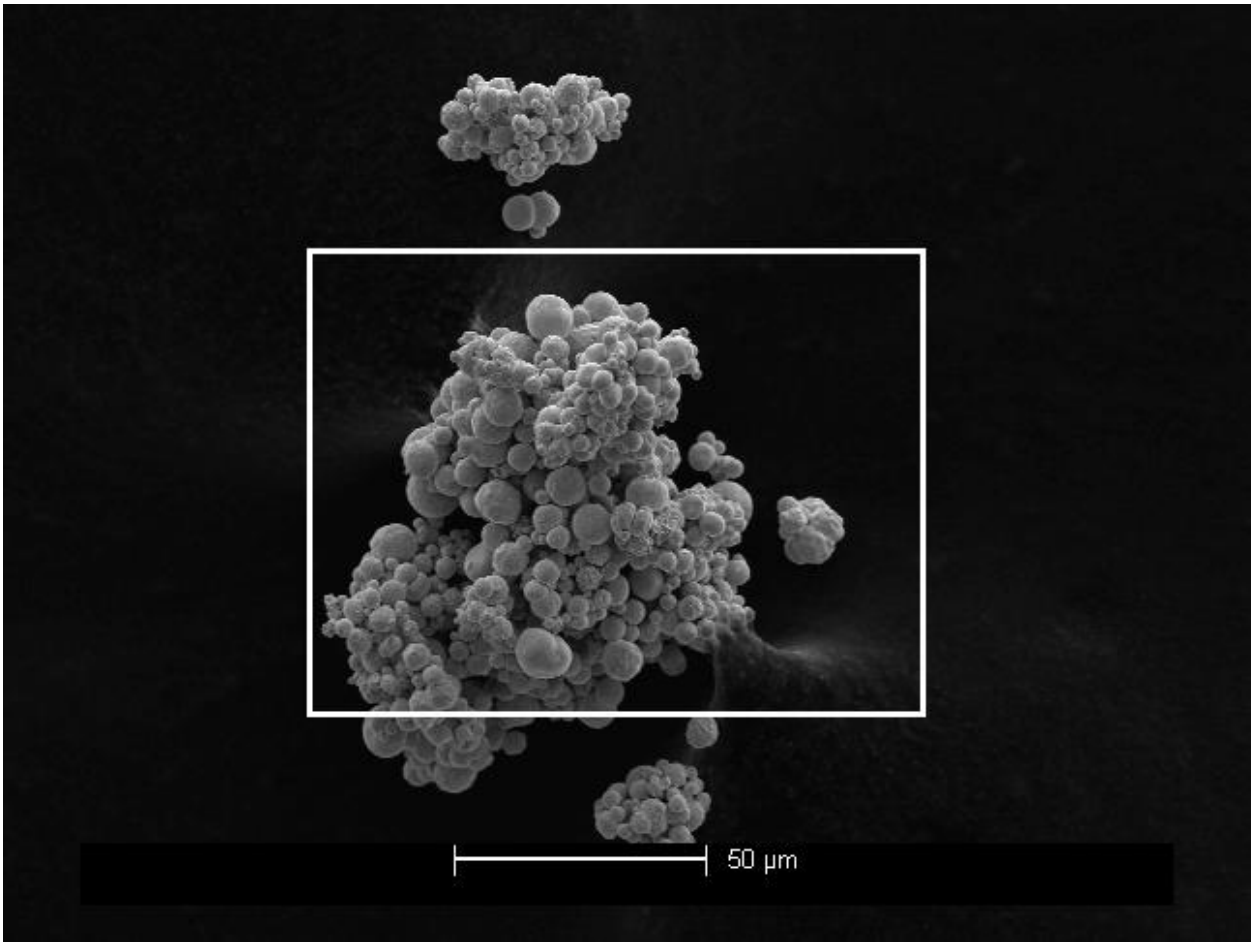

Figure S31. New medium 5.5-9.0 micron gold powder (region A in Figure S30).

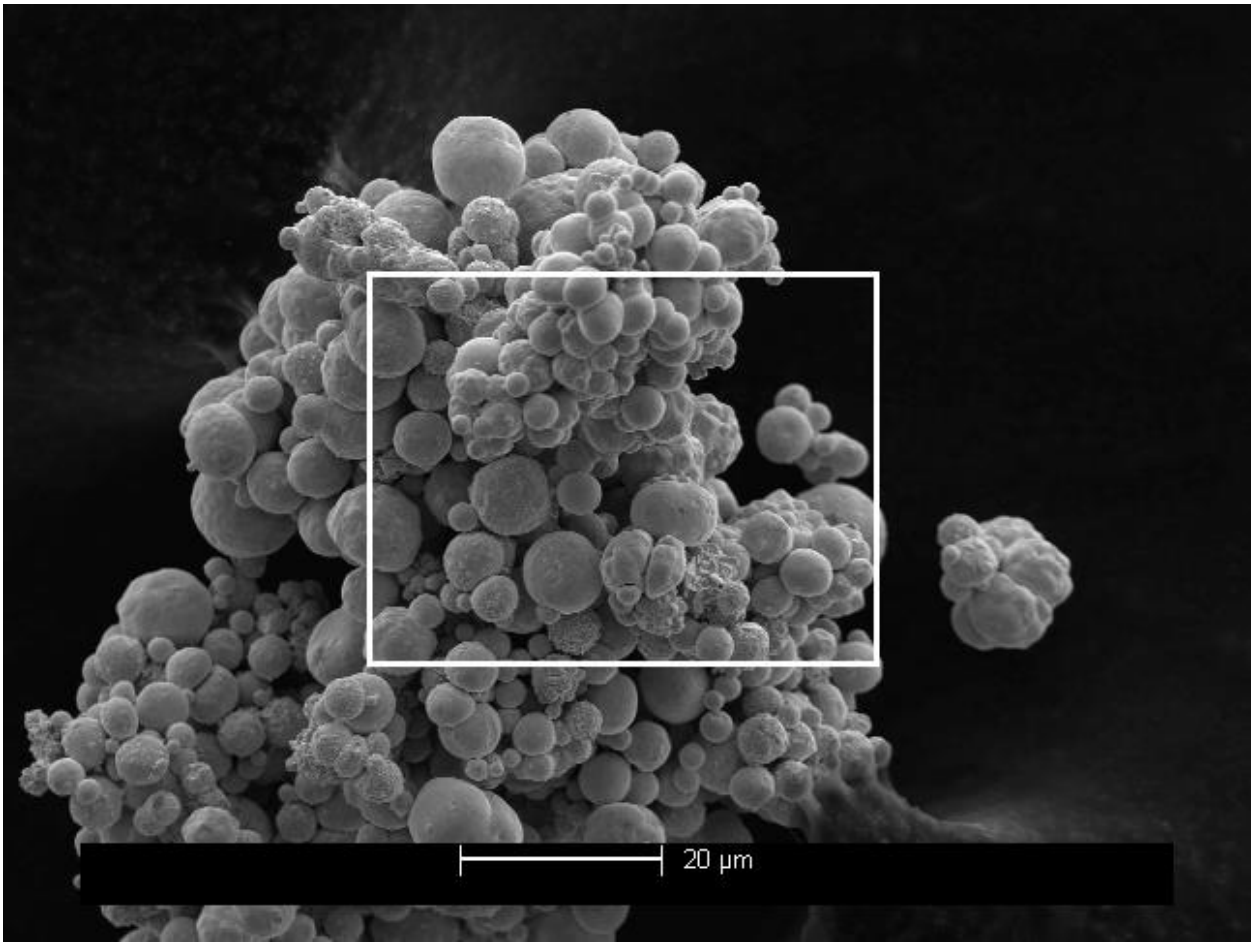

Figure S32. New medium 5.5-9.0 micron gold powder (boxed area in Figure S31).

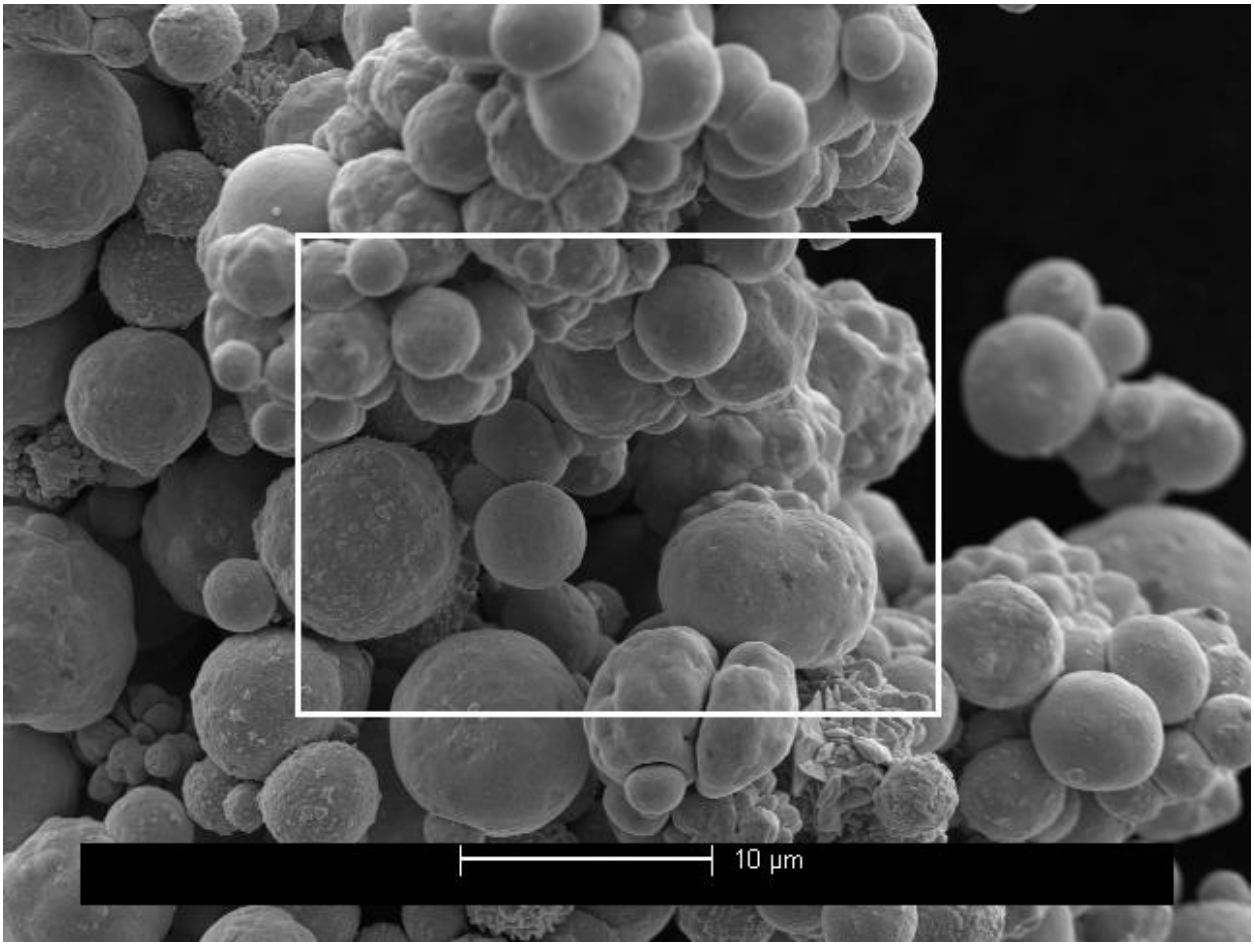

Figure S33. New medium 5.5-9.0 micron gold powder (boxed area in Figure S32).

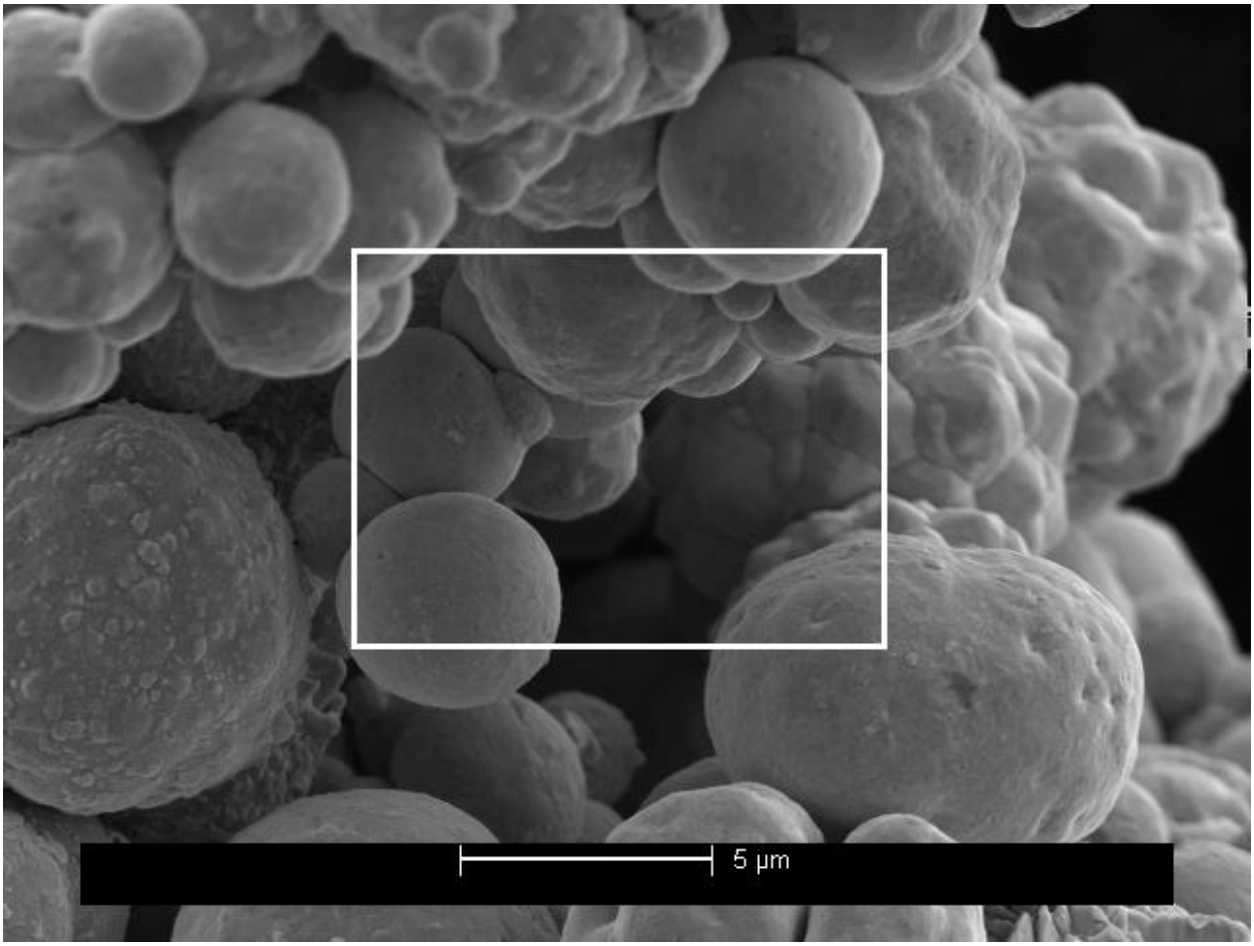

Figure S34. New medium 5.5-9.0 micron gold powder (boxed area in Figure S33).

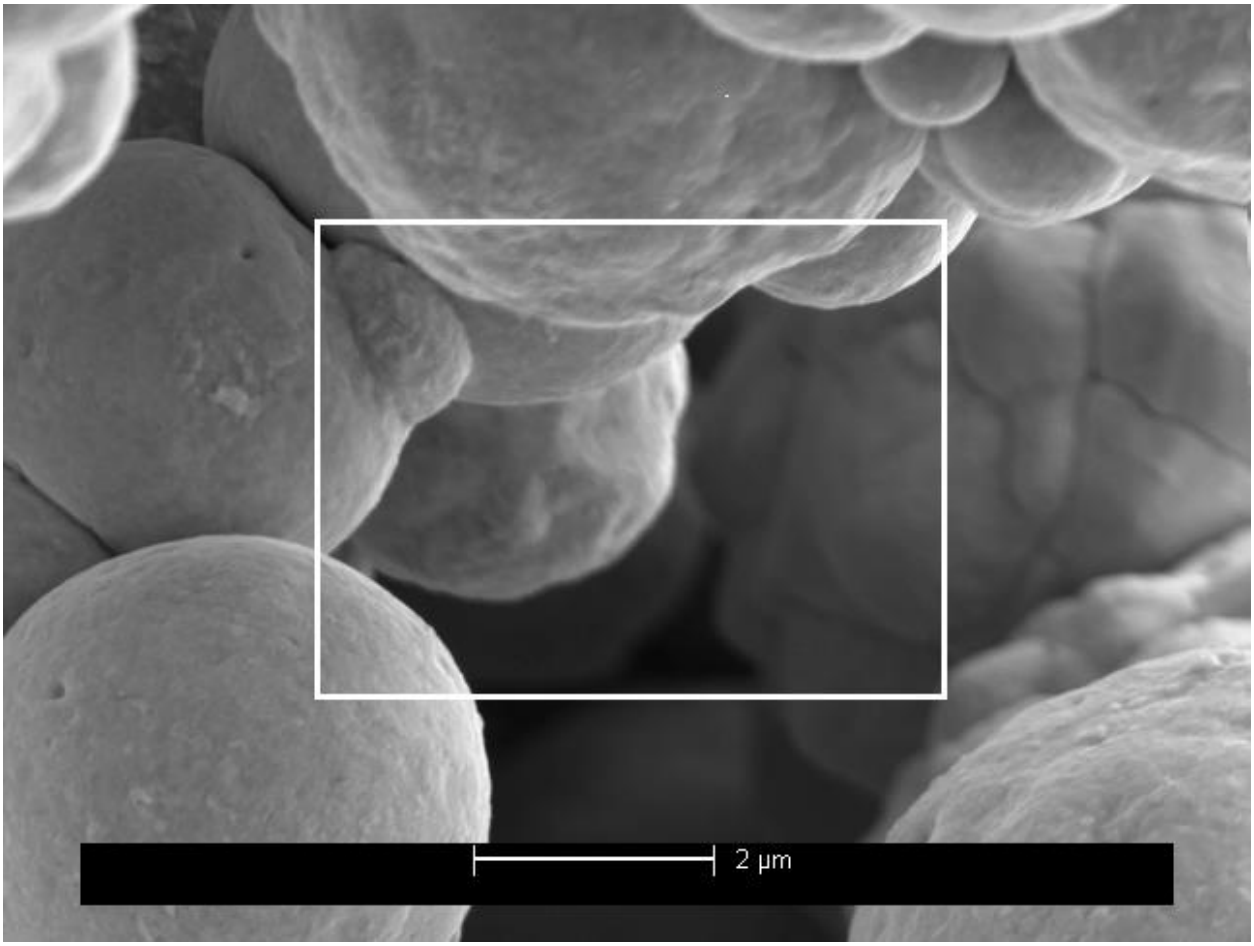

Figure S35. New medium 5.5-9.0 micron gold powder (boxed area in Figure S34).

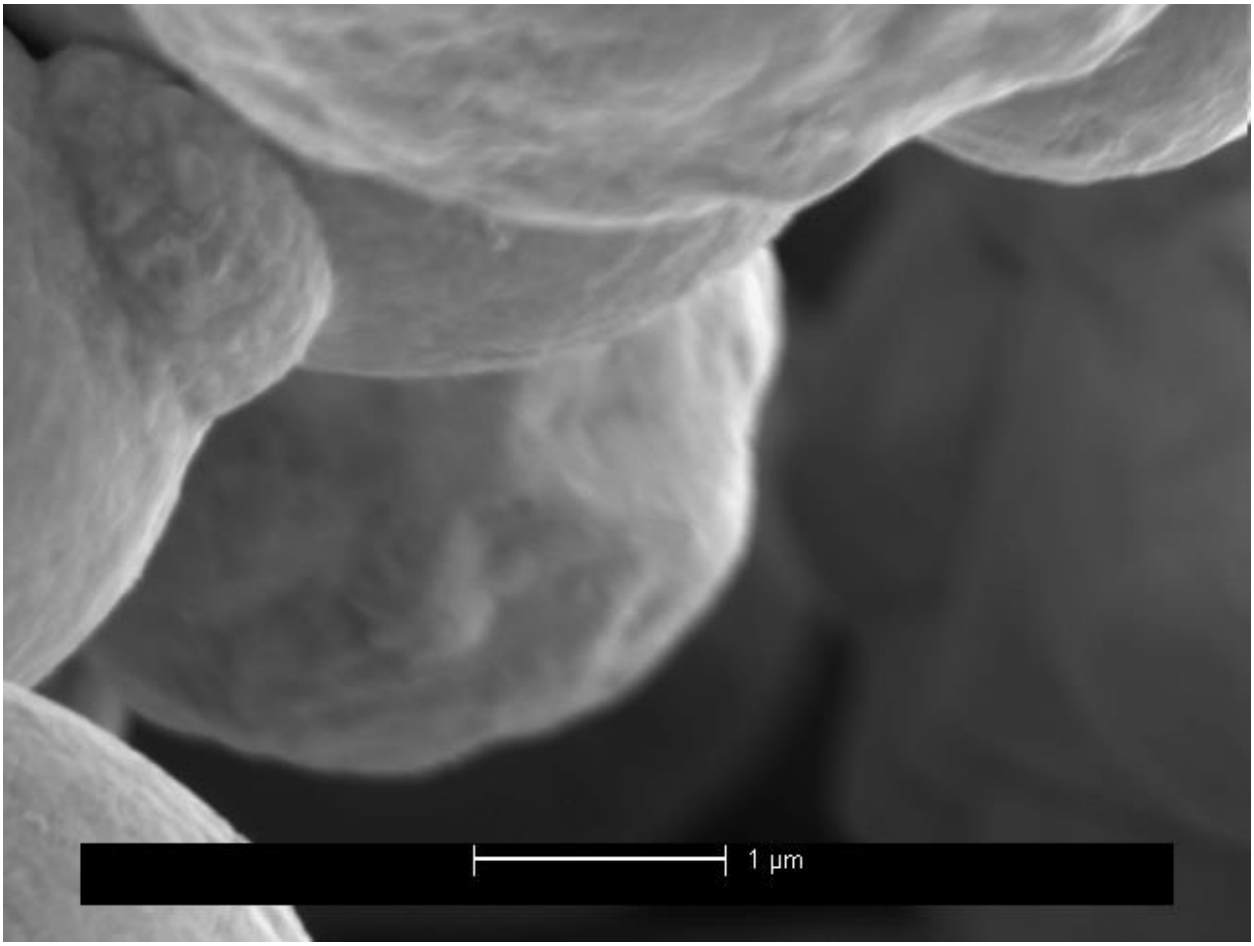

Figure S36. New medium 5.5-9.0 micron gold powder (boxed area in Figure S35).

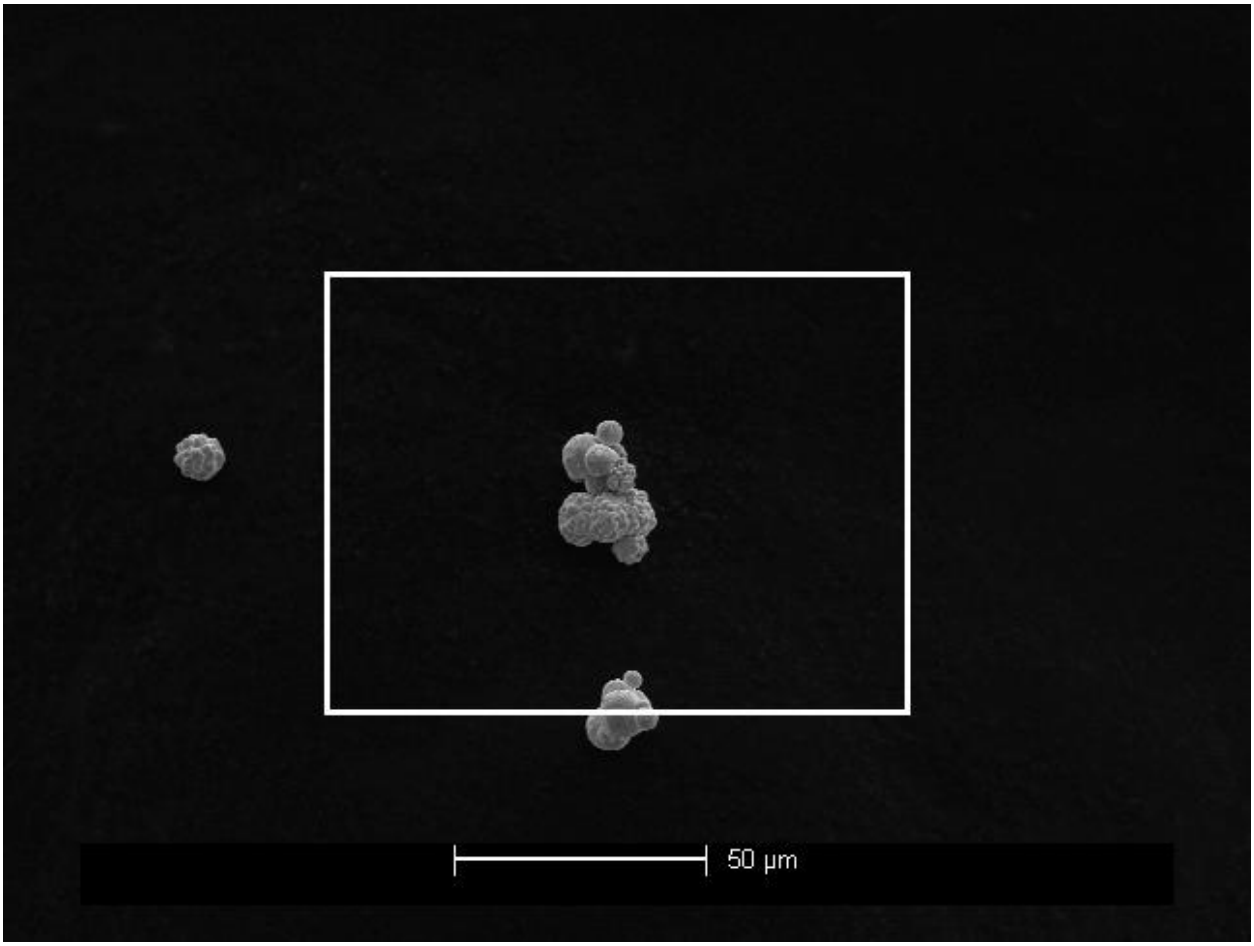

Figure S37. New medium 5.5-9.0 micron gold powder (region B in Figure S30).

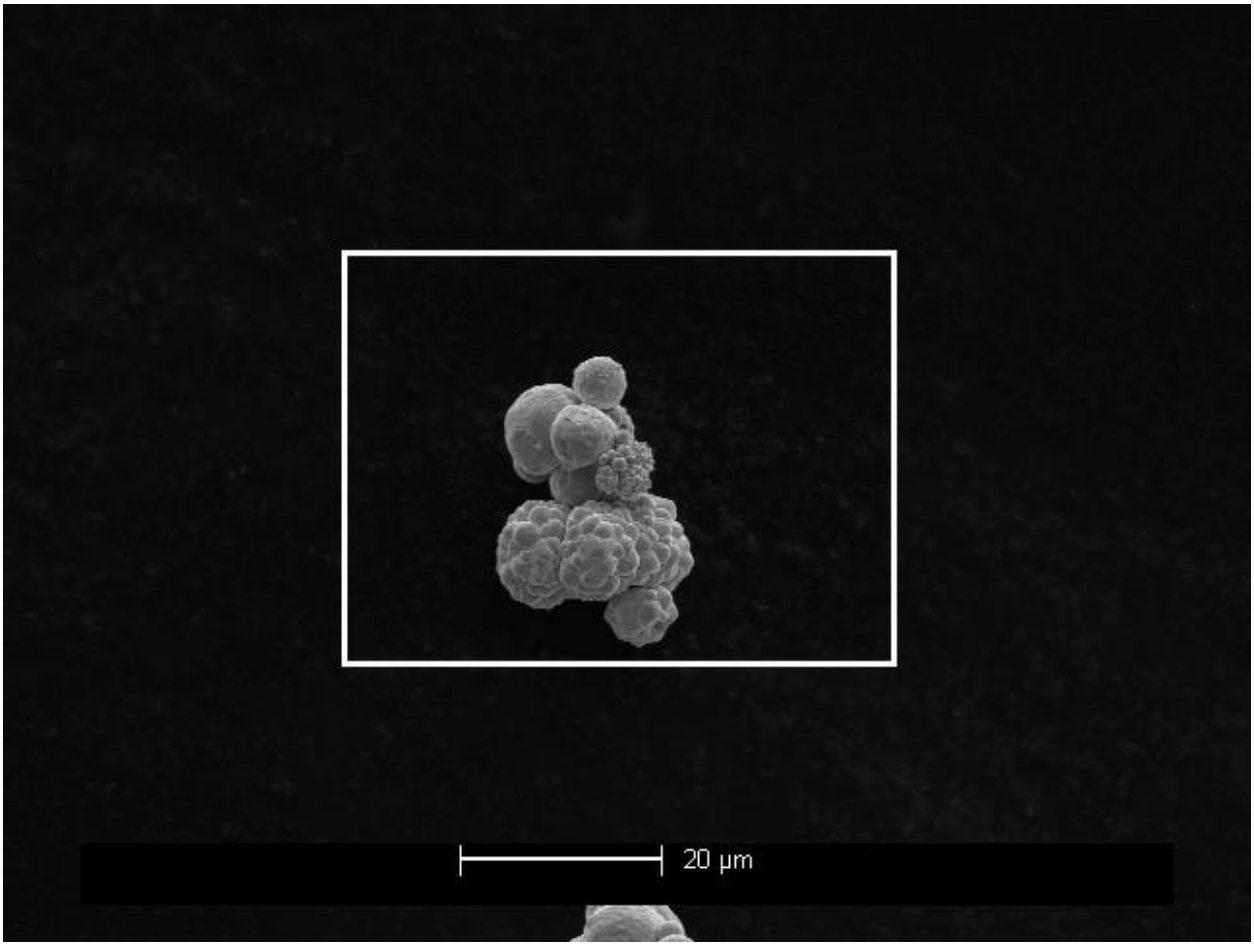

Figure S38. New medium 5.5-9.0 micron gold powder (boxed area in Figure S37).

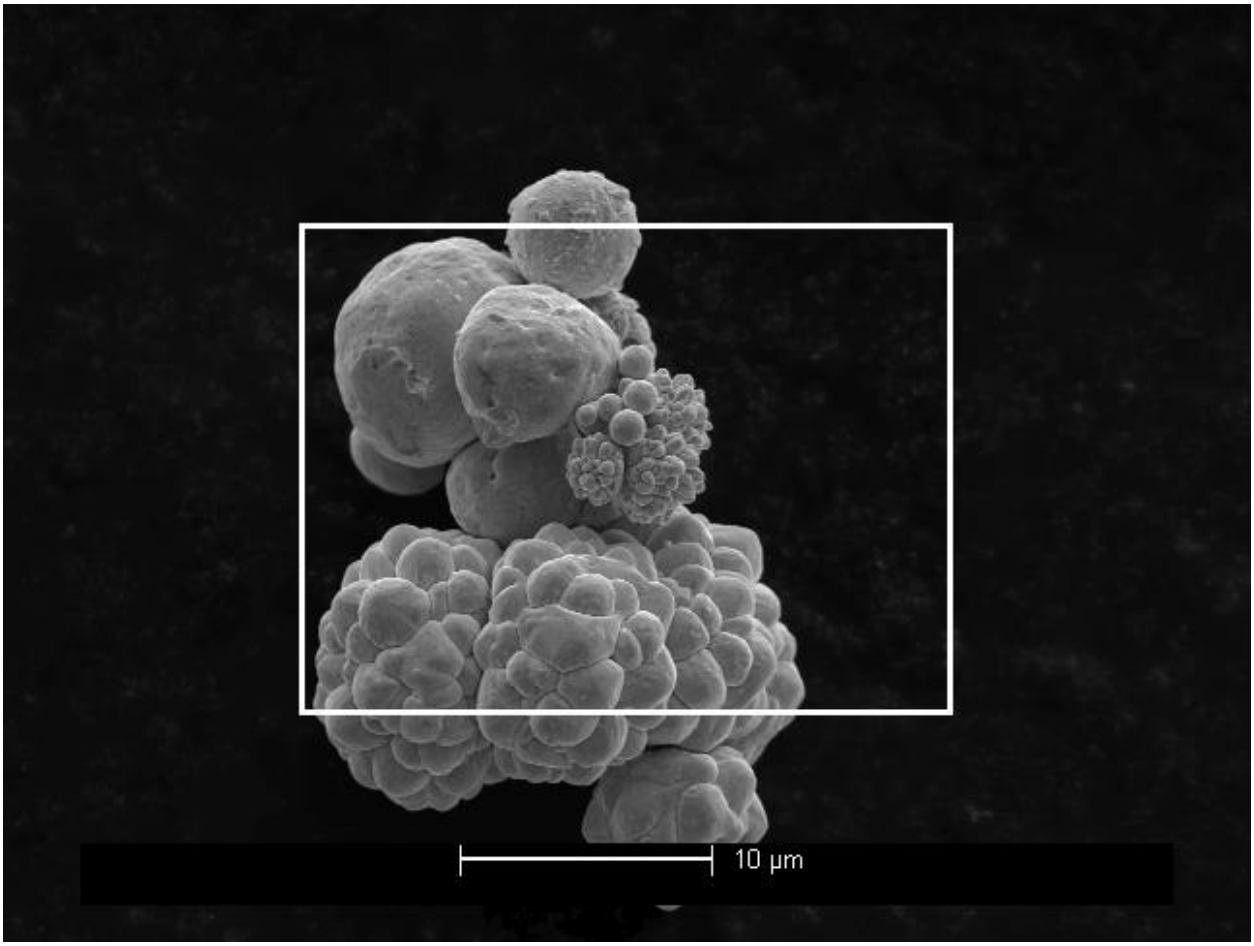

Figure S39. New medium 5.5-9.0 micron gold powder (boxed area in Figure S38).

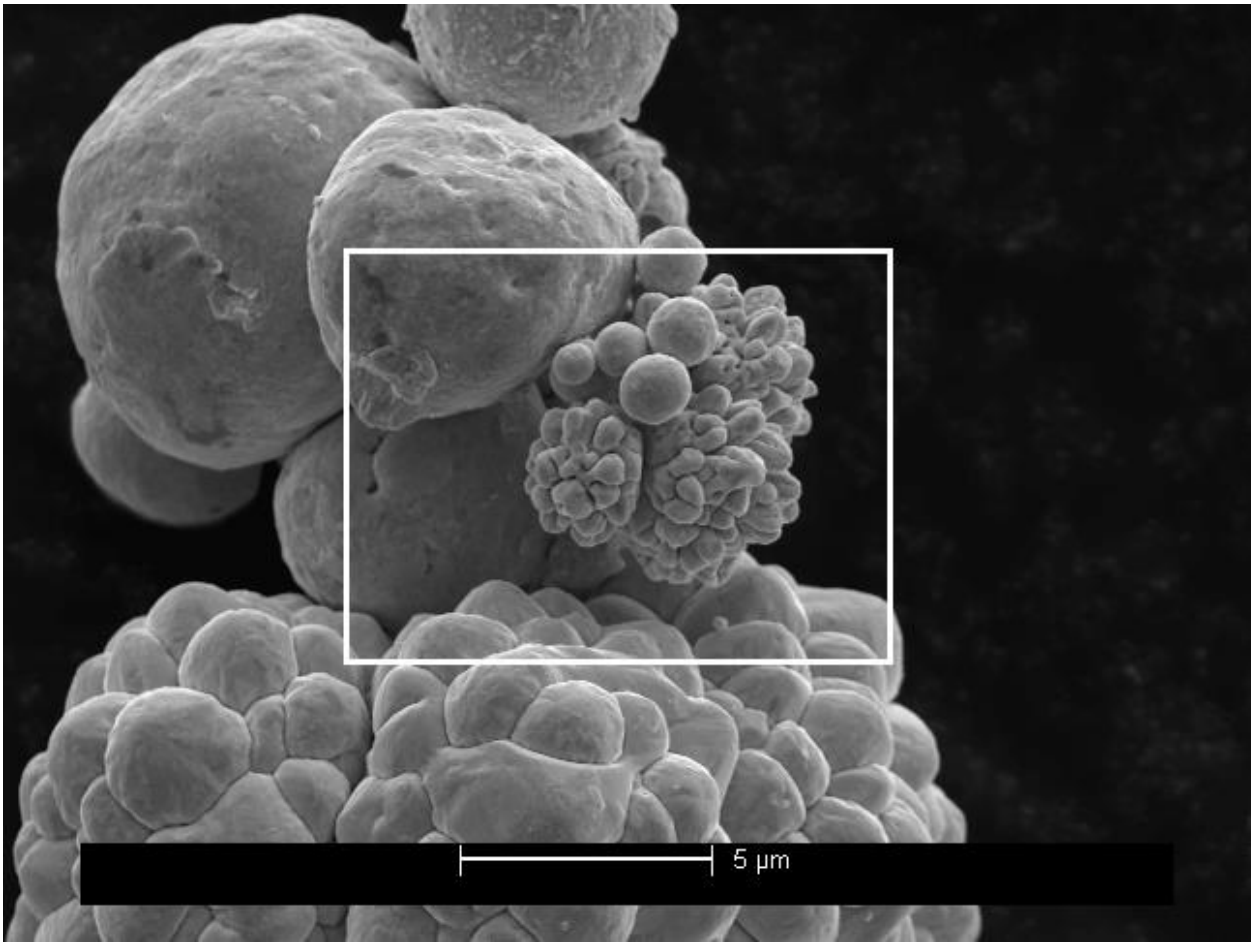

Figure S40. New medium 5.5-9.0 micron gold powder (boxed area in Figure S39).

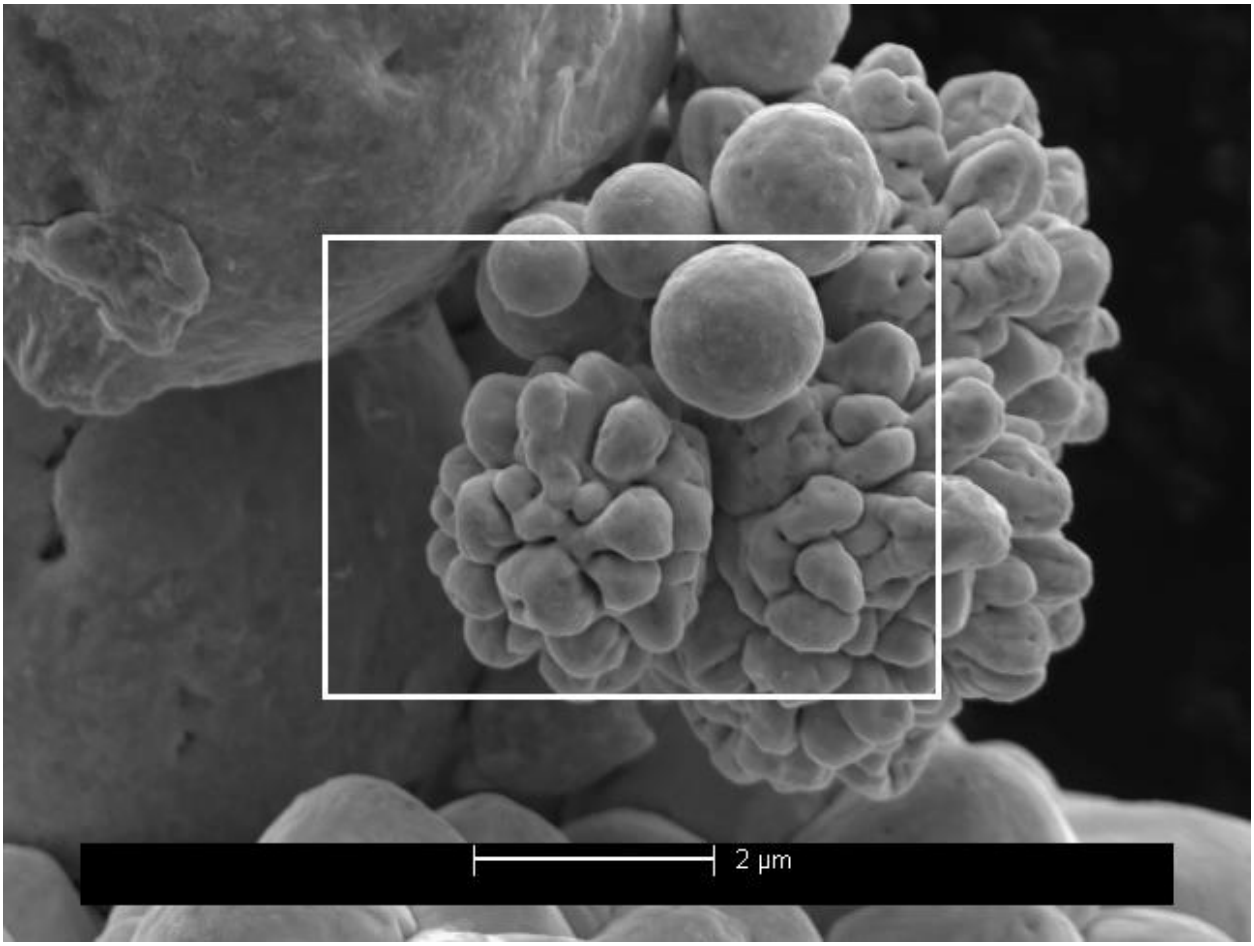

Figure S41. New medium 5.5-9.0 micron gold powder (boxed area in Figure S39).

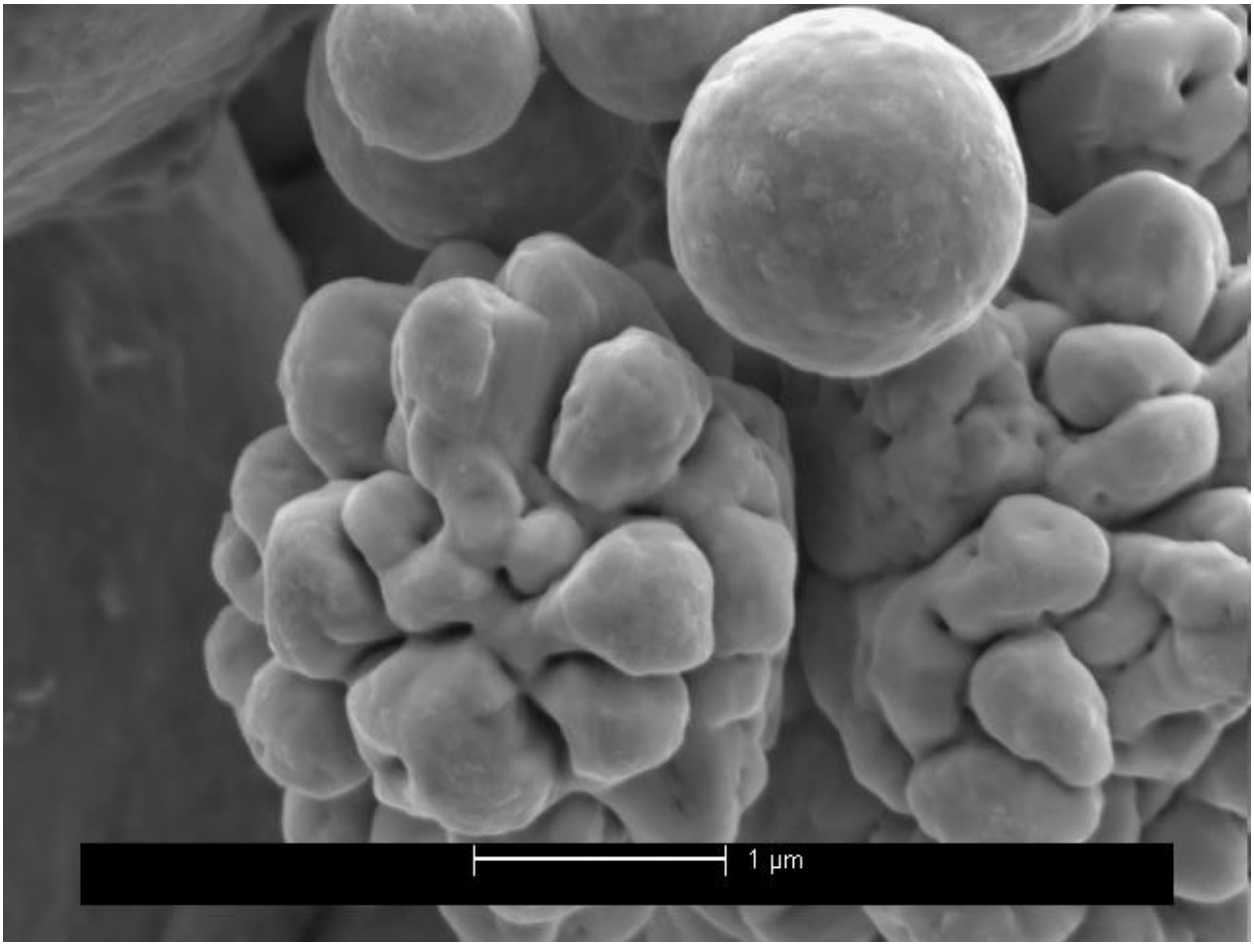

Figure S42. New medium 5.5-9.0 micron gold powder (boxed area in Figure S40).

SEM of used medium 5.5-9.0 micron gold powder

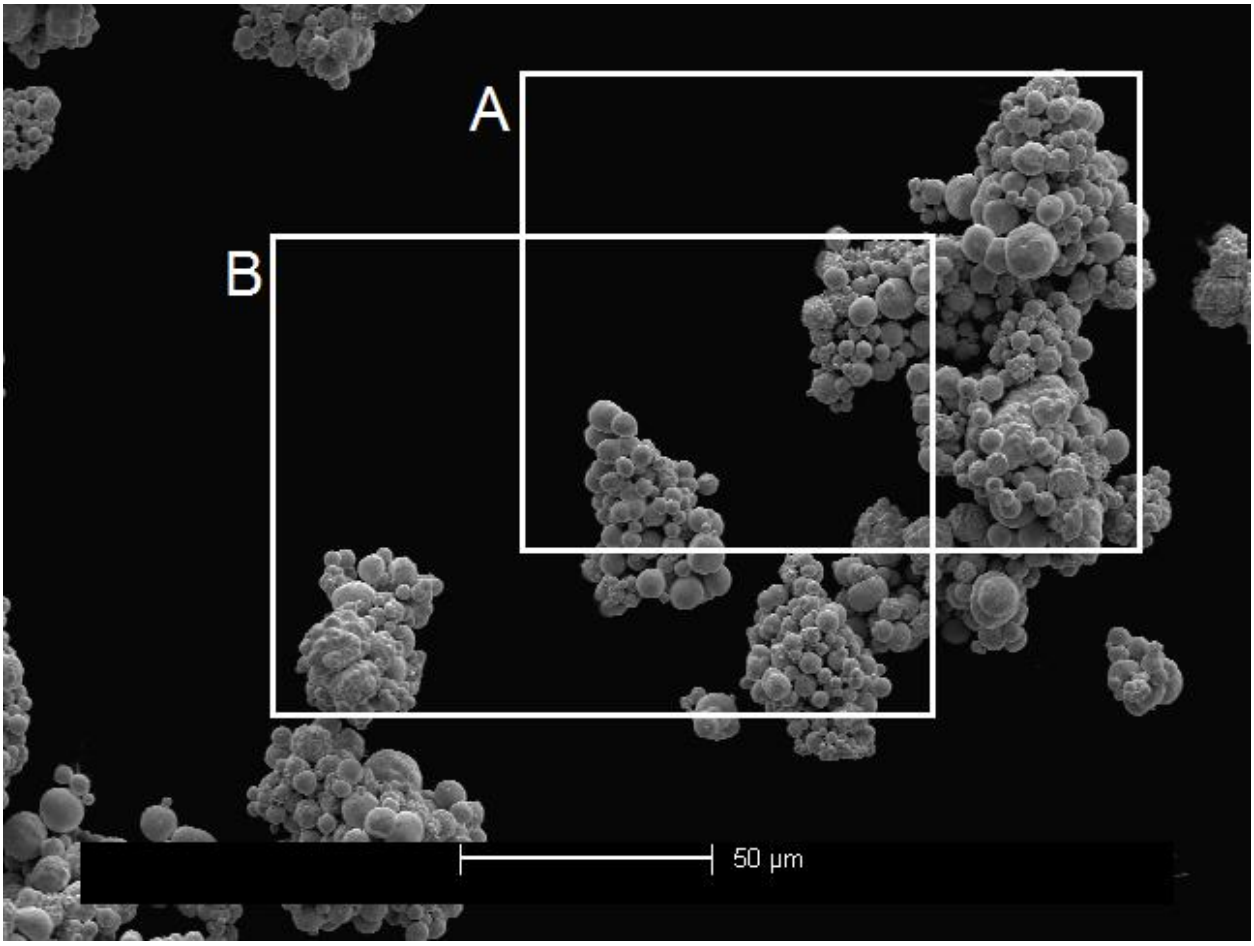

Figure S43. Used medium 5.5-9.0 micron gold powder (broad view with regions indicated).

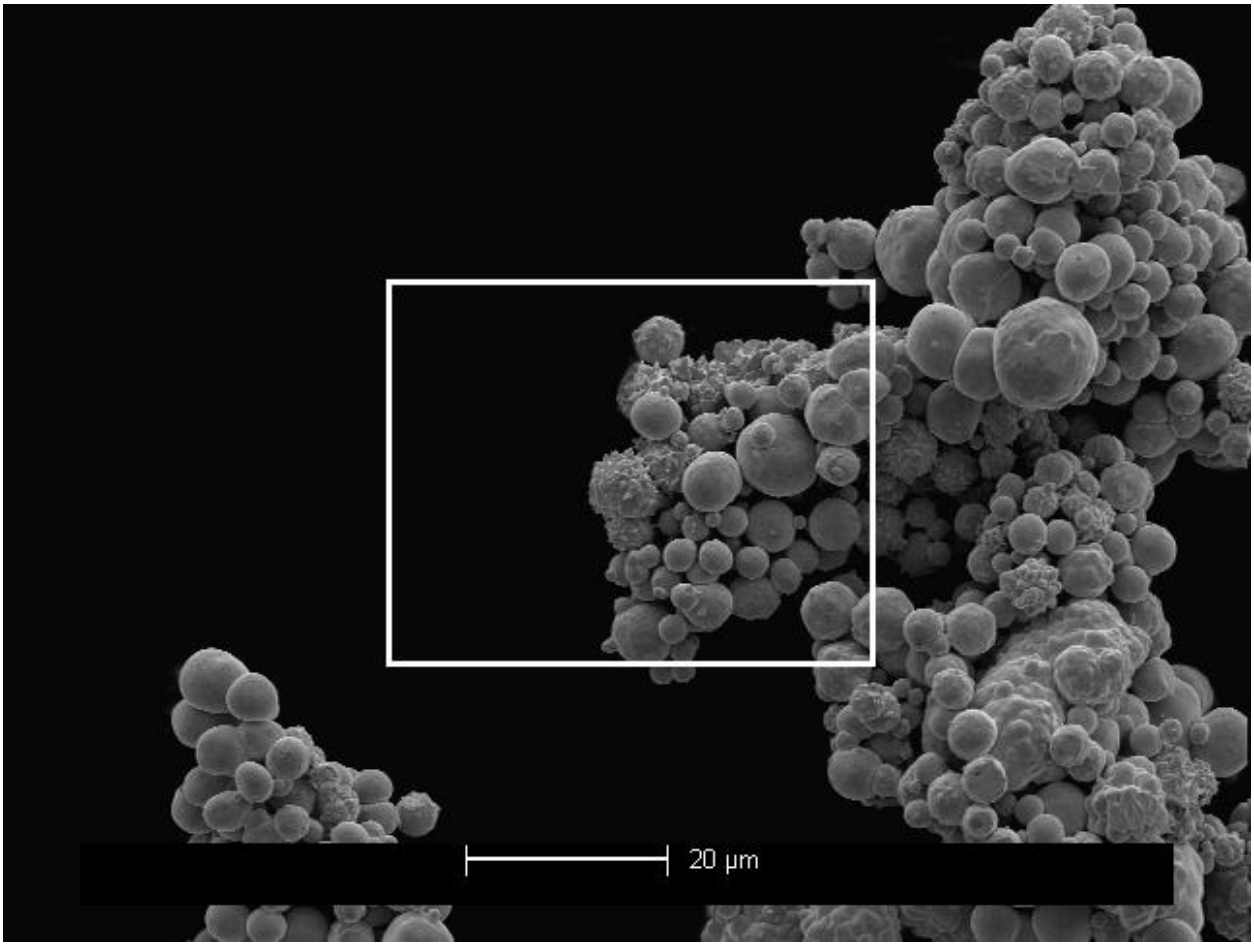

Figure S44. Used medium 5.5-9.0 micron gold powder (region A in Figure S43).

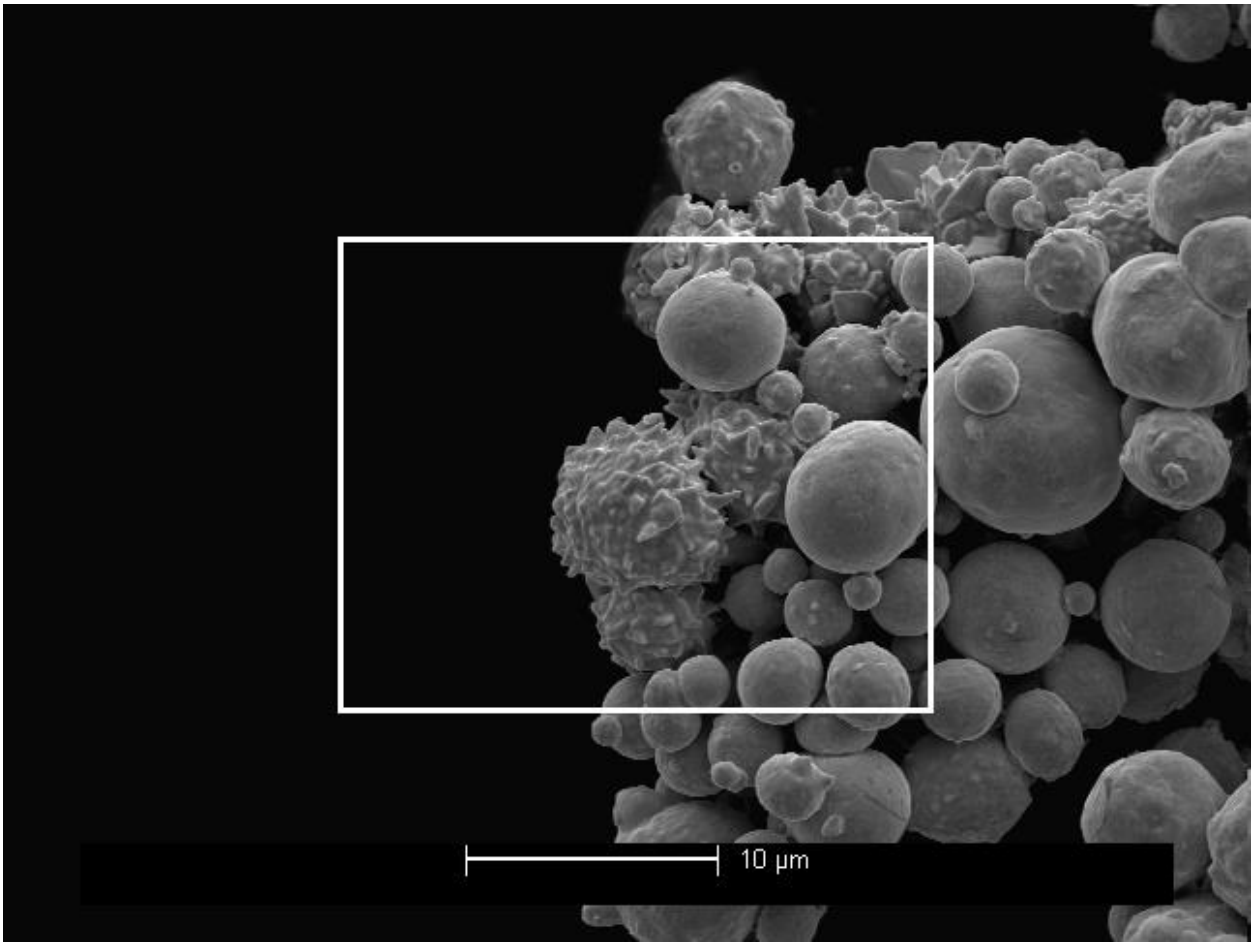

Figure S45. Used medium 5.5-9.0 micron gold powder (boxed area in Figure S43).

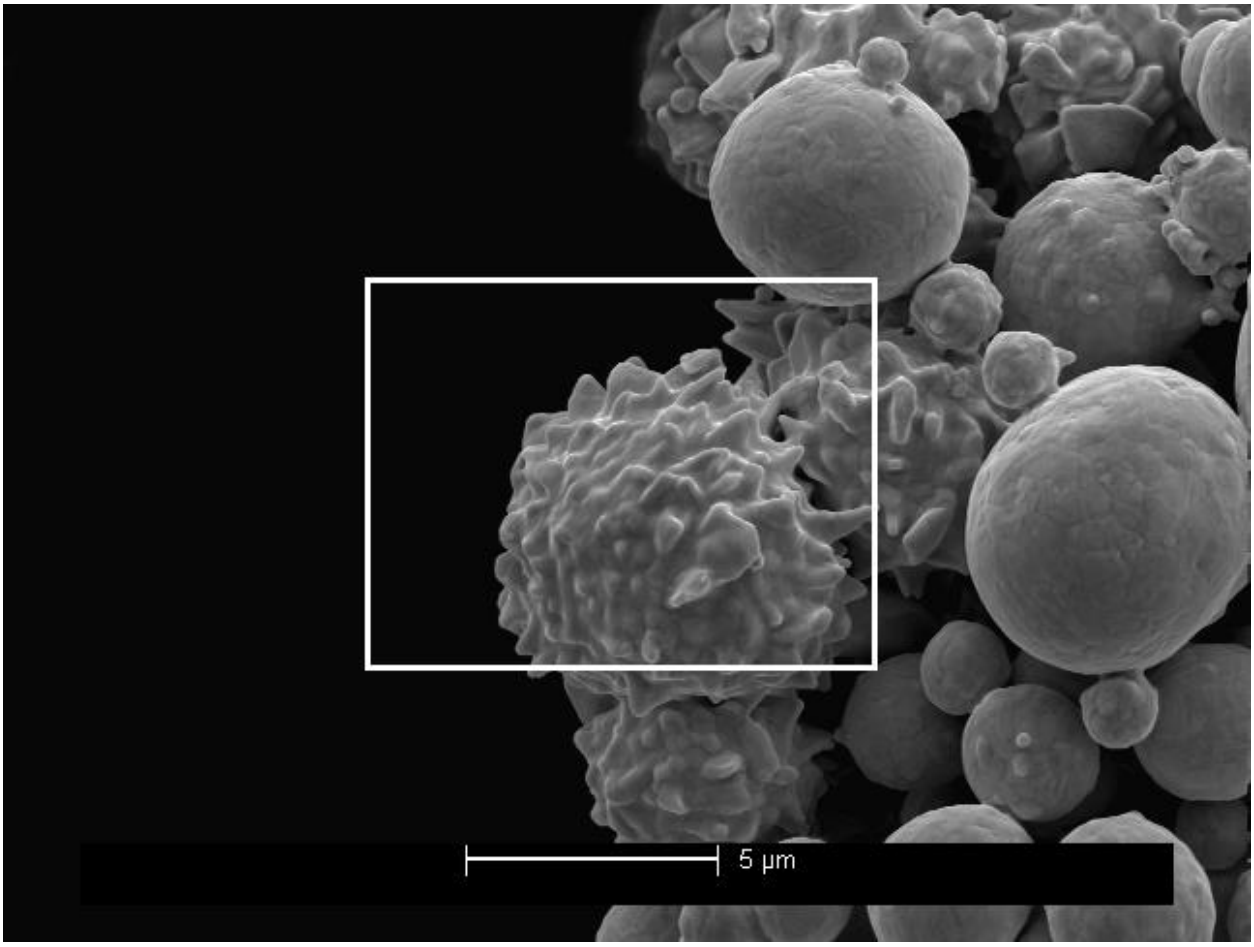

Figure S46. Used medium 5.5-9.0 micron gold powder (boxed area in Figure S45).

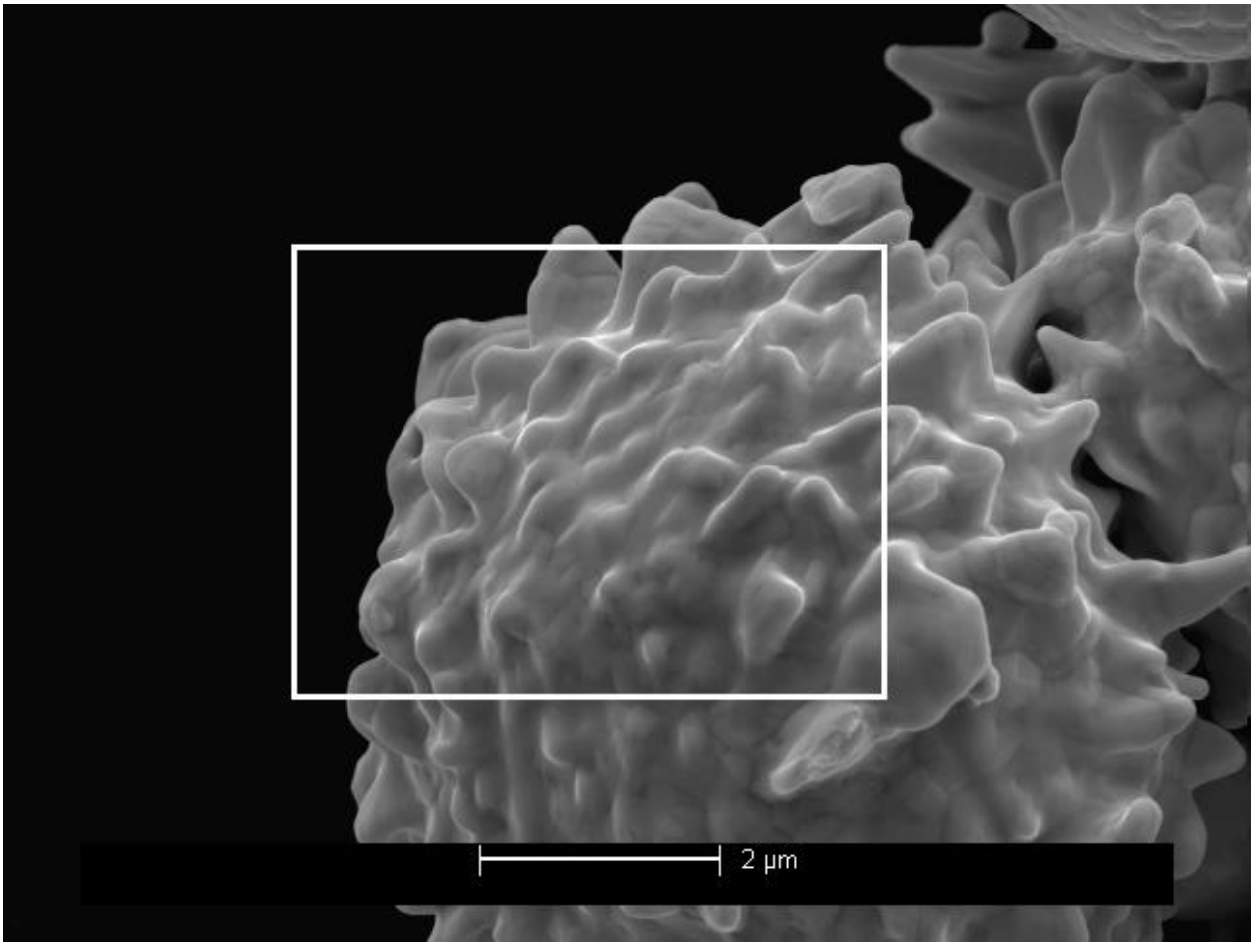

Figure S47. Used medium 5.5-9.0 micron gold powder (boxed area in Figure S46).

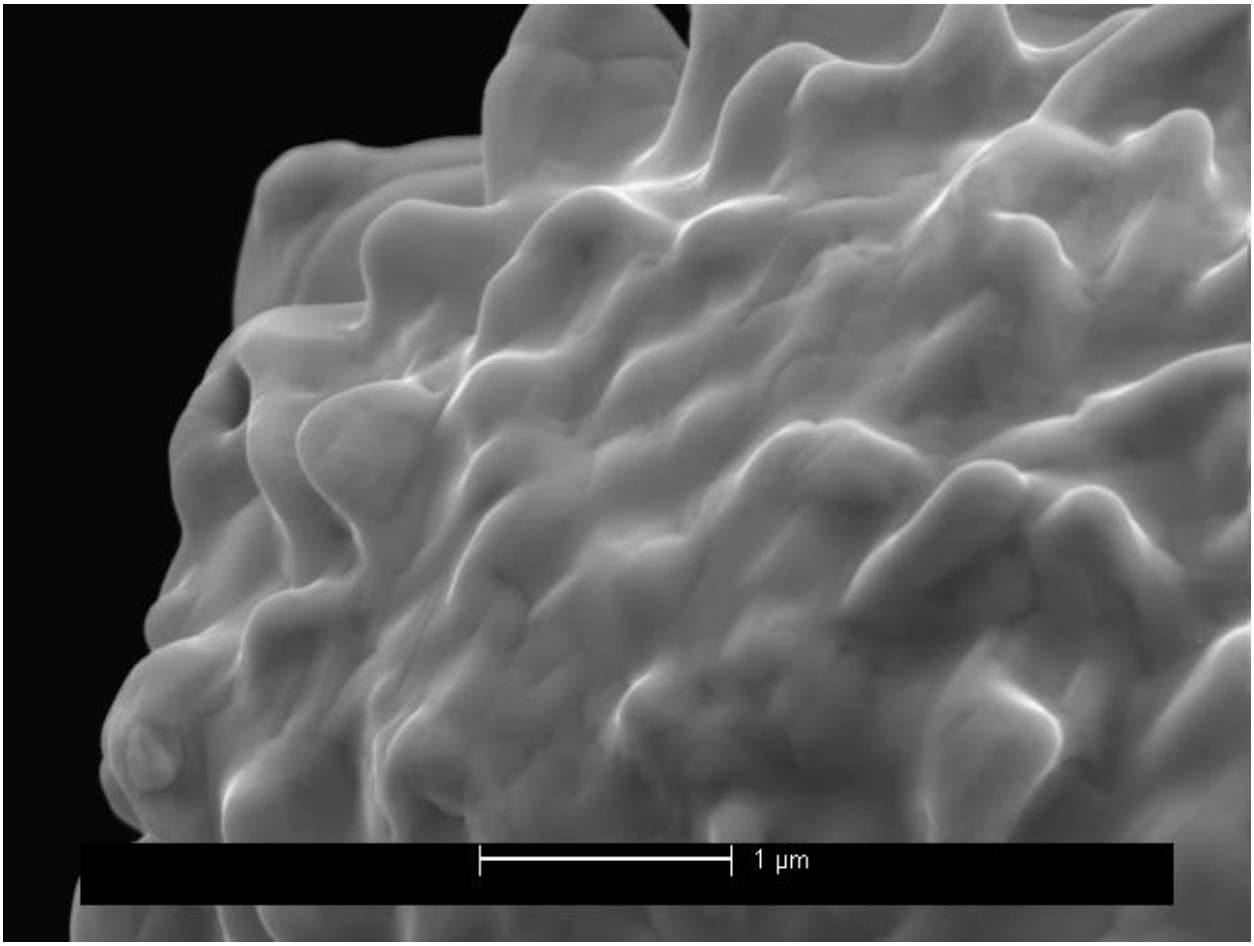

Figure S48. Used medium 5.5-9.0 micron gold powder (boxed area in Figure S47).

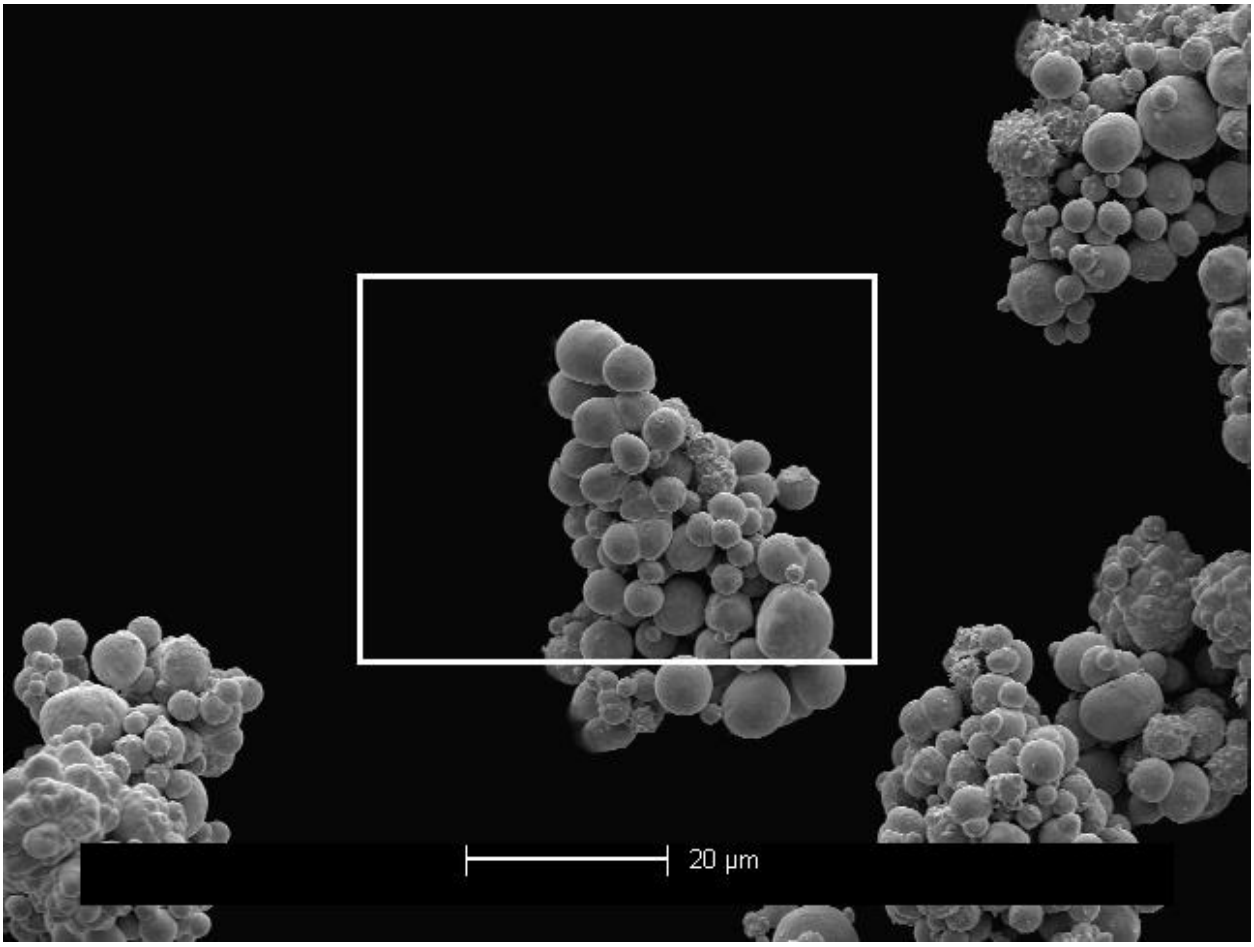

Figure S49. Used medium 5.5-9.0 micron gold powder (region B in Figure S43).

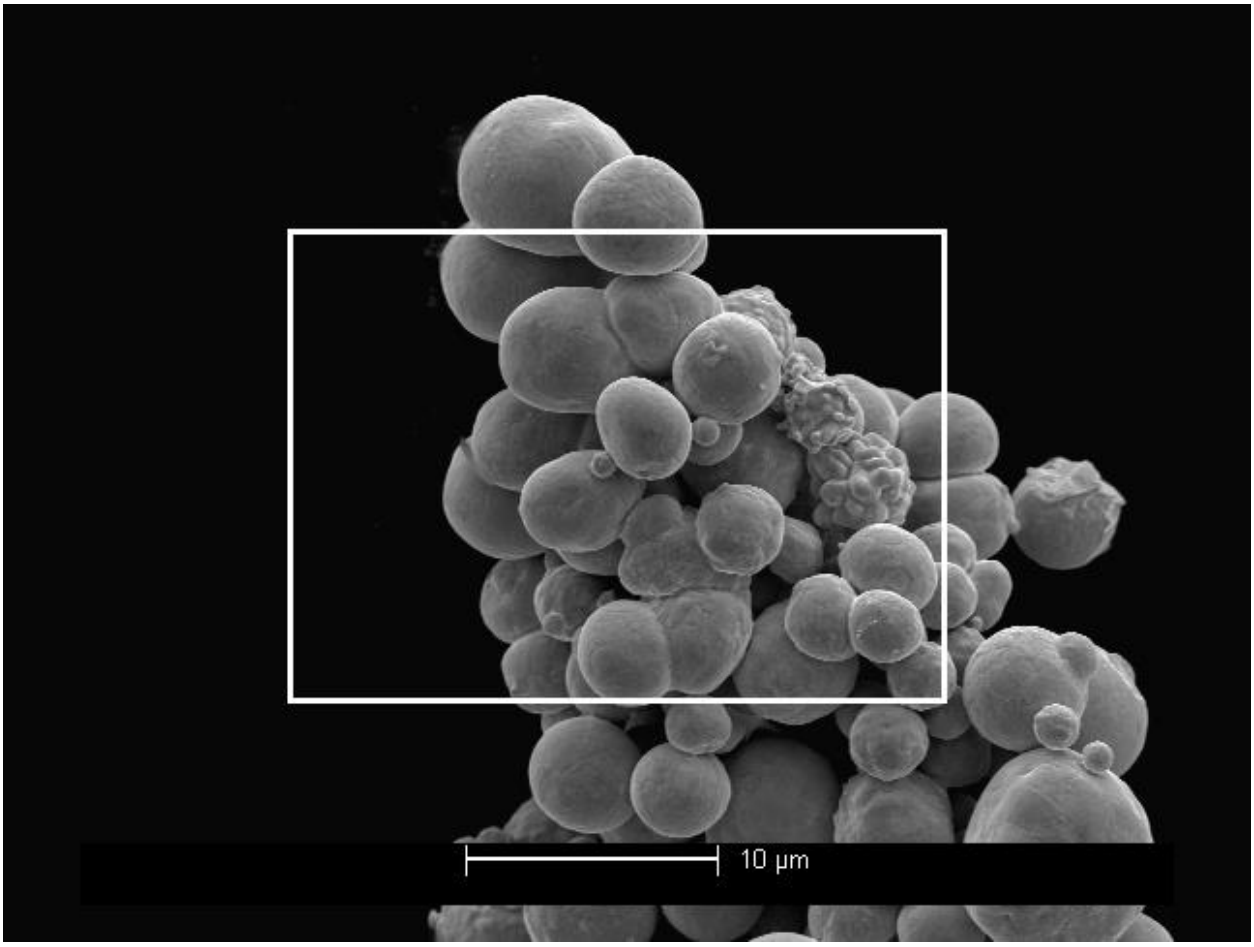

Figure S50. Used medium 5.5-9.0 micron gold powder (boxed area in Figure S49).

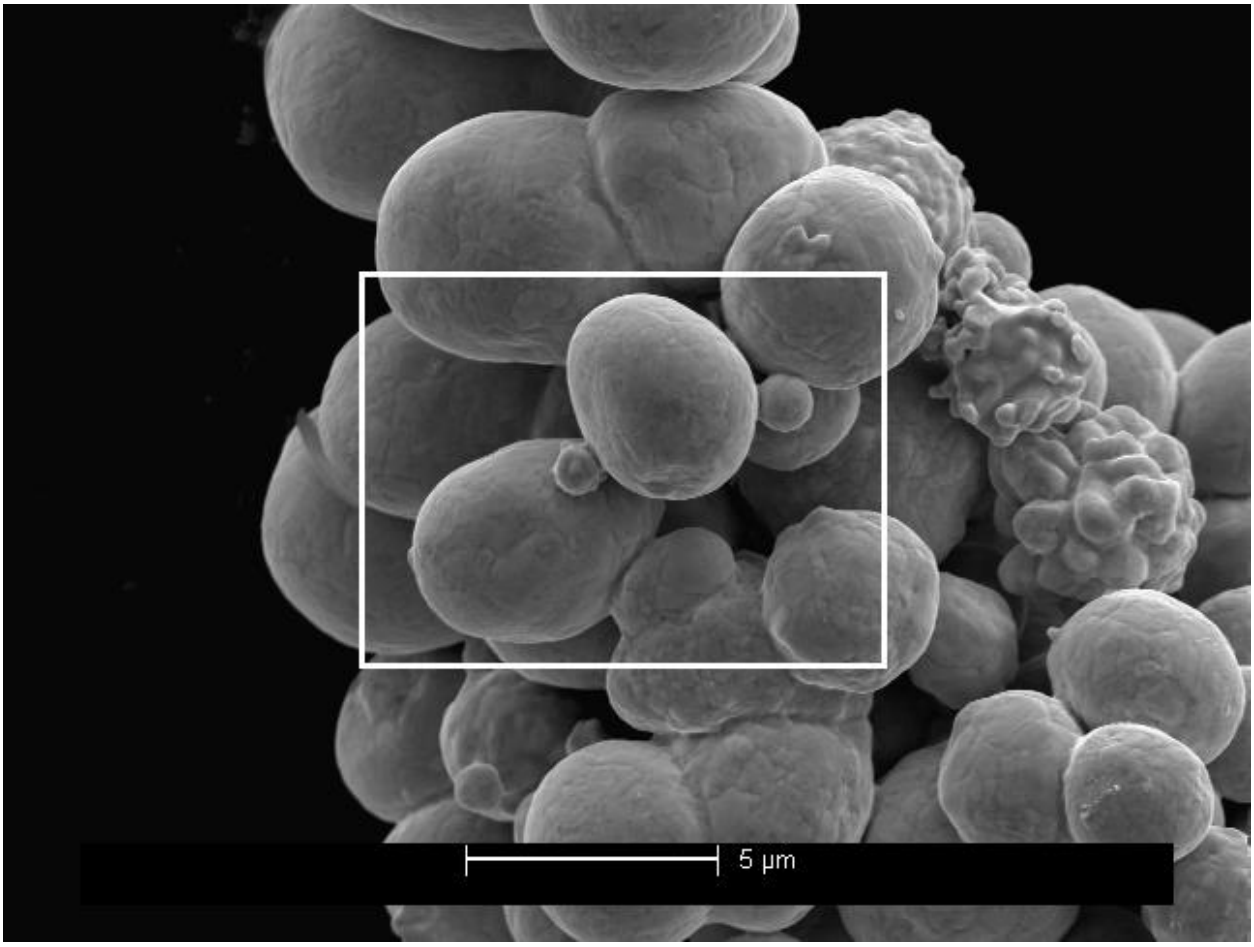

Figure S51. Used medium 5.5-9.0 micron gold powder (boxed area in Figure S50).

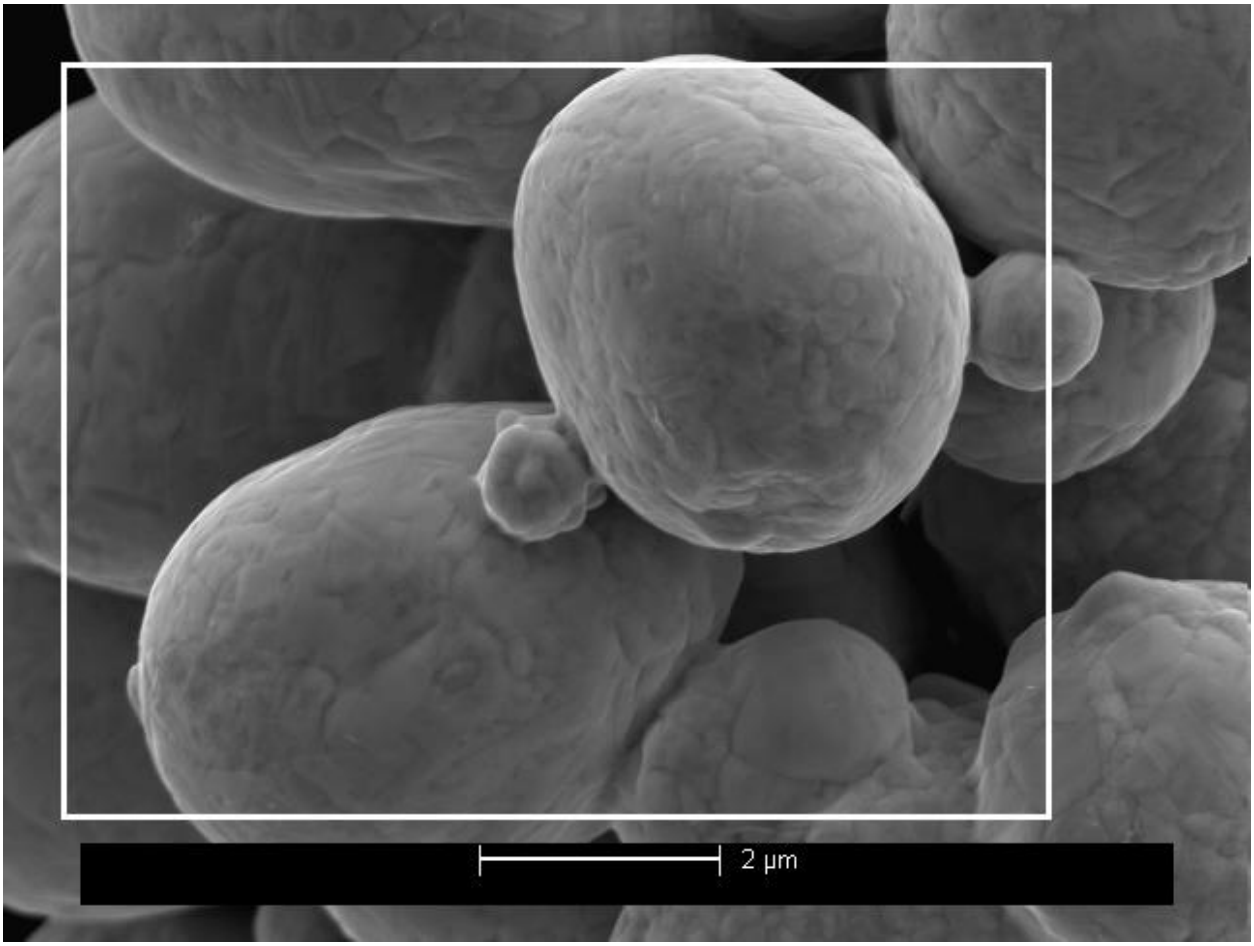

Figure S52. Used medium 5.5-9.0 micron gold powder (boxed area in Figure S51).

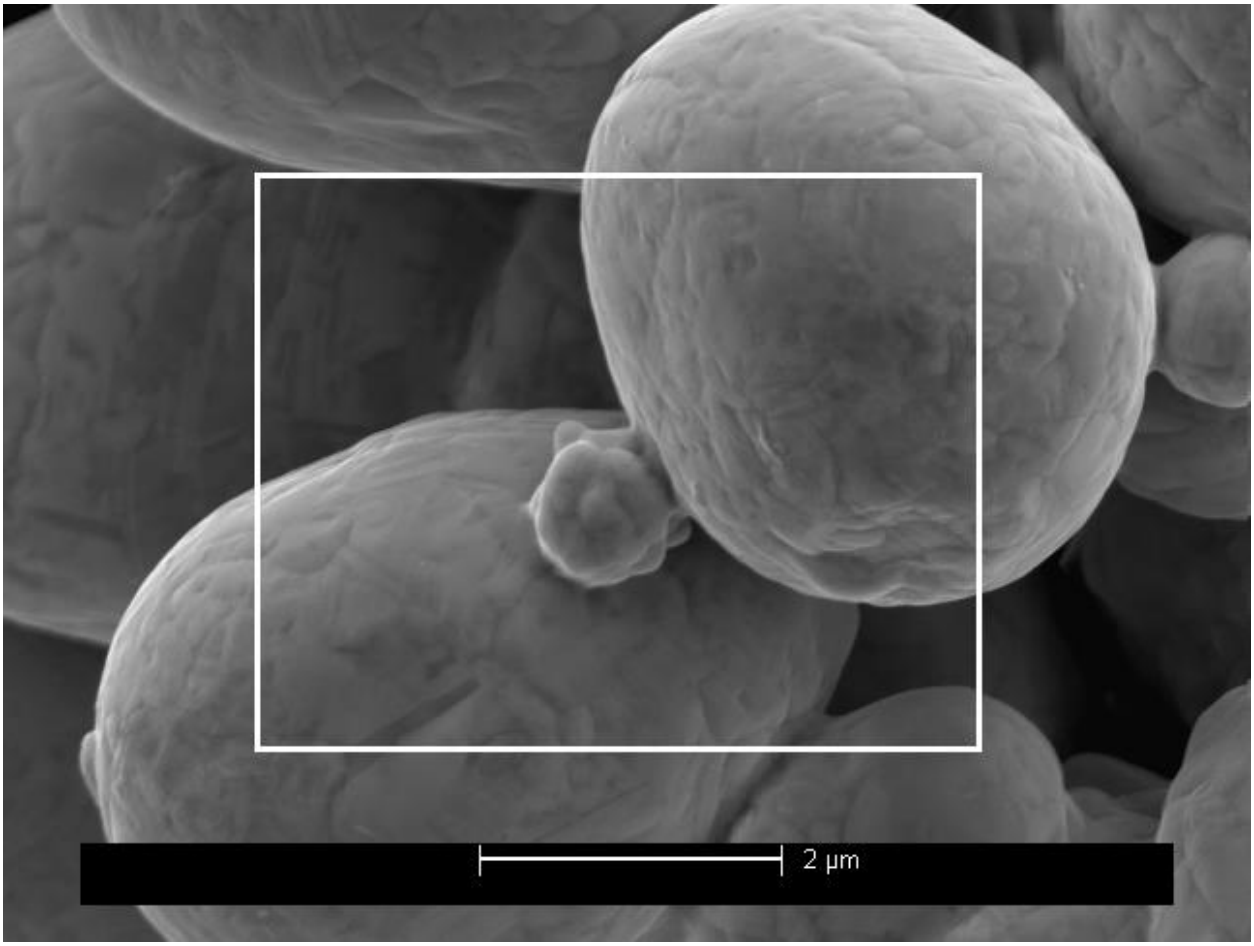

Figure S53. Used medium 5.5-9.0 micron gold powder (boxed area in Figure S52).

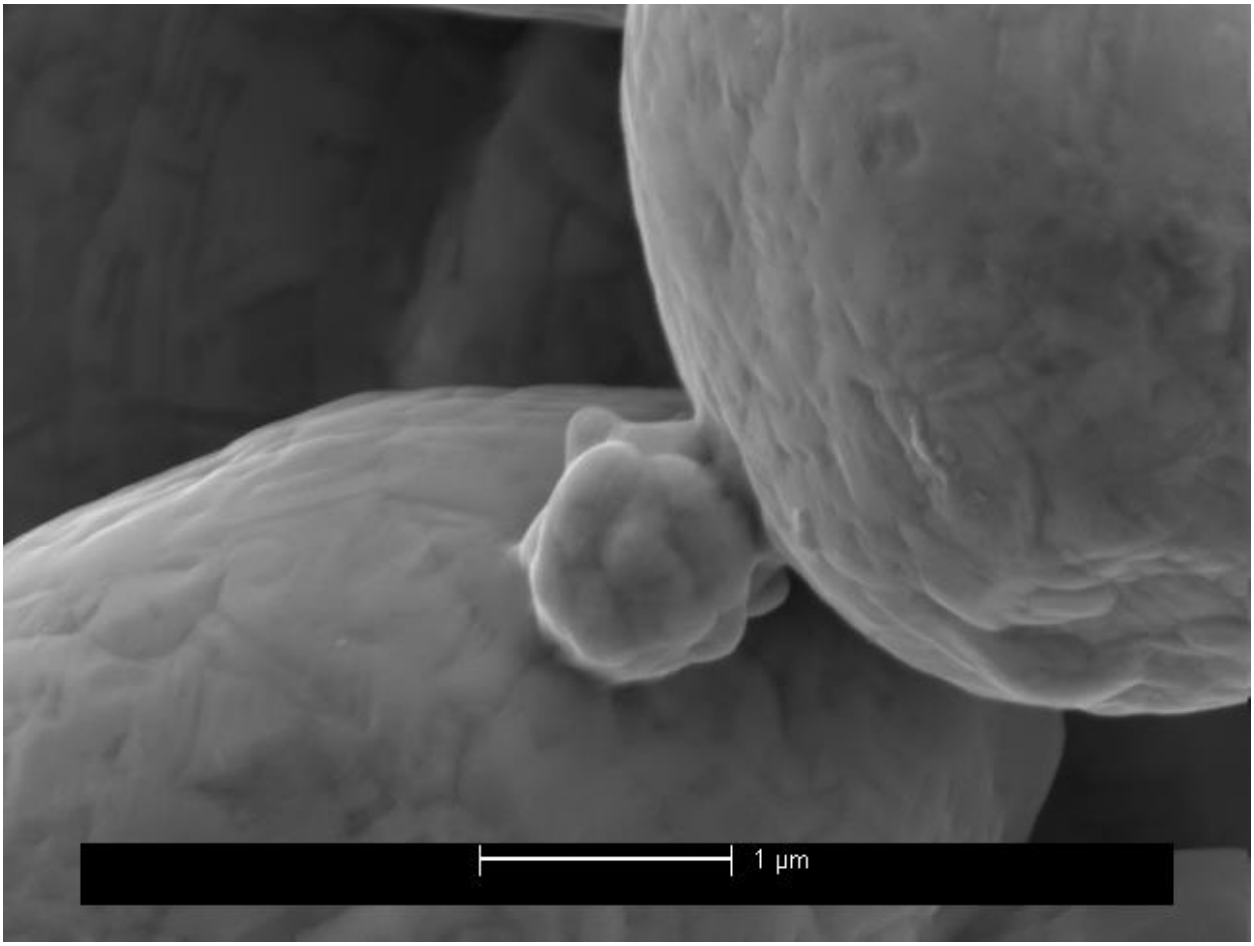

Figure S54. Used medium 5.5-9.0 micron gold powder (boxed area in Figure S53).

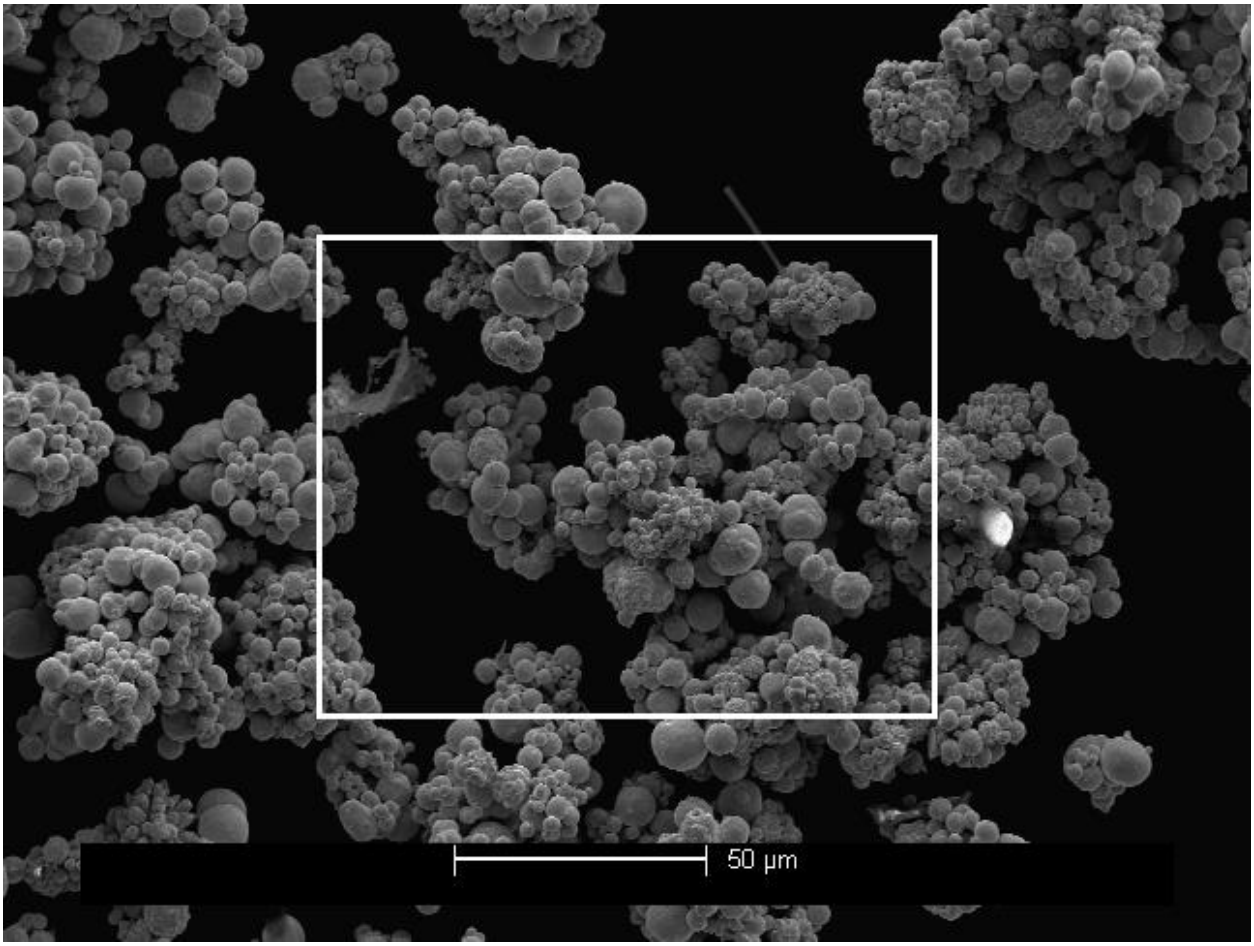

Figure S55. Used medium 5.5-9.0 micron gold powder (region C, not shown in Figure S43).

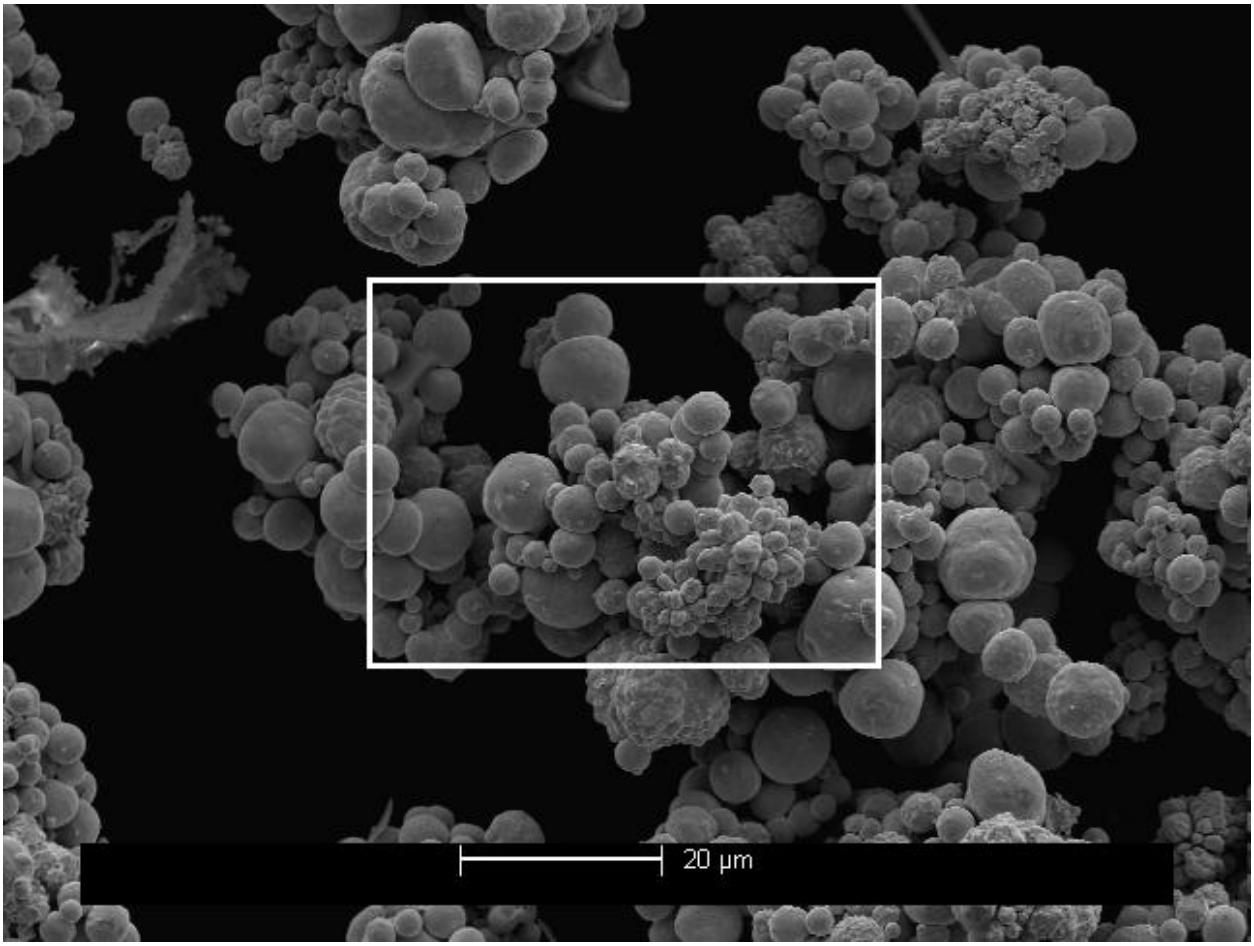

Figure S56. Used medium 5.5-9.0 micron gold powder (boxed area in Figure S55).

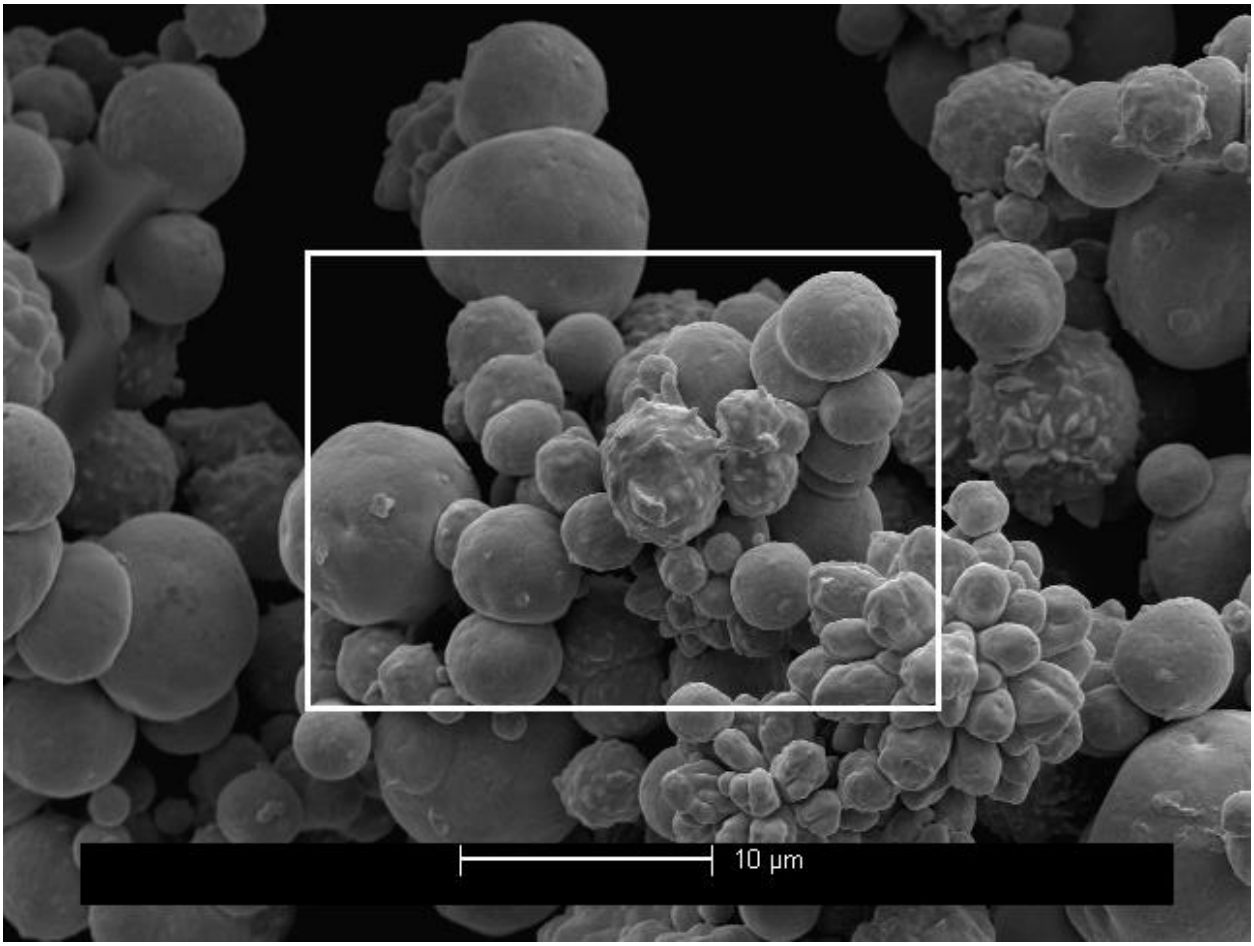

Figure S57. Used medium 5.5-9.0 micron gold powder (boxed area in Figure S56).

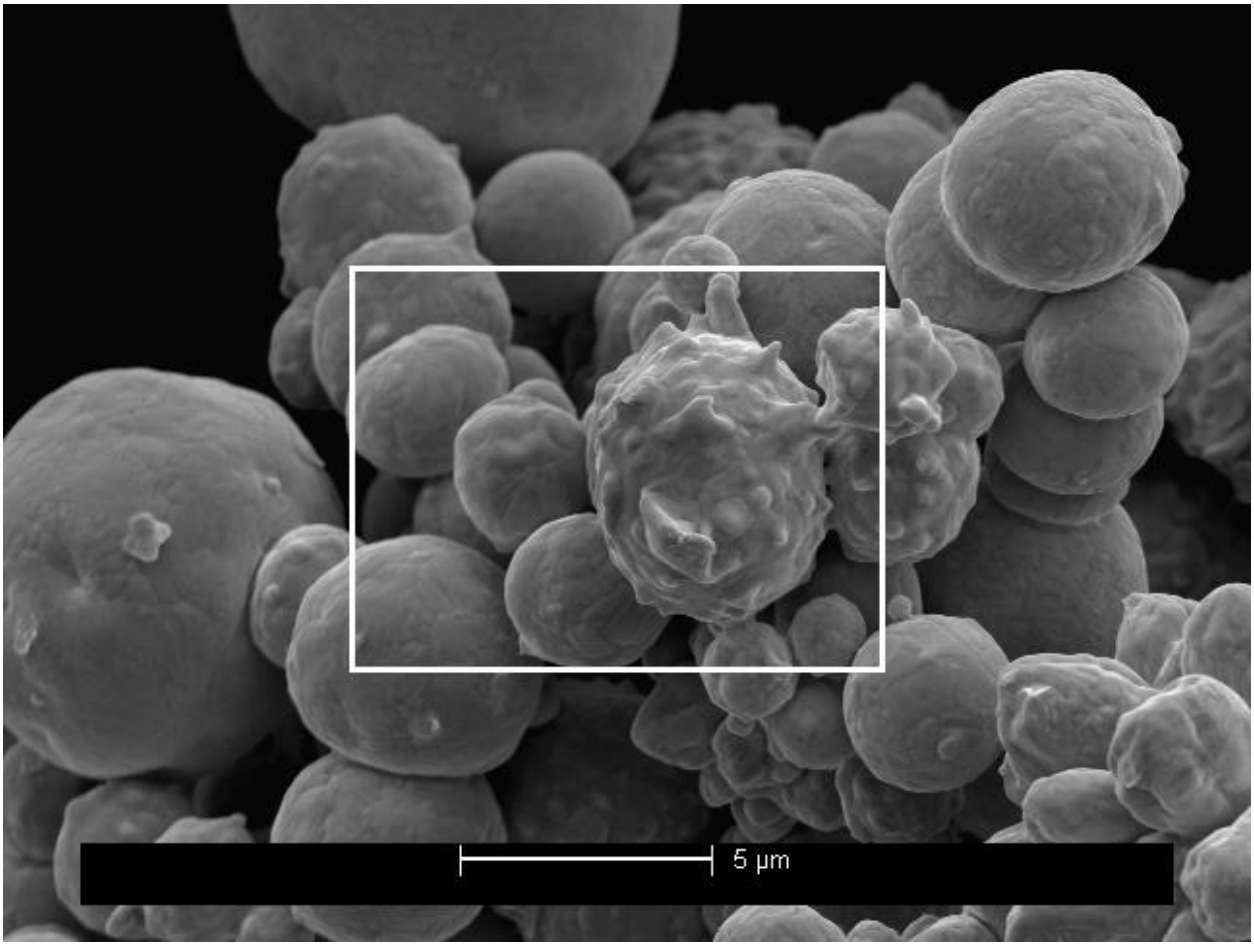

Figure S58. Used medium 5.5-9.0 micron gold powder (boxed area in Figure S57).

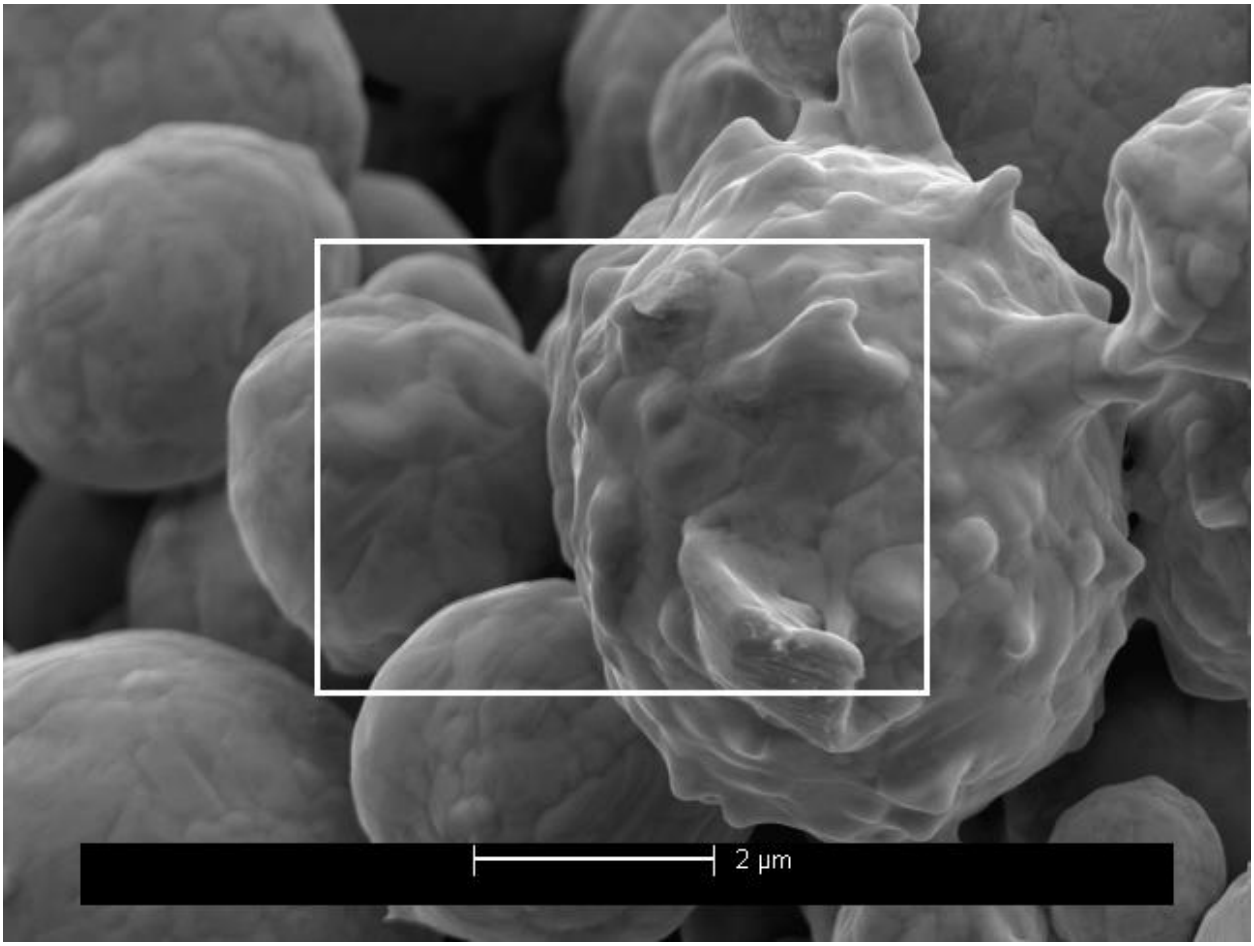

Figure S59. Used medium 5.5-9.0 micron gold powder (boxed area in Figure S58).

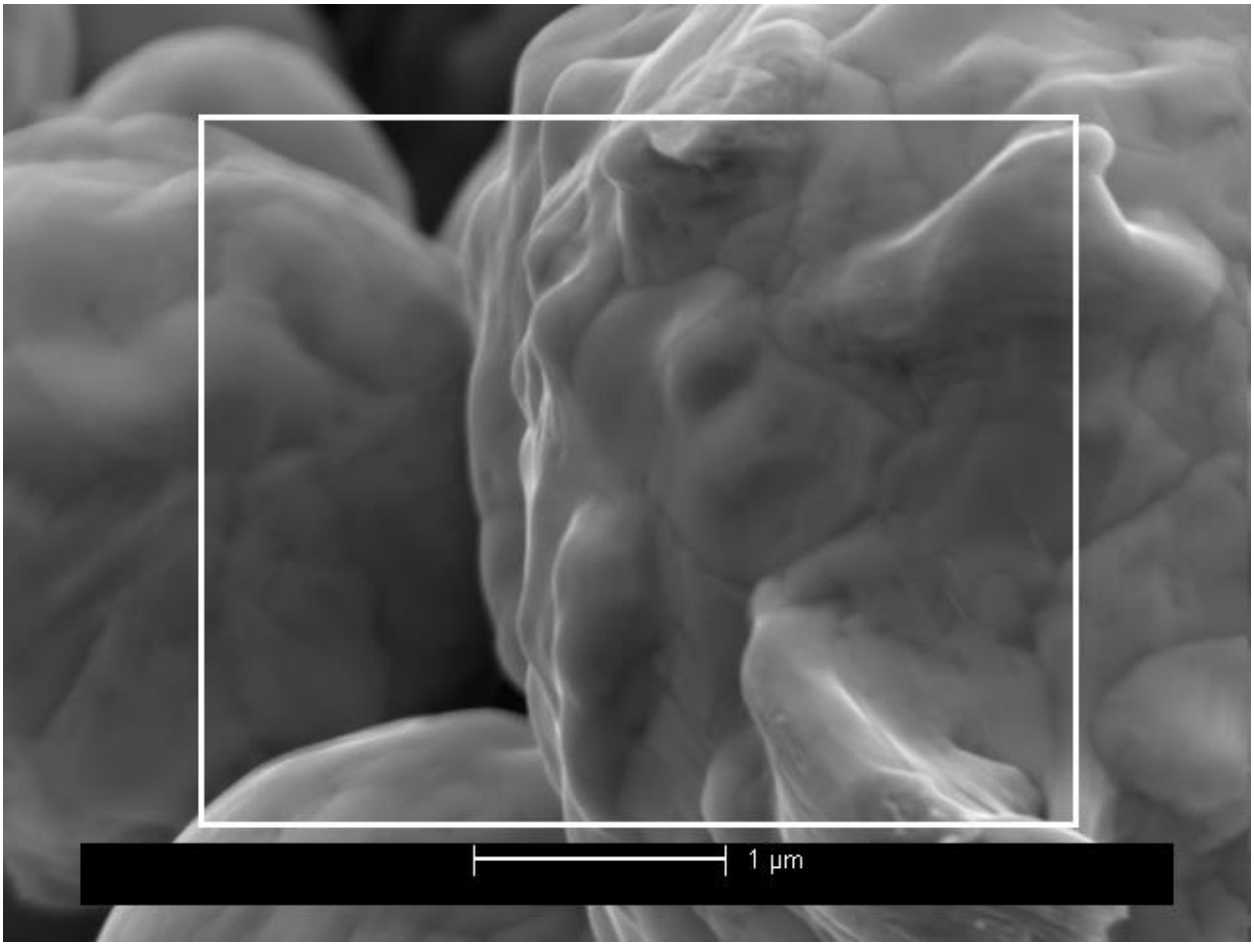

Figure S60. Used medium 5.5-9.0 micron gold powder (boxed area in Figure S59).

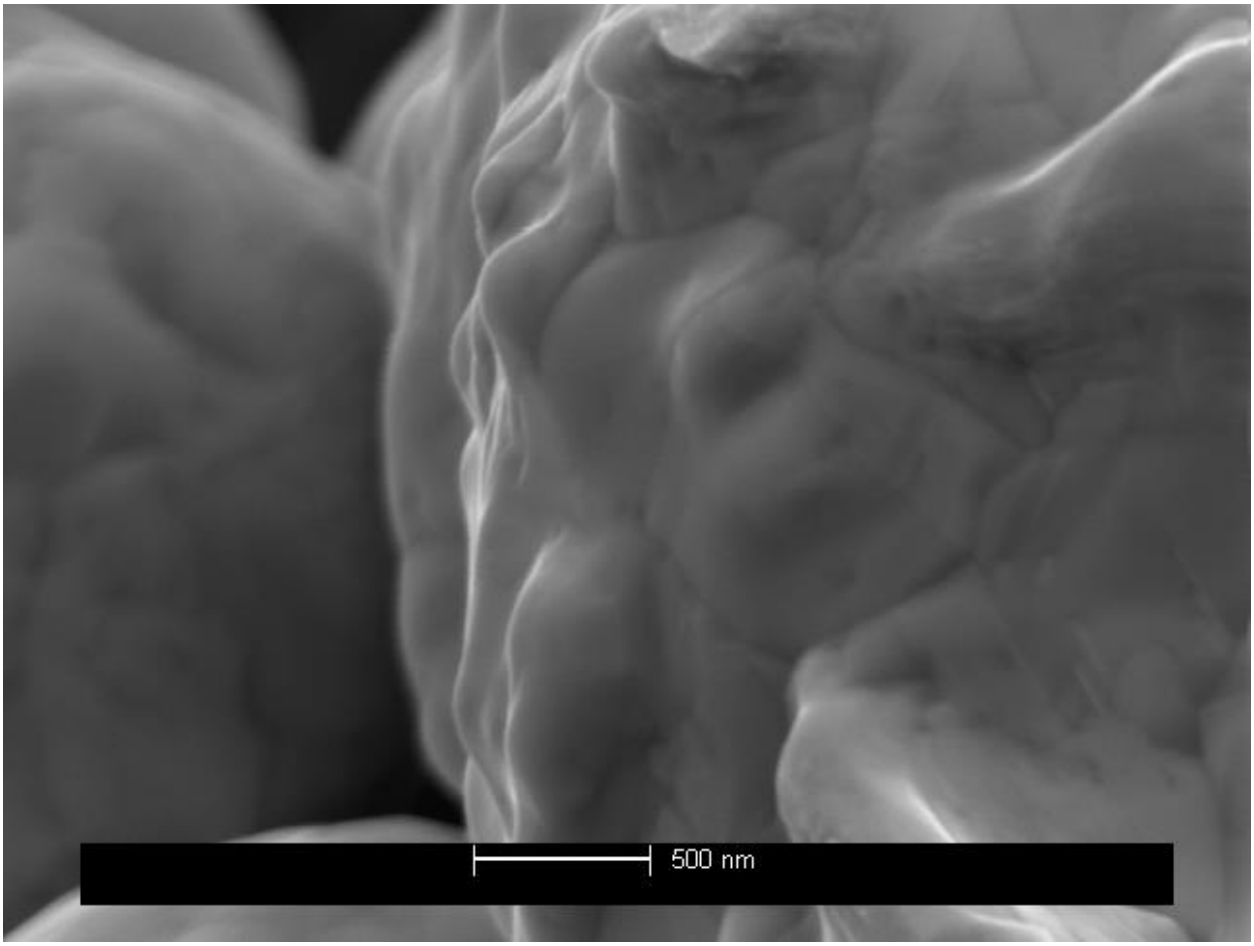

Figure S61. Used medium 5.5-9.0 micron gold powder (boxed area in Figure S60).

SEM of new large bulk gold powder

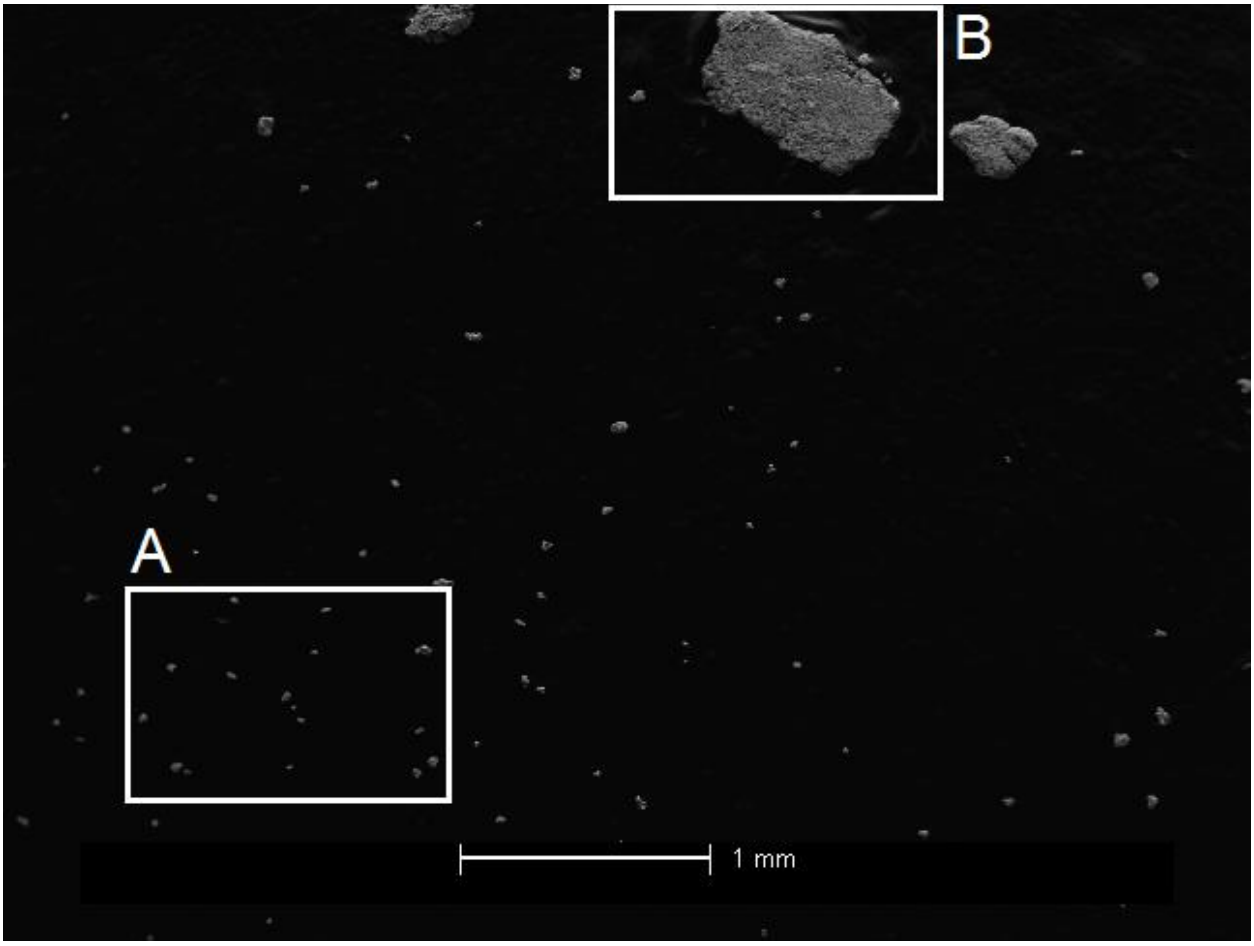

Figure S62. New large bulk gold powder (broad view with regions indicated).

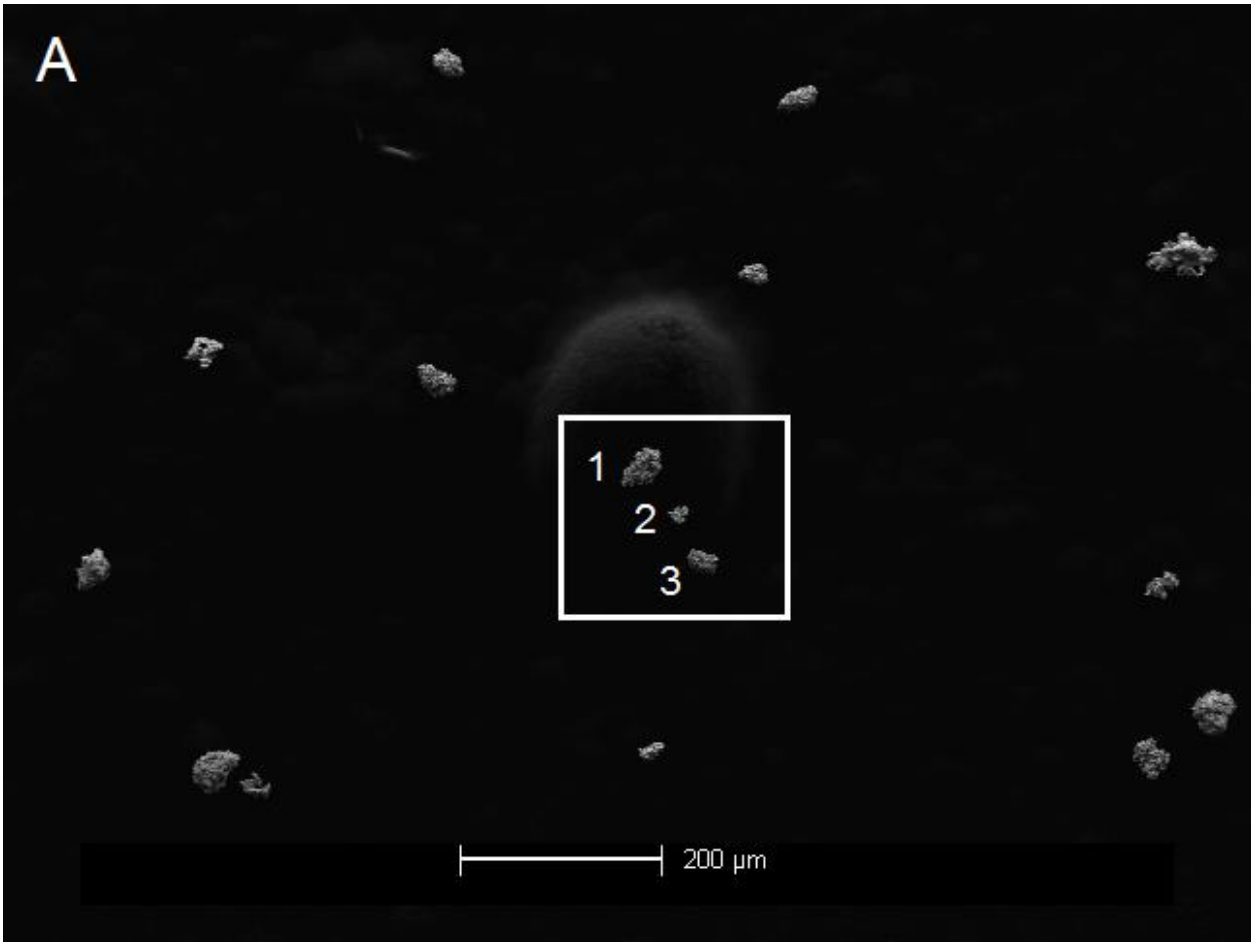

Figure S63. New large bulk gold powder with selected particles numbered (region A in Figure S62).

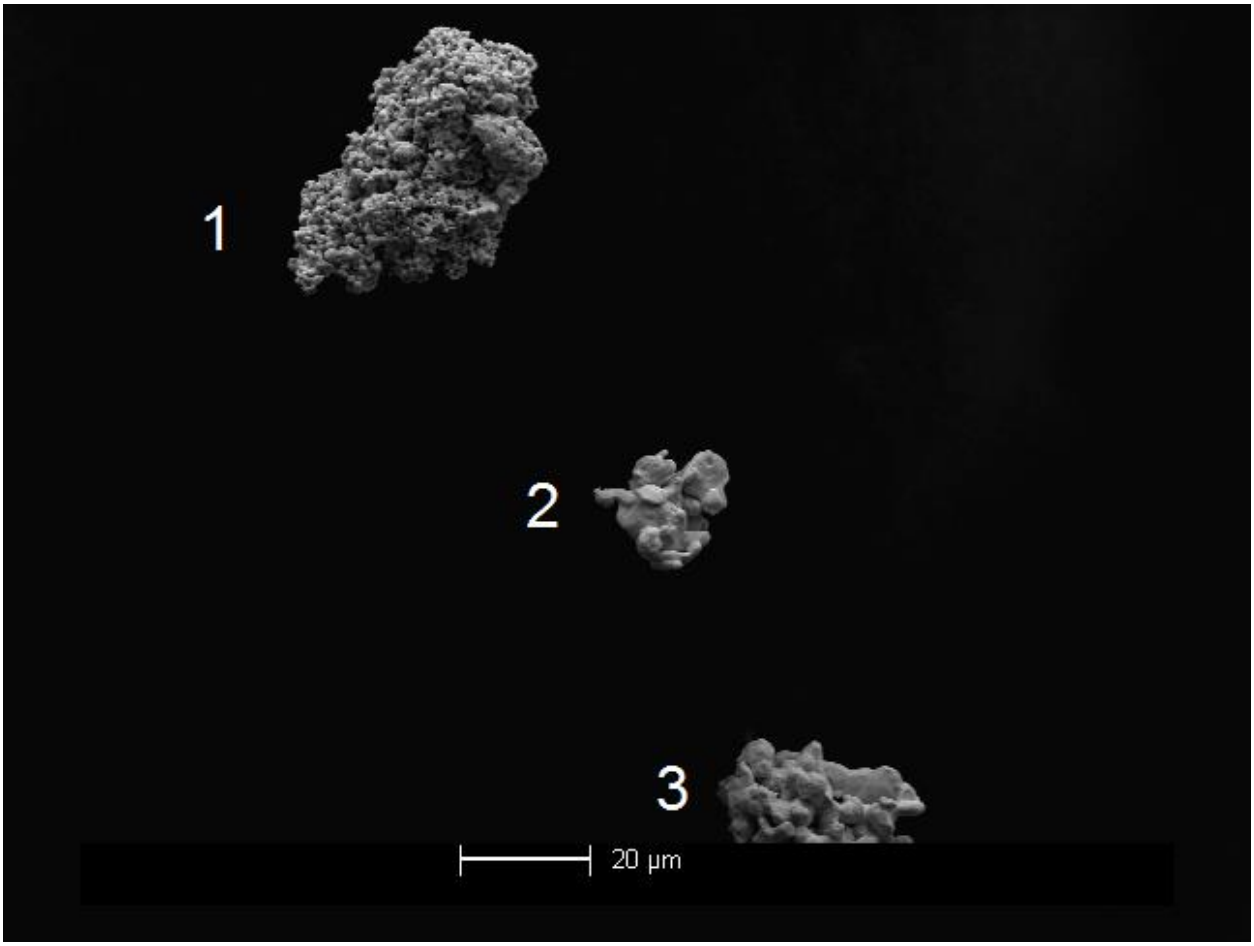

Figure S64. New large bulk gold powder with particles numbered (boxed area in Figure S63).

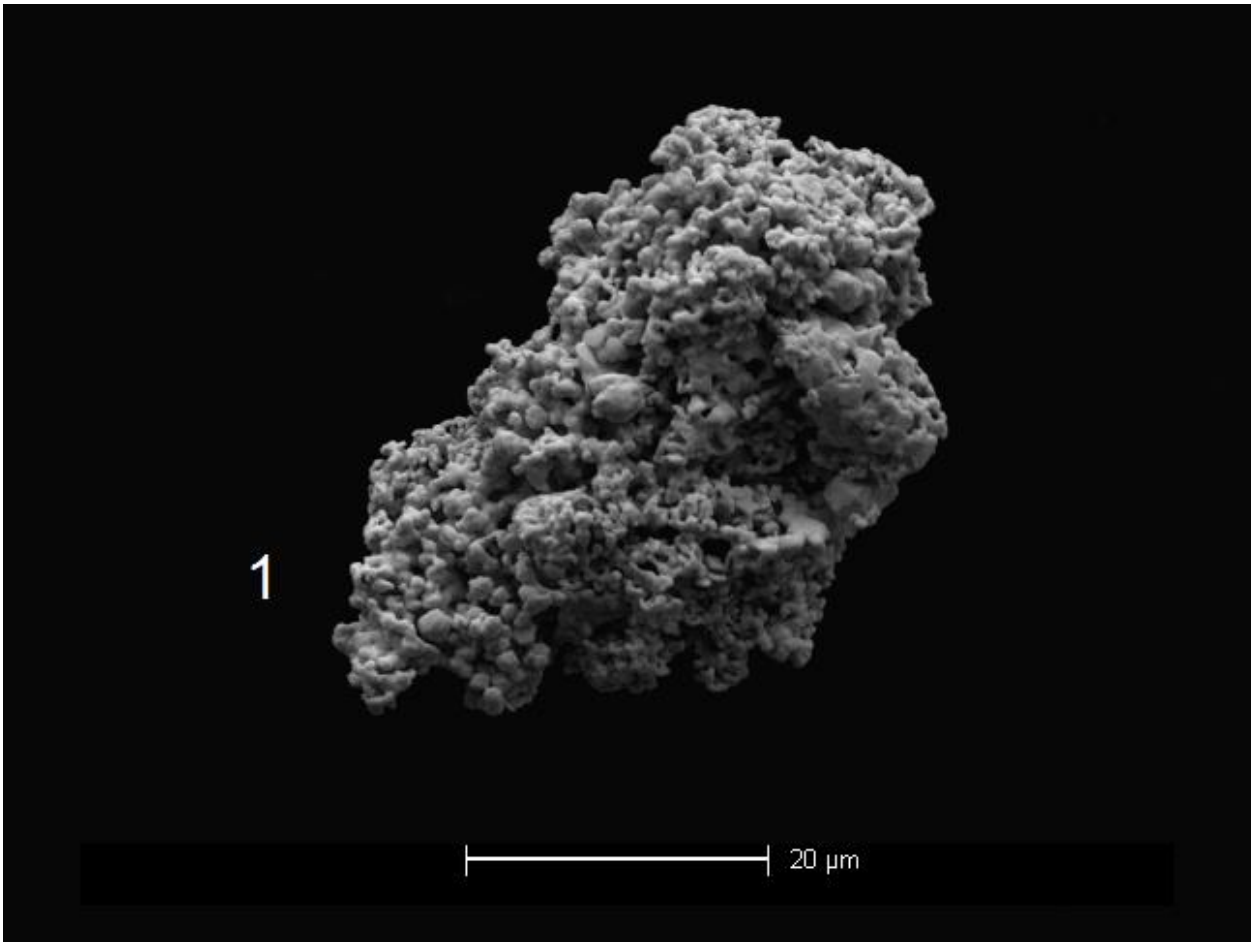

Figure S65. New large bulk gold powder (particle 1 in Figure S64).

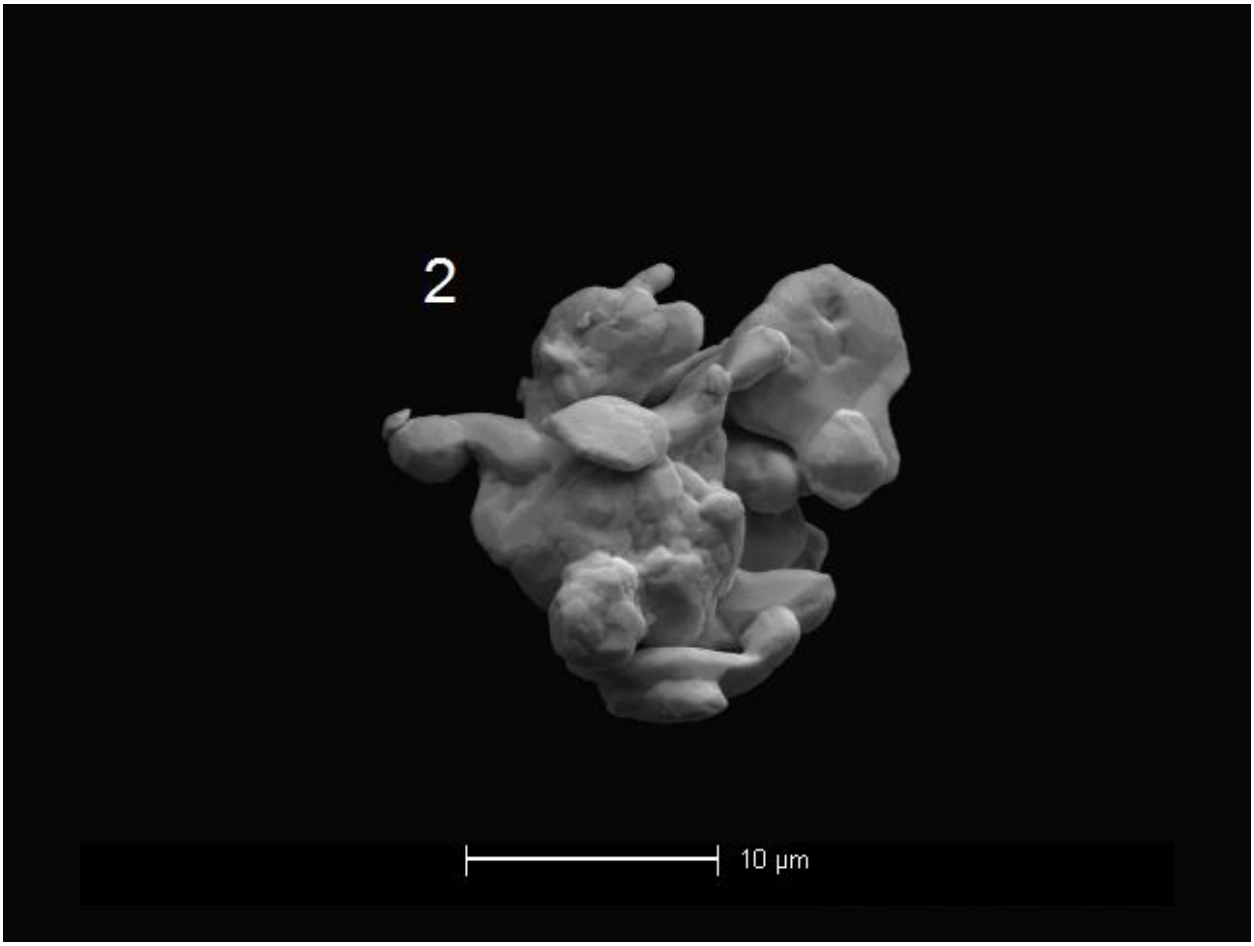

Figure S66. New large bulk gold powder (particle 2 in Figure S64).

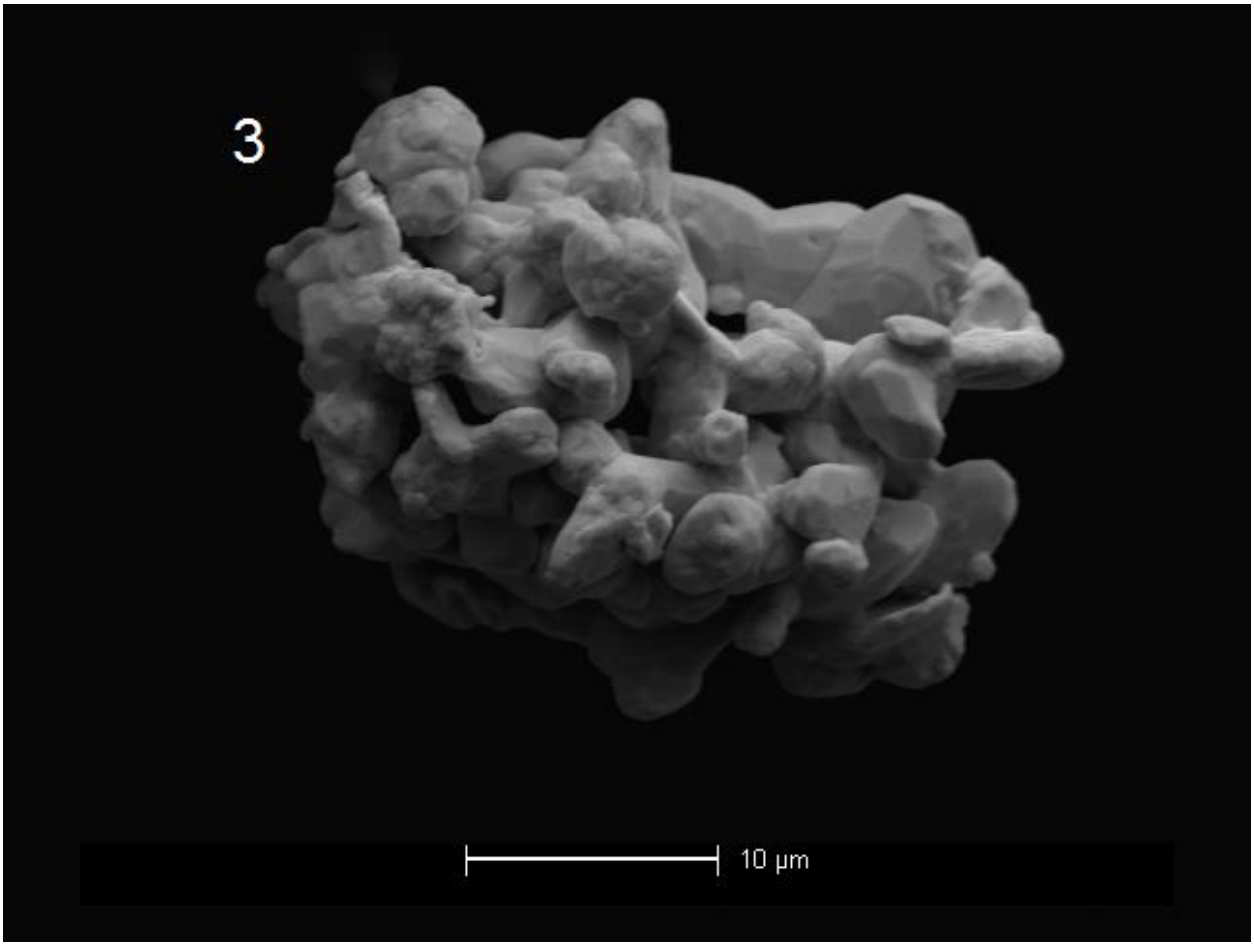

Figure S67. New large bulk gold powder (particle 3 in Figure S64).

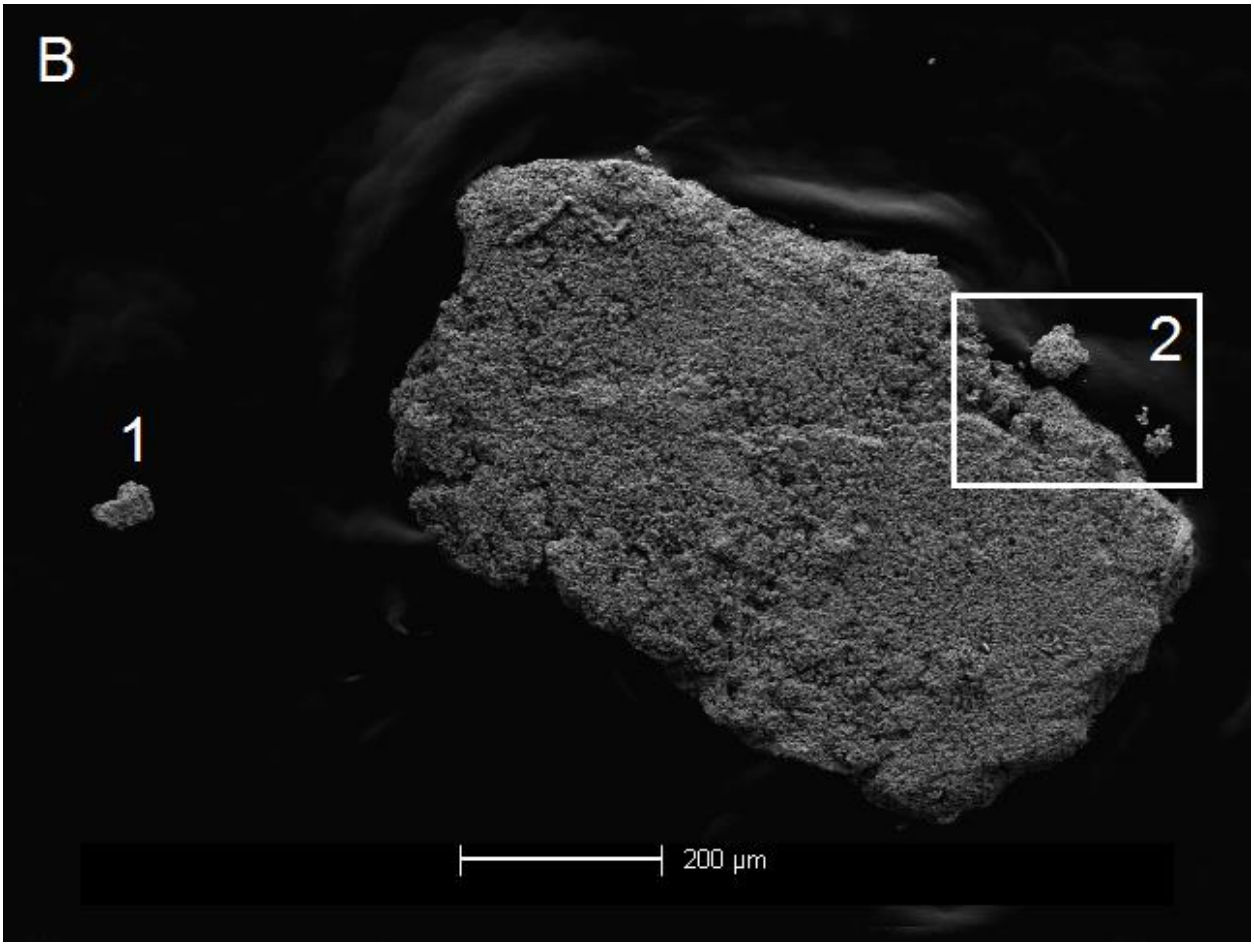

Figure S68. New large bulk gold powder with selected areas numbered (region B in Figure S62).

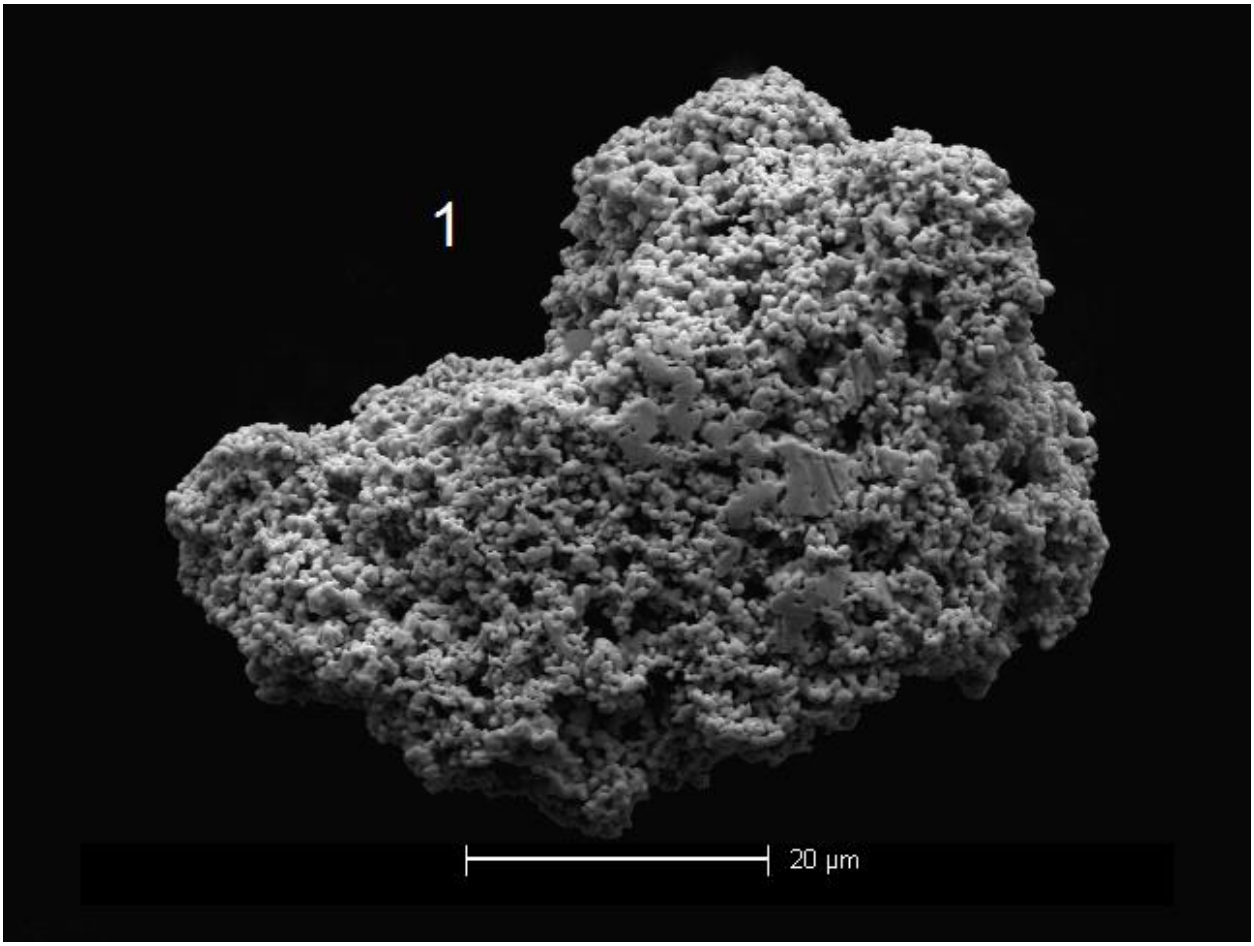

Figure S69. New large bulk gold powder (area 1 in Figure S68).

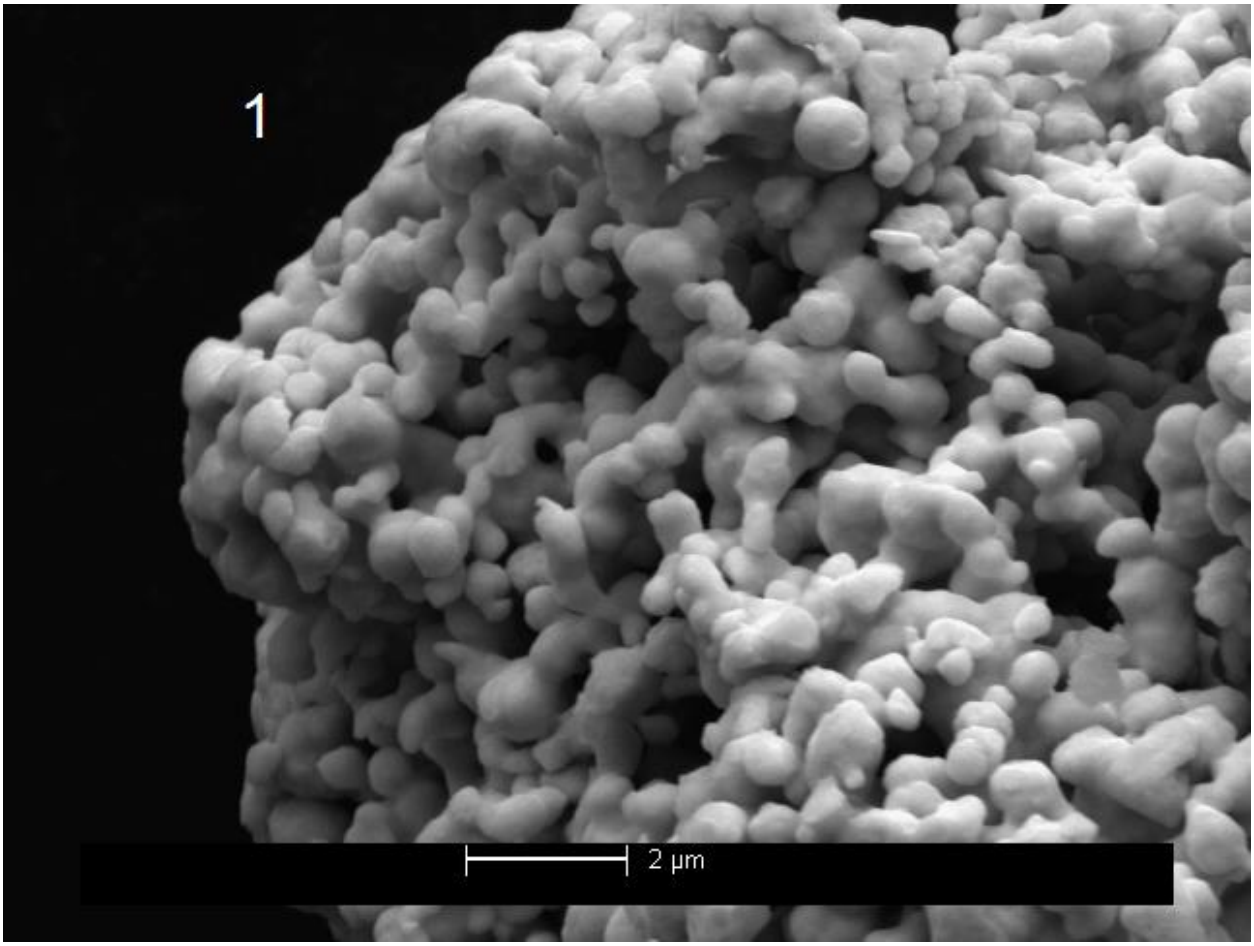

Figure S70. New large bulk gold powder (area 1 in Figure S68, zoomed in).

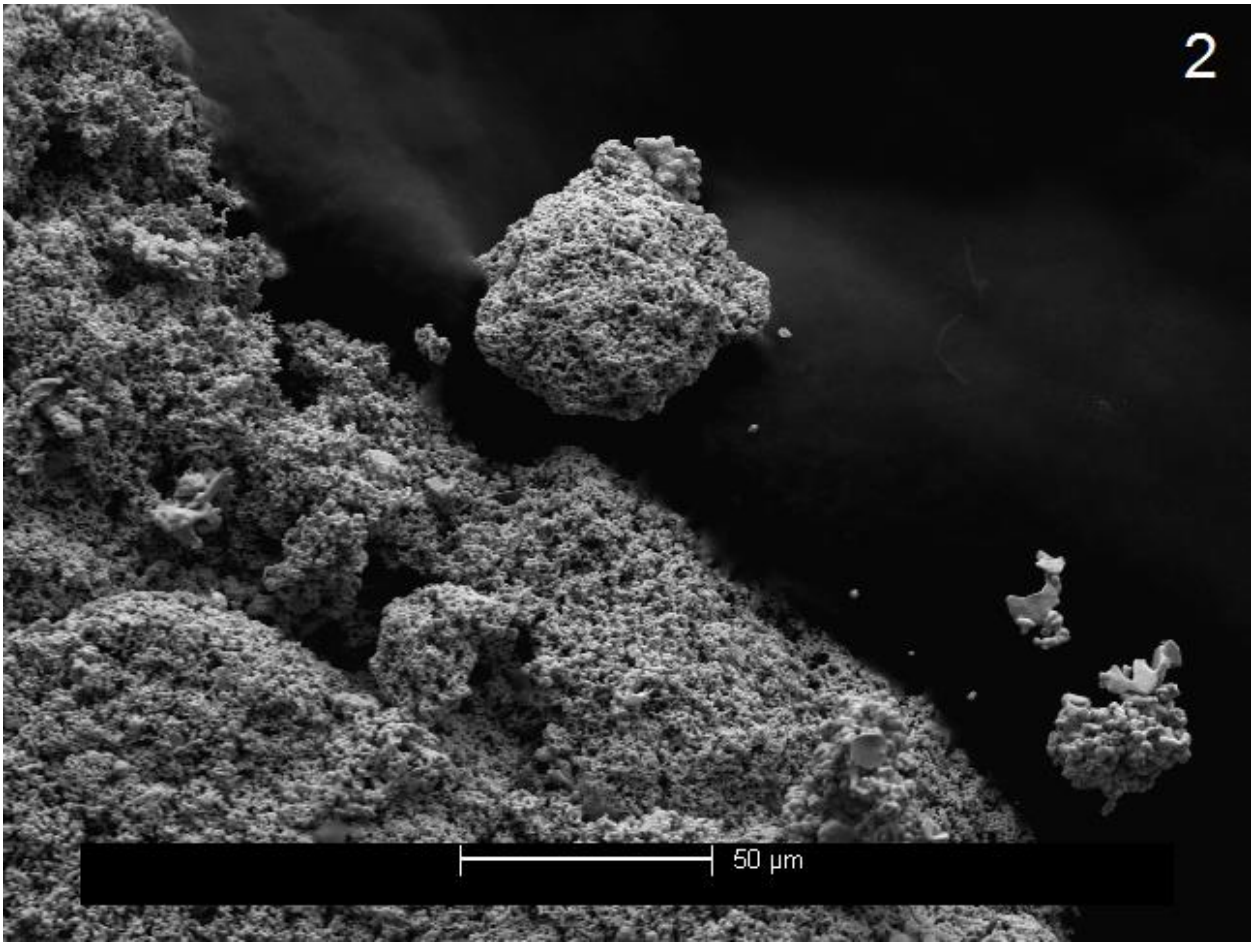

Figure S71. New large bulk gold powder (area 2 in Figure S68).

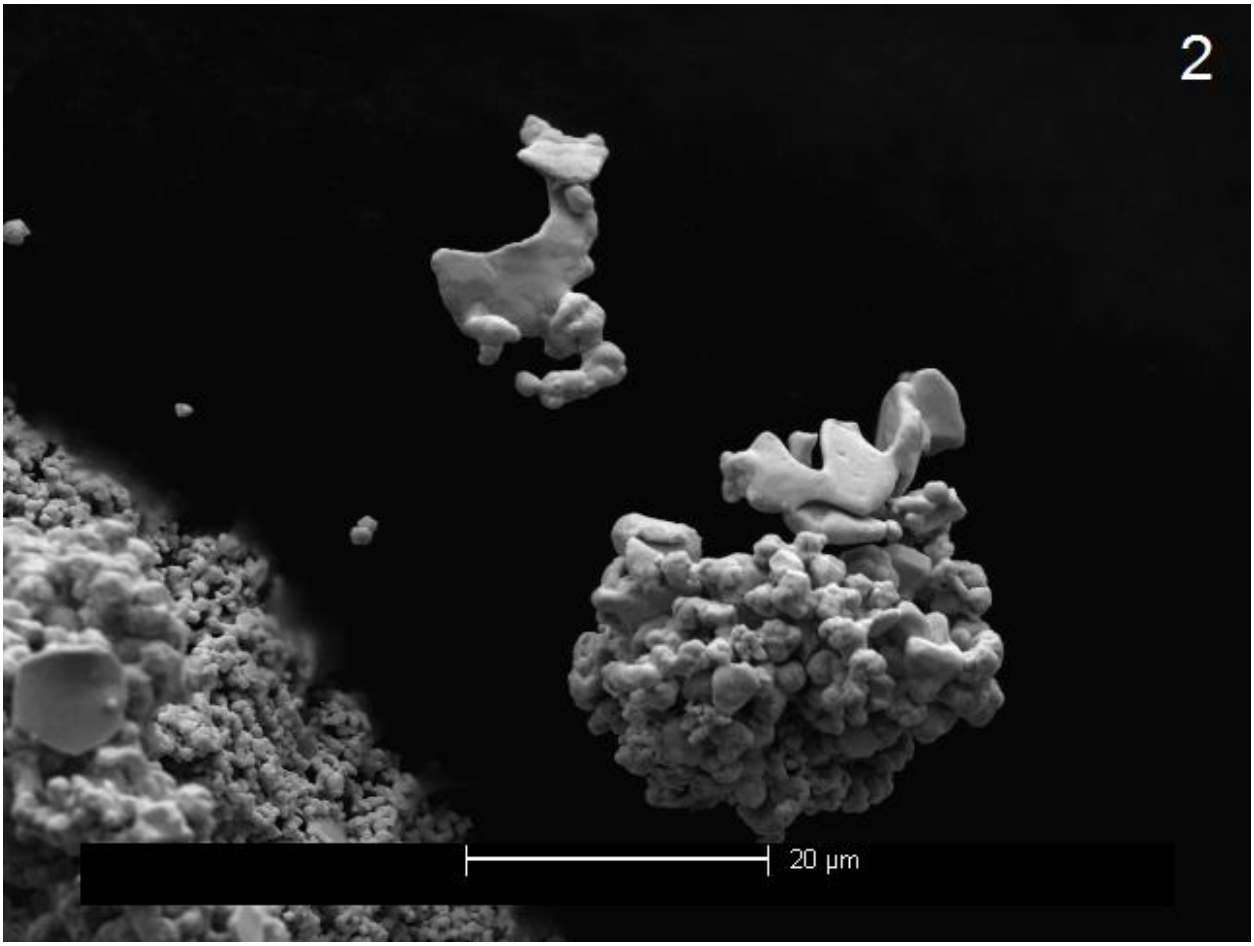

Figure S72. New large bulk gold powder (area 2 in Figure S68, zoomed in).

SEM of used large bulk gold powder

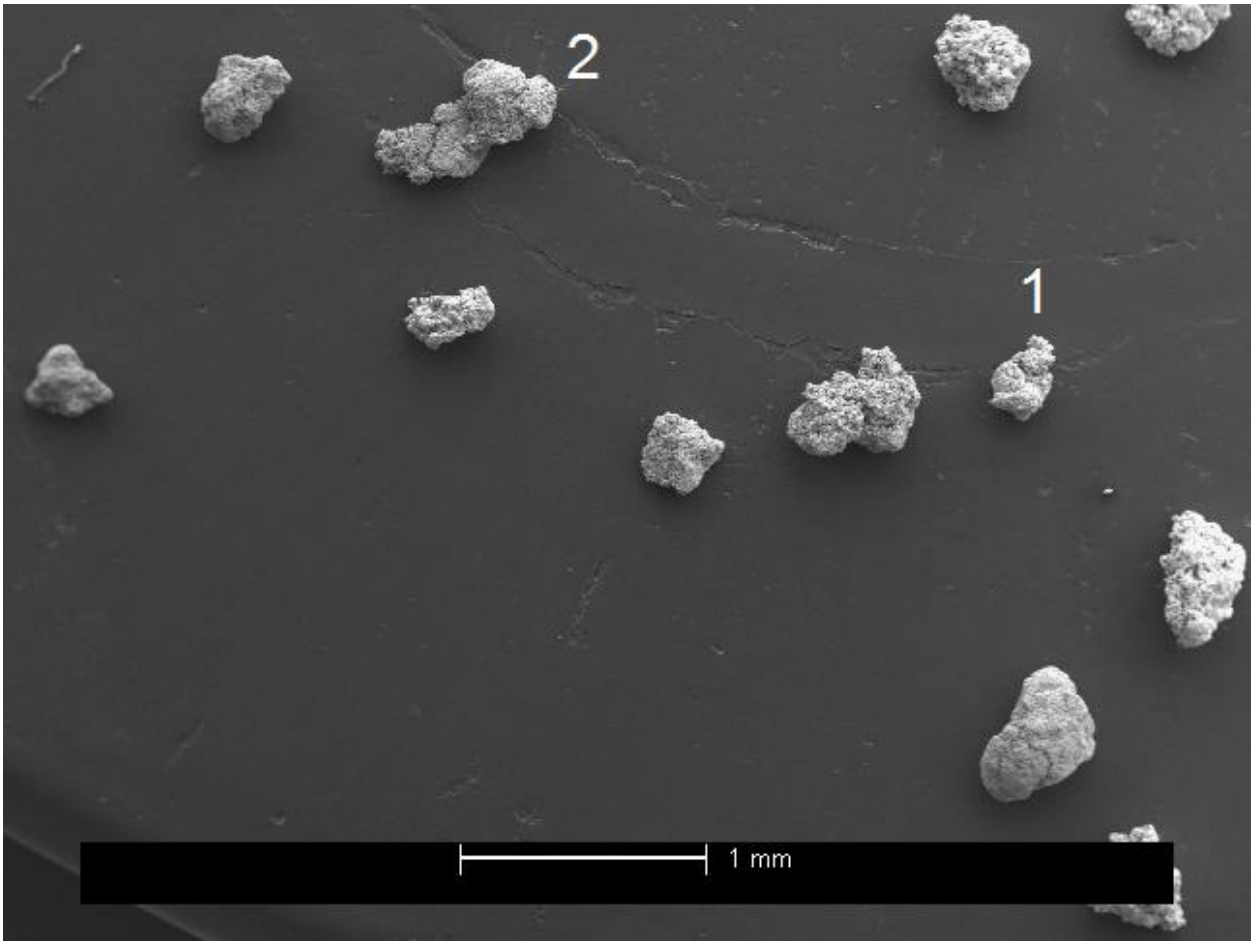

Figure S73. Used large bulk gold powder (broad view with selected particles indicated).

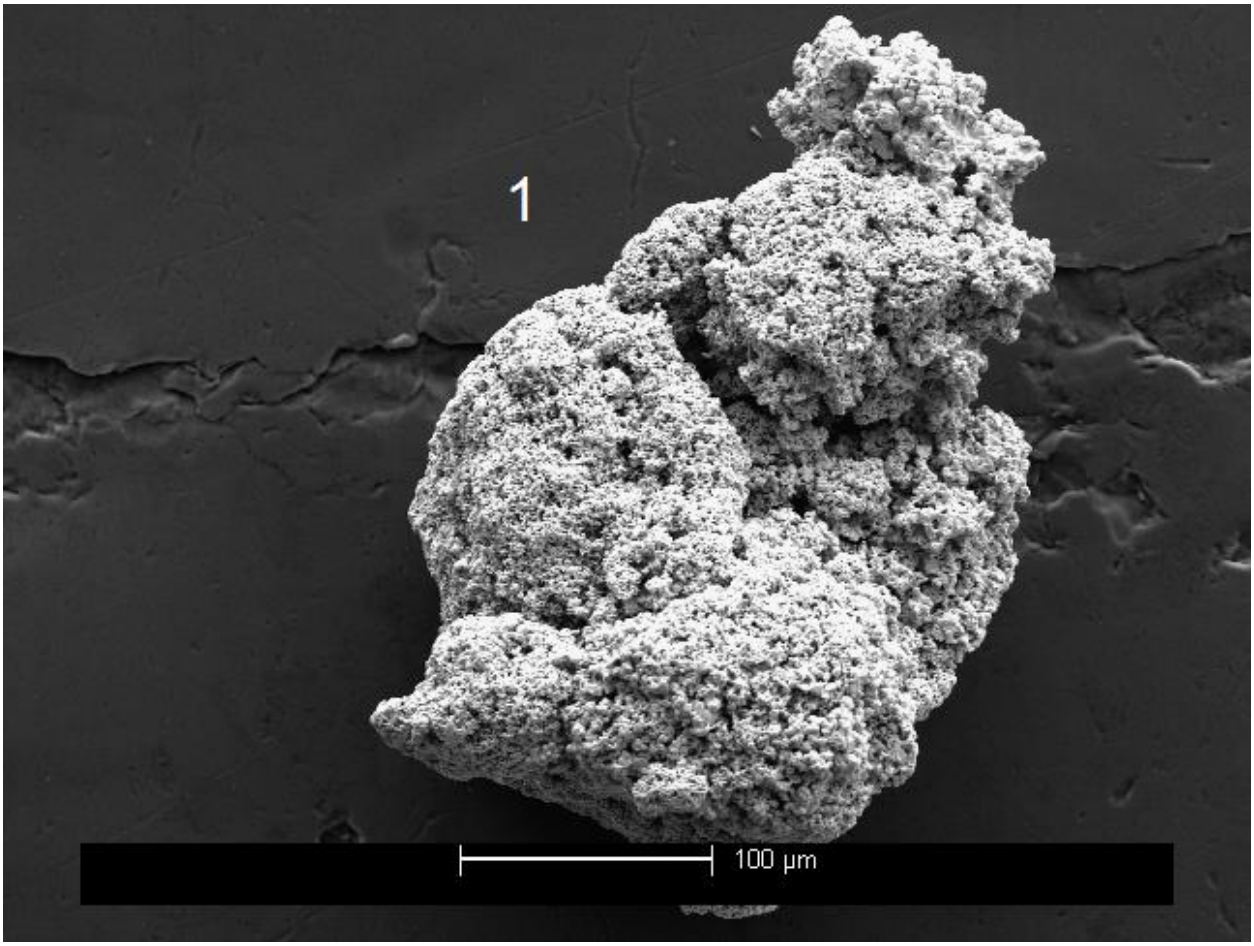

Figure S74. Used large bulk gold powder (particle 1 in Figure S73).

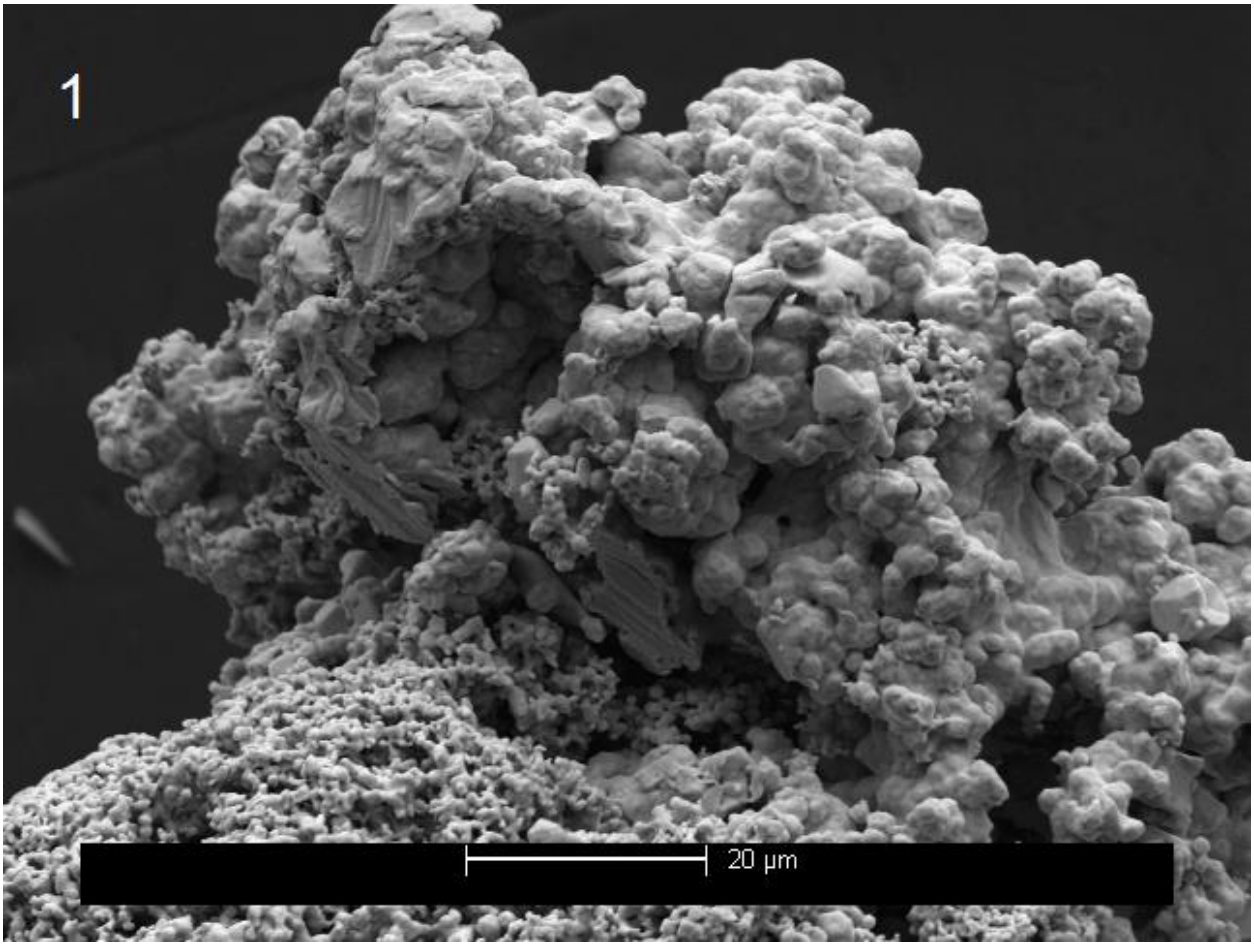

Figure S75. Used large bulk gold powder (particle 1 in Figure S73, zoomed in).

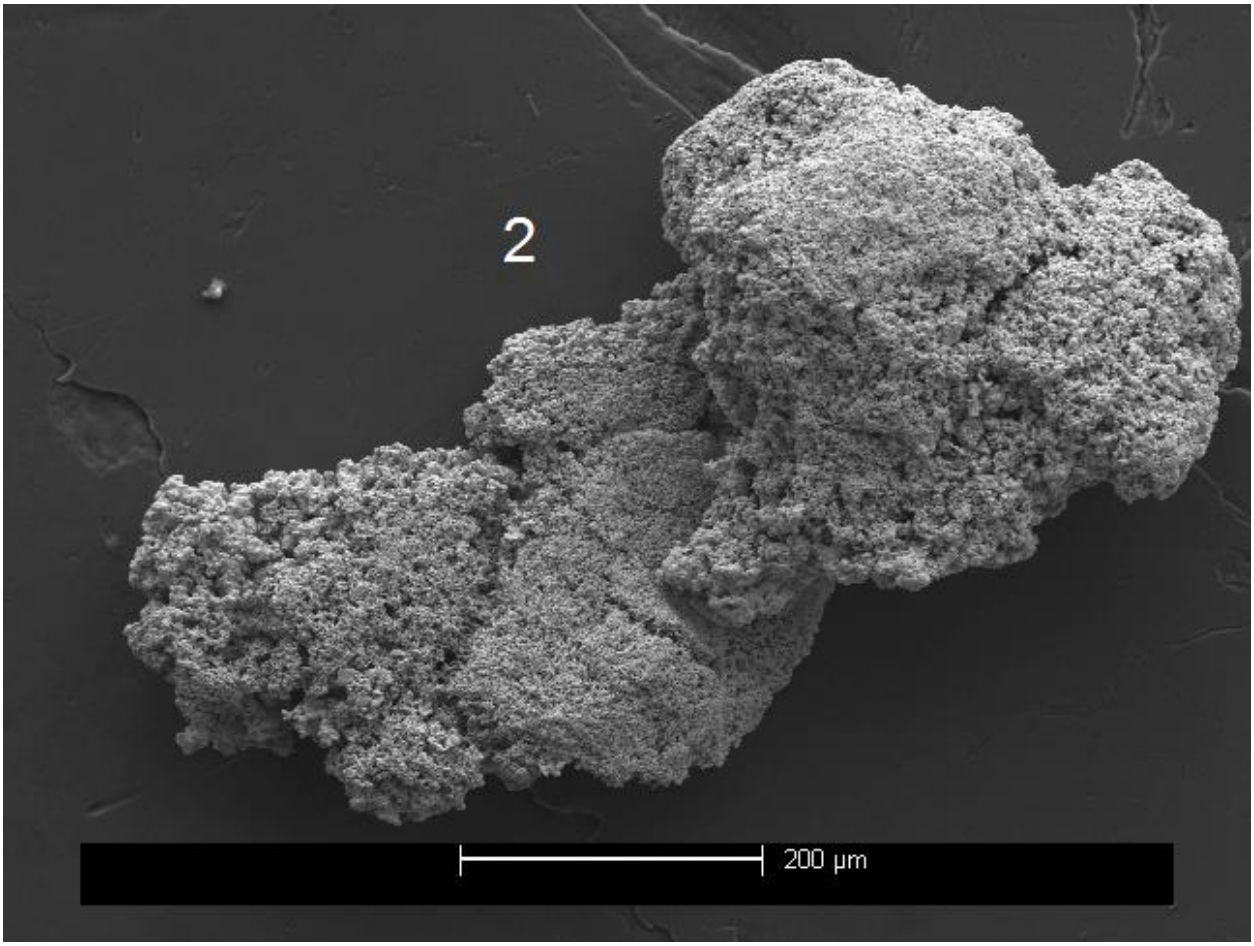

Figure S76. Used large bulk gold powder (particle 2 in Figure S73).

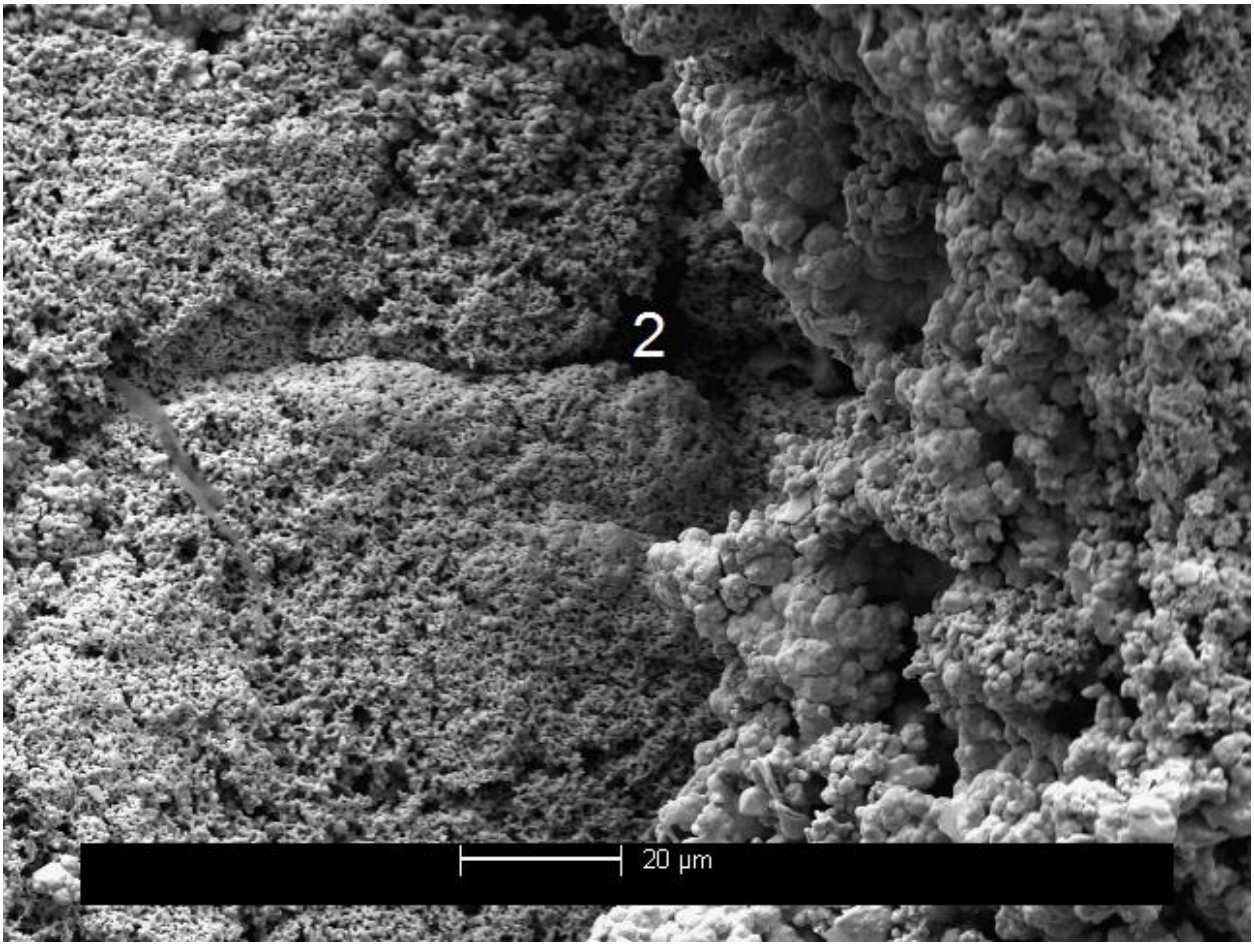

Figure S77. Used large bulk gold powder (particle 2 in Figure S73, zoomed in.